Optical dating of quartz from young deposits

From single-aliquot to single-grain

The research discussed in the present thesis has been mainly carried out at the RD&M department and at the Netherlands Centre for Luminescence dating (NCL), R^3, Faculty of Applied Sciences, Delft University of Technology, Mekelweg 15, 2629 JB Delft, The Netherlands; and, for a short time, at the Risø National Laboratory, DK-4000, Roskilde, Denmark.

Optical dating of quartz from young deposits

From single-aliquot to single-grain

PROEFSCHRIFT

ter verkrijging van de graad van doctor
aan de Technische Universiteit Delft,
op gezag van de Rector Magnificus Prof. dr. ir. J.T. Fokkema,
voorzitter van het College voor Promoties,
in het openbaar te verdedigen op maandag 1 mei 2006 om 12.30 uur
door

Mirko BALLARINI

Laurea di dottore in Fisica
Universiteit Torino, Italië
geboren te Torino, Italië

Dit proefschrift is goedgekeurd door de promotoren:

Prof. dr. ir. C.W.E. van Eijk
Prof. A.G. Wintle

Samenstelling promotiecommissie:

Rector Magnificus	voorzitter
Prof. dr. ir. C.W.E. van Eijk	Technische Universiteit Delft, promotor
Prof. A.G. Wintle	Univ. of Wales, Aberystwyth, UK, promotor
Prof. dr. ir. M. J. F. Stive	Technische Universiteit Delft
Prof. dr. U. Radtke	University of Cologne, Germany
Prof. dr. ir. M. F. P. Bierkens	Universiteit Utrecht
Prof. dr. I. M. de Schepper	Technische Universiteit Delft
Dr. J. Wallinga	Technische Universiteit Delft

ISBN XXXXXXXXXX

Keywords: Optically Stimulated Luminescence, Quaternary, quartz, insufficient bleaching, single aliquot, single grain

Published and distributed by IOS Press under the imprint Delft University Press

Publisher & Distributor
IOS Press
Nieuwe Hemweg 6b
1013 BG Amsterdam
Netherlands
fax:+31-20-687 0019
email: info@iospress.nl

Distributor in the USA and Canada
IOS Press, Inc.
4052 Rachel Manor Drive
Fairfax, VA 22032
USA
fax:+1-703-323 3668
email: sales@iospress.com

PRINTED IN THE NETHERLANDS

When a baby holds his parents finger for the first time,
they both know that it will be forever.

Episode IV - A NEW HOPE

A long time ago in a Galaxy far, far away…

It is a period of confusion. The Republic of Luminescence Dating is fighting against the evil that makes most of their optical dates unusable. The Poor Bleaching appears to have affected all the quartz samples in the Galaxy like a virus, with disastrous consequences for correct age estimates.

The reliability of the Republic is in danger. Engineers have secretly developed a magnificent weapon to assist the Republic in the war, the Single Grain method, but its tremendous power is still beyond their control. Within the Senate, some old members are skeptical, and disapprove the use of such a terrible weapon fearing destabilization of their own power.

Pursued by the Council, a limited number of Jedi Knights is called to the difficult mission of controlling the Single Grain method and turning it against the Poor Bleaching...

Contents

1 Introduction **1**
1.1 Contents overview . . . 3

2 Optical dating of young coastal dunes on a decadal time scale **5**
2.1 Introduction . . . 6
2.2 Study area and independent age control . . . 7
2.3 OSL dating . . . 8
2.3.1 Sample preparation . . . 8
2.3.2 OSL measurements . . . 8
2.3.3 Dose-rate determination . . . 10
2.4 Results and discussion . . . 12
2.4.1 Degree of resetting . . . 12
2.4.2 Reproducibility and precision . . . 12
2.4.3 Comparison with independent age control . . . 13
2.5 Conclusions . . . 14

3 Optical dating using single grains of quartz - A review **17**
3.1 Introduction . . . 18
3.2 Single Aliquot methods . . . 20
3.3 Luminescence measurements of individual grains . . . 25
3.3.1 Initial results from individual sand-sized grains . . . 25
3.3.2 Single grain facilities . . . 25
3.3.3 Procedures for single grain measurements . . . 27
3.3.4 Single grain decay curves . . . 30
3.3.5 Signal intensity . . . 31
3.3.6 Rejection criteria . . . 33
3.4 Equivalent dose distributions . . . 36
3.4.1 Histograms . . . 37
3.4.2 Probability density function (PDF) . . . 37
3.4.3 Radial plots . . . 37
3.5 Palaeodose determination . . . 38
3.5.1 Cumulative frequencies and probability plots . . . 39
3.5.2 The common, the central and the minimum age model . . . 39
3.5.3 The finite mixture model . . . 40

3.5.4 The leading edge (LE) method . . . 41
3.5.5 Comparison of internal and external uncertainties (IEU) . . . 41
3.6 Case studies of the analysis of single grain dose distributions . . . 42
3.7 Determining the palaeodose: which is the most reliable method? . . . 45
3.8 Improving the quality of single grain measurements . . . 46
3.9 Summary and conclusions . . . 47

4 Spatial variation of dose rate from beta sources as measured using single grains 53
4.1 Introduction . . . 54
4.2 Equipment . . . 55
4.2.1 Experimental procedure . . . 55
4.3 Results . . . 56
4.4 Discussion . . . 61
4.5 Conclusions . . . 62

5 Optimizing detection filters for single grain optical dating of quartz 65
5.1 Introduction . . . 66
5.2 Filter selection criteria . . . 67
5.3 Characterization of detection filters . . . 69
5.3.1 First criterion - high OSL transmission . . . 69
5.3.2 Second criterion - low background noise . . . 71
5.4 Experimental comparison . . . 72
5.4.1 Samples and experimental details . . . 72
5.4.2 Light detection efficiency . . . 72
5.4.3 Selection of the most suitable filter configuration based on RSE comparisons . . . 73
5.5 Discussion . . . 76
5.6 Conclusions . . . 77
5.7 Acknowledgements . . . 77

6 A modified SAR protocol for optical dating of individual grains from young quartz samples 81
6.1 Introduction . . . 82
6.2 Development of a modified SAR protocol . . . 83
6.2.1 Instrumentation . . . 84
6.2.2 Description of the experiments and results . . . 86
6.2.3 Discussion . . . 91
6.3 Validation of the modified SAR protocol for young natural quartz samples . . . 93
6.3.1 Samples . . . 93
6.3.2 Experimental details . . . 93
6.3.3 Equivalent dose determination . . . 98
6.3.4 Results and discussion . . . 99
6.4 Conclusions . . . 102

7 Analysis of equivalent dose distributions for single grains of quartz from modern deposits 107

7.1 Introduction . . . 108
7.2 Samples and instrumentation . . . 109
7.3 Experimental details . . . 109
7.4 Rejection criteria . . . 111
7.5 Equivalent dose calculation . . . 111
7.6 Results and discussion . . . 112
7.6.1 Sample TX02-8 . . . 112
7.6.2 Sample TX02-23 . . . 115
7.7 Conclusions . . . 116

8 Optical dating of fluvial deposits with excellent age control provided by a wrecked Roman barge (Rhine delta, The Netherlands) 119

8.1 Introduction . . . 120
8.2 Optical dating . . . 121
8.3 The Roman barge . . . 122
8.4 Samples and experiments . . . 124
8.4.1 Dose rate determination . . . 124
8.4.2 Single aliquot equivalent dose determination . . . 125
8.4.3 Single grain equivalent dose determination . . . 126
8.5 Results . . . 127
8.5.1 Dose rate . . . 127
8.5.2 Single aliquot . . . 128
8.5.3 Single grain . . . 128
8.6 Discussion . . . 131
8.6.1 Single-aliquot . . . 131
8.6.2 Single-grain . . . 134
8.7 Summary and conclusions . . . 134

Summary and Conclusions 137

Samenvatting en conclusies 141

Acknowledgements 145

Curriculum Vitae 147

Chapter 1

Introduction

During the past fifteen years, Optically Stimulated Luminescence (OSL) techniques have been successfully used as tools for establishing absolute chronologies for late Quaternary deposits. OSL dating relies on the fact that sedimentary minerals such as quartz, feldspars or zircons, experience ionizing radiation from the radioactive decay of radionuclides present in the soil. As a consequence, free electrons and free holes are excited and may be subsequently trapped in crystal defects within the material. Trapped charge is sensitive to light and is removed by sunlight exposure during transportation of the mineral grains. As the grains are deposited and shielded from light by overlying sediments, the charge build-up process begins. Thus, the amount of trapped charge can be used as a chronometer for estimating the burial time of a mineral grain. Within OSL methods, electrons are liberated by optical stimulation; these, in turn, may recombine with charge carriers of the opposite sign and produce luminescence that can be detected by a photomultiplier tube. A simple representation of the luminescence process is shown in Fig. 1.1.

Optical dating of quartz from young deposits - From single-aliquot to single-grain

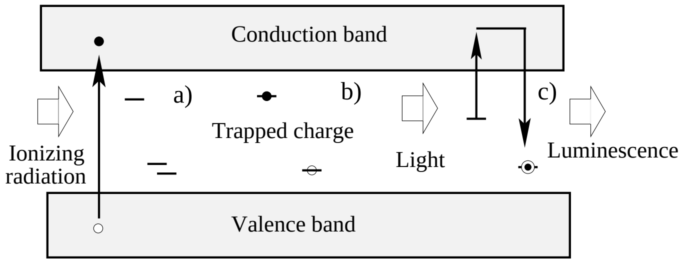

Figure 1.1: Schematic of the simplest model for OSL involving one trap and one radiative recombination center. (a) An electron and a hole are created due to ionizing radiation; (b) the electron is trapped in a lattice defect and depending on the trap depth the halflife can be several million years; (c) optical stimulation causes detrapping of the electron that might recombine with a hole and produce emission of light (luminescence).

In order to estimate the burial dose (known as equivalent dose, D_e), the luminescence signal resulting from exposure to the natural ionizing radiation is measured and compared to the ones resulting from several different laboratory irradiations. To calculate an age also requires knowledge of the rate at which the natural dose was absorbed by the grains. This is calculated by measuring the dose rate due to the various radionuclides within the sample and the (small) contribution of cosmic rays. Once the equivalent dose and the dose rate are known, the last depositional age of a sample is given by the following formula:

$$Age(a) = \frac{equivalent\ dose\ (Gy)}{dose\ rate\ (Gy/a)}$$

Although determining the dose rate is a relatively straightforward procedure, estimating the equivalent dose is a more challenging task. This is due to the fact that the light exposure experienced by some grains prior to sedimentation might not be enough to reset the OSL signal to zero (this is referred to as poor bleaching). As a result, the depositional dose received by those grains is added on the top of a pre-depositional dose, leading to an overestimation of the age of the deposit. Unwanted dose overestimation effects due to poor bleaching are more pronounced for young deposits, as the remnant dose may be of the same magnitude as the dose to be estimated. The challenge is to assess whether insufficient bleaching occurred for some grains within a sample and to estimate the correct equivalent dose from a differently-bleached population of grains.

Early procedures adopted in OSL dating made use of large aliquots consisting of thousands of grains for D_e calculation. With such an approach, only aliquots consisting of sufficiently bleached grains give an accurate burial dose. If a sample consists of a mixture of bleached and unbleached grains, different aliquots would produce different equivalent doses, revealing heterogeneous bleaching.

Recent advances in optical dating facilities, made it possible to measure the luminescence of single grains of quartz. The main advantage of single-grain (SG) over multi-grain techniques is that the D_e of each grain can be measured separately. Thus, the presence of insufficiently bleached grains can be directly inferred from dose-distribution analysis. Samples whose grains had their luminescence signal fully zeroed, show Gaussian-like distributions, while samples containing a fraction of incompletely zeroed grains show skewed distributions.

Although SG techniques are a powerful tool for recognizing poor bleaching, the method is not without problems. The first complication is that the luminescence signal from individual grains is extremely weak, and that only a few grains among hundreds show enough sensitivity to produce a measurable OSL signal. As a consequence, a large number of grains has to be measured in order to obtain meaningful statistics for dose-distribution analysis. Another problem is that no widely-accepted method has been proposed yet for estimating the burial dose from a mixed distribution of differently bleached grains.

Additional problems arise when single grain techniques are applied to very young sediments due to the extremely weak natural luminescence signal, which is dominated by noise. Also, poor bleaching can seriously affect correct D_e estimates of young samples, in that the amount of the pre-depositional dose can be as large as the post-depositional burial dose received by a grain.

The aim of this thesis is to develop a robust protocol for optical dating of individual grains from young quartz samples. Such a protocol is tested on two young aeolian samples that were well- and poorly-bleached before deposition, respectively, and on a few samples taken from an archaeological site (180 - 200 AD).

1.1 Contents overview

In **Chapter 2** we validate the existing protocol for multigrain OSL dating on aeolian very well-bleached samples. These are taken from a “perfect" environment where quartz grains have experienced many bleaching cycles prior to deposition and thus are expected to be well-bleached. This particular nature of our samples combined with a tight independent age control for the area given by maps, makes it possible to (1) determine whether these samples are indeed well-bleached, (2) test the reproducibility of OSL dating results using large aliquots and (3) date very young deposits using conventional OSL methods.

Chapter 3 reviews from the first attempts at dealing with poorly-bleached materials to the modern approach of single-grain techniques (methods for measurement of single grains and for analyzing data). Potential and limits of single-grain methods are discussed in detail.

Instruments for SG dating are such that 4800 grains can be measured within a single run. Regenerative doses, used to build up the dose-response curve of a grain, are administered simultaneously to all the grains through a β-source. It is crucial for correct dose estimations that the source irradiate the grains homogeneously. This issue is discussed in more detail in **Chapter 4** and sources available in our laboratories are tested.

Crucial for luminescence dating of young sediments is the optimization of instruments in a manner that the maximum light output with respect to instrumental noise is obtained. One approach is to optimize detection filters. Although this may not be an issue for dating of relatively old samples, this issue is of relevance for young grains, for which the luminescence signal is weak. The use of a number of alternative filters for SG dating is discussed in **Chapter 5**.

In **Chapter 6** we aim at developing a protocol suitable for single-grain optical dating of young quartz deposits. The main features of the existing protocol used for large aliquot

OSL are tested and if necessary adjusted to be suitable for measuring young single grains. The newly developed protocol is then validated using two samples that have been already successfully dated in Chapter 2 by means of large aliquots (~ 300 years).

The protocol developed in the previous chapter is further tested on two difficult-to-date samples (**Chapter 7**). One is well-bleached and estimated to be less than ten years old; the other is presumably younger than one year but poorly-bleached (age of 73 ± 24 years from large aliquot works). We show that SG dating has great potential on these kind of samples but further investigations are needed in order to provide reliable equivalent dose estimates.

SG dating has been used in **Chapter 8** as a tool for investigating incomplete resetting of fluvial deposits. A very well preserved Roman barge has been recently found in The Netherlands, which was dated to be from 180-200 AD by means of archaeological findings. Multigrain optical dating results were in good agreement with archaeological evidences, but dose distributions appeared to be slightly skewed. Through SG techniques, grains from two samples that were responsible for dose overestimation were easily recognized and removed. However, equivalent doses calculated from individual grains somewhat underestimate the age of the barge. The reasons are unknown and investigations on more samples are needed.

Chapter 2

Optical dating of young coastal dunes on a decadal time scale

Quaternary Science Reviews, 22 (2003) 1011-101

M. Ballarini[a], J. Wallinga[b], A.S. Murray[a], S. van Heteren[c], A.P. Oost[d], A.J.J. Bos[b], C.W.E. van Eijk[b]

[a] *Nordic Laboratory for Luminescence Dating, Department of Earth Sciences, Aarhus University, Risø National Laboratory, DK-4000 Roskilde, Denmark.*

[b] *Radiation Technology Group, IRI, Delft University of Technology, Netherlands Centre for Luminescence dating, Mekelweg 15, NL-2629 JB Delft, The Netherlands.*

[c] *Netherlands Institute of Applied Geoscience TNO - National Geological Survey, P.O. Box 80015, NL-3508 TA Utrecht, The Netherlands.*

[d] *National Institute for Coastal and Marine Management/RIKZ, P.O. Box 207, NL-9750 AE Haren,*
The Netherlands.

Optical dating of quartz from young deposits - From single-aliquot to single-grain

Abstract

We explore the use of quartz optically stimulated luminescence (OSL) dating for reconstructing coastal evolution on a timescale of decades to a few hundred years. Samples are taken from the accretionary south-west coast of Texel, a barrier island just offshore of the northern Netherlands. The ages of dune ridges are known from historical sources; an excellent chronology with a decadal accuracy exists for the past 260 years. OSL ages of less than 10 years on the youngest samples indicate that the OSL signal of the quartz grains is very well zeroed prior to deposition and burial. OSL ages of five samples from a 250-year-old dune ridge are indistinguishable, and the OSL ages on 17 out of 20 samples are in excellent agreement with the well-known independent age controls. Our results highlight the potential of OSL dating for high-resolution reconstruction of coastal evolution over the past few centuries.

2.1 Introduction

Over the last few years luminescence dating has been improved considerably, both in the methods for the estimation of the equivalent dose, D_e (with the development of the single-aliquot regenerative-dose (SAR) protocol, Murray and Wintle, 2000) and in the measurement facilities (Bøtter-Jensen and Murray, 1999). Using these new methods and procedures, quartz optically stimulated luminescence (OSL) dating has been shown to give accurate results for samples from a wide range of depositional environments and for a wide range of ages (Murray and Olley, 2002). Modern deposits have been sampled to investigate offsets due to incomplete removal of the OSL signal in fluvial (Stokes *et al.*, 2001) and glacial (Rhodes, 2000) environments. A very young age ($<$ 5 years) has been reported for a modern beach sand (Banerjee *et al.*, 2001). So far, however, no systematic study of the accuracy of OSL ages on deposits younger than a few hundred years has been presented.

In this paper, we present quartz OSL dating results on coastal-dune sand from the south-west coast of the island of Texel (The Netherlands); these deposits formed over the last three hundred years. The timing of formation of the sequence of dunes at the study location is accurately known from historical maps and documents. The sand grains in these dunes are likely to have experienced several bleaching cycles while washed on the beach and during subsequent aeolian transport, before being trapped and buried in a coastal dune. We therefore expect these grains to be well bleached, i.e. there should be negligible charge remaining in the easy-to-bleach OSL traps at the time of burial. The aim of our study is threefold: 1) Determine whether these deposits are indeed well bleached; 2) Investigate the reproducibility of OSL dating results on young deposits and 3) Demonstrate the potential of quartz OSL dating for determining the time of formation of coastal-dune ridges formed during the past three hundred years. Reconstructing coastal evolution on a century to decadal time scale allows insight into coastal-system dynamics; this is of importance for the development of coastal-management tools and policies, and in particular for coastal-defence planning. Demonstration of the validity of quartz OSL dating on these time scales and in these environments has the potential to revolutionise research in this area, as accurate and precise age estimation of sandy coastal deposits has hitherto not been possible.

2.2 Study area and independent age control

Texel is a barrier island offthe north-west coast of The Netherlands (Fig. 2.1).

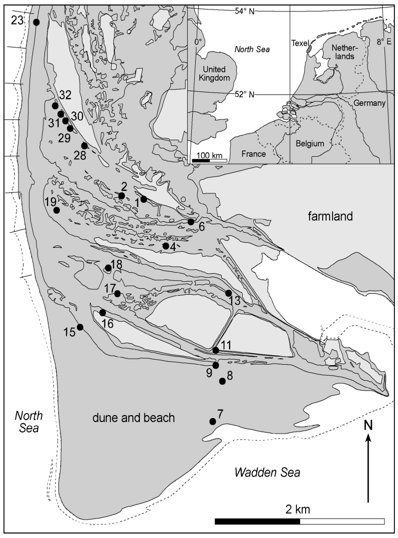

Figure 2.1: Location of south-west Texel in the North Sea coast of The Netherlands. Lines in the dune-and-beach area, representing the +5-m contour (relative to mean sea level), show the most prominent dune ridges.

The core of the island is formed by a slightly elevated ice-pushed ridge composed of till, formed during a stillstand phase in the recession of the Middle-Saalian (Oxygen Isotope Stage 6) ice sheet (Ter Wee, 1962). The south-west part of the island is made up of a sequence of dune ridges, formed parallel to the coast over the last few centuries. The island has been growing in a south-westerly direction, allowing the preservation of most of the dune ridges after their formation, up to the present day. Growth of the island is a result of shoals merging with the island periodically. Following their formation within the confines of the ebb-tidal delta south-west of Texel, shoals are separated from the island by a flood-dominated tidal channel. When a shoal and adjacent channel migrate northward, the channel usually erodes part of the island before it is abandoned. After connecting to the island the shoal forms a significant sediment source; sand blown from the shoal, by this stage forming a wide beach, is captured by pioneer vegetation (dune grass) and, more recently, man-made sand fences, and develops into a dune ridge parallel to the coast. Once the dune ridge is separated from the sediment source by a new ridge, development stops and the dune becomes entirely stabilized by vegetation. The dune ridges are generally about 5-10 meters high, although some reach a height of 15 meters. Although blowouts do occur, most ridges remain linear, indicating that they are more-or-less stable after formation.

Following merger of a shoal, a number of ridges can develop rather quickly. When the next channel approaches, sediment supply diminishes and dune-ridge development may cease locally. Since the middle of the 19^{th} century, an increasing part of the west coast of the island has been eroding. In the 20^{th} century alone, up to 1 km of land has been lost. To stem this loss, a beach-nourishment program, in which sand from elsewhere is dumped on the beach, has been implemented in the last few years.

Detailed information on the Pleistocene and Holocene formation of Texel is provided by Sha (1990). The recent coastal development of the island is very well documented in historical records and maps. Accurate maps that can be readily related to existing landmarks and to the present grid system are available from AD 1749; after 1800 AD, a new map in this series has been produced initially at a decadal frequency, and at shorter time intervals later on.

2.3 OSL dating

2.3.1 Sample preparation

Sand-sized quartz separates from 20 samples were used in this study. Samples were taken from a depth of 30 to 85 cm below the surface on the seaward slopes of ridges. We took care to pick locations where ridges had maintained their linear form to minimize the risk of sampling sand that experienced reworking after formation of the dune. First a hole was dug with a shovel, and then PVC tube (diameter 10 cm, length 40 cm) was hammered into the internal face, capped and sealed with black tape.

The tubes were opened in subdued orange light. Samples for equivalent dose determination were obtained from the center of the cores, while the outer parts were used for -spectrometry and water-content determination. Material from both ends of the tube was discarded. The samples were wet sieved to obtain the 180-212 μm fraction, which was then treated with HCl, H_2O_2, concentrated (40%) HF, and finally with HCl again. Sample purity was checked by exposure to infrared (IR) light; no significant IR-OSL sensitivity was observed in any of the samples.

2.3.2 OSL measurements

Measurements were undertaken using an automated TL/OSL reader (Bøtter-Jensen and Murray, 1999). Stimulation with blue LEDs (470 ± 30 nm) was performed at 125°C; the resulting OSL signal was detected through 7 mm of U-340 filter. We used the OSL signal from the first 0.8 seconds of stimulation, and subtracted the background signal as observed during the last 4 seconds of stimulation. The Single-Aliquot Regenerative-dose (SAR) protocol (Murray and Wintle, 2000) was used for the equivalent-dose determination. Test doses were heated to 160°C prior to measurement.

It is important to investigate the influence of preheating (especially for very young samples), because thermal treatment prior to measurements may transfer charge from light-insensitive traps to light-sensitive ones (Rhodes, 2000; Wintle and Murray, 2000). Plateau tests for two samples (TX02-7 and TX02-32) show the D_e to be independent of preheat temperature below 200°C when 10 s preheats were used (Fig. 2.2).

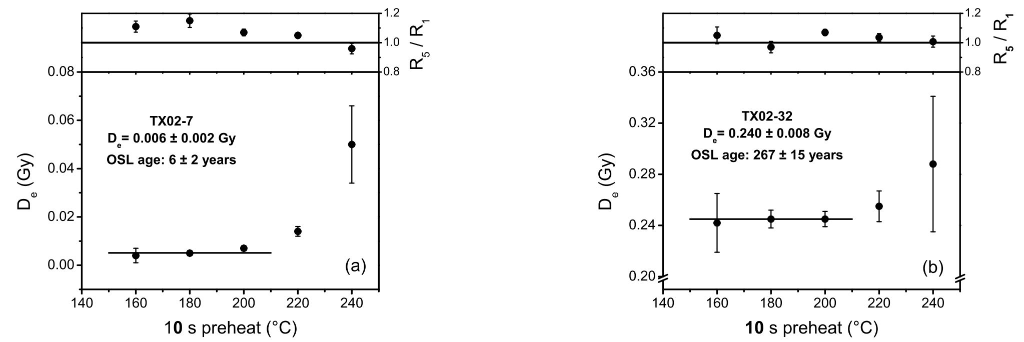

Figure 2.2: Equivalent dose and recycling ratio (cf. Murray and Wintle, 2000) as a function of the preheat temperature for sample TX02-7 (a) and for sample TX02-32 (b). The mean value obtained on three aliquots is presented with the standard error on the mean. Both graphs indicate that the equivalent dose (D_e) is independent of the preheat temperature up to 200°C. Recycling ratios are close to unity for sample TX02-32, but tend to be high for sample TX02-7 when preheat temperatures of 160°C or 180°C are used. Based on these experiments, we selected a preheat temperature of 190°C for routine measurements.

For more stringent preheats a rising trend in the D_e was observed, probably due to thermal transfer (Rhodes, 2000). To investigate this, a thermal-transfer test was conducted in which a number of aliquots were optically bleached (two times 40 s exposure to blue light from LEDs at ambient temperature separated by a pause of 4000 s) after which their equivalent dose was measured using the SAR procedure. We found that the dependency of the apparent equivalent dose on preheat temperature matches the rise in D_e found for the preheat-plateau measurement. This observation confirms that the rising trend in the latter is a result of thermal transfer during preheating of the natural, and should be avoided if possible.

Although the SAR protocol monitors sensitivity changes during the measurement sequence, it cannot detect changes in trapping sensitivity occurring prior to administration of the first test dose (Murray and Wintle, 2000; Wallinga *et al.*, 2000a;b). To provide an overall test of the reliability of the protocol, we carried out a dose-recovery test (Wallinga *et al.*, 2000b). This test is similar to the thermal transfer test described above, except that a laboratory dose was administered after the initial optical bleaching, and before the first heating of the sample. Measured and given doses were found to be indistinguishable for 10 s preheats up to 200°C (weighted mean $1.04 \pm 0.01, n = 4$), and the ratio of measured to given dose showed a rising trend due to thermal transfer above that temperature. This test shows that no significant change in trapping efficiency occurs during the first heating of the sample. Sensitivity changes during the measurement protocol, as monitored by OSL response to the test dose, were found to be negligible. Although we applied the full SAR procedure, a simple regeneration procedure, without sensitivity correction, would probably have sufficed.

Ideally, regenerative doses used in the SAR procedure should encompass the natural dose to allow equivalent-dose determination by interpolation between the regenerative points. However, this was not possible for the youngest samples studied here, because their equivalent dose was too small. For these samples the D_e was interpolated between the origin and the first regeneration dose ($R_1 = 0.07$ Gy; Fig. 2.3).

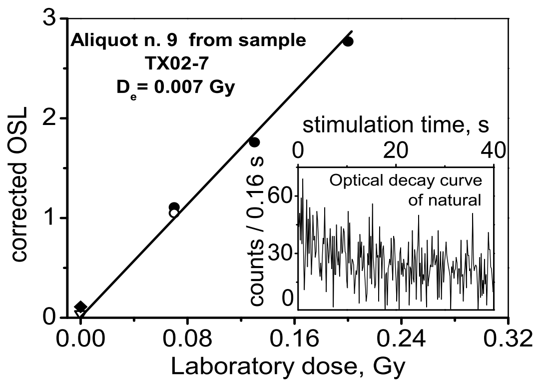

Figure 2.3: Typical dose-response curve for an aliquot from sample TX02-7 (D_e= 5.9 ± 2.0 mGy). Filled circles represent the regenerated-dose points (R_1, R_2, and R_3) while the open circle indicates the recycling point (R_5). The test-dose-corrected OSL natural (filled diamond) and the recuperation point (R_4, open triangle) are also shown. To determine the equivalent dose of this and other young samples we used interpolation between the origin and the first dose point (R_1). A test dose of 0.7 Gy was used for this sample. A natural stimulation curve is shown in the inset.

We thus assume that the dose-response curve passes through the origin; this assumption seems valid as the recuperation signal observed for these samples is negligible.

To avoid offsets due to thermal transfer, we decided to use a 10 s preheat at 190°C for all samples. At least twelve aliquots were measured for each sample; the equivalent doses obtained are presented in Table 2.1.

2.3.3 Dose-rate determination

High-resolution γ-spectrometry was used for the estimation of the natural dose rate (Murray *et al.*, 1987), using material taken from the sample tube as described in section 2.3.1. A contribution from cosmic rays was calculated based on the depth of the samples using equation (2) given by Prescott and Hutton (1994). The 'in situ' water content of the samples was used to calculate water content attenuation factors, with an uncertainty of ±4% on the measured value. Radionuclide concentration, sample depths, water contents and resulting dose rates are presented in Table 2.1.

Table 2.1: Summary of radionuclide analysis, dose rates, equivalent doses, OSL results and independent age control

Sample	Radionuclide concentration[a] (Bq kg^{-1})				Water content	Sample depth	Dose rate[b]	Equivalent dose[c]	OSL age[d]	OSL age[d]	Independent age range
	^{238}U	^{226}Ra	^{232}Th	^{40}K	(%)	(cm)	(Gy ka^{-1})	(mGy)	(years)	(AD)	(AD)
TX02-1	2 ± 4	3.7 ± 0.7	4.7 ± 0.6	196 ± 17	4 ± 4	55	0.94 ± 0.04	233 ± 10	248 ± 11	1754 ± 11	1738 − 1749
TX02-2	7 ± 3	4.5 ± 0.3	5.3 ± 0.3	188 ± 6	9 ± 4	60	0.92 ± 0.04	202 ± 7	220 ± 12	1782 ± 12	1774 − 1795
TX02-4	6 ± 4	4.7 ± 0.3	6.5 ± 0.3	192 ± 6	5 ± 4	55	0.98 ± 0.04	143 ± 6	145 ± 9	1857 ± 9	1855 − 1863
TX02-6	1 ± 3	3.3 ± 0.2	4.4 ± 0.2	157 ± 5	4 ± 4	60	0.82 ± 0.03	133 ± 6	163 ± 10	1839 ± 10	1795 − 1838
TX02-7	5 ± 4	3.9 ± 0.6	4.3 ± 0.5	179 ± 15	2 ± 4	28	0.92 ± 0.05	5.9 ± 2.0*	6 ± 2	1996 ± 2	1996 − 2002
TX02-8	2 ± 4	2.8 ± 0.6	4.3 ± 0.5	155 ± 15	5 ± 4	40	0.81 ± 0.05	6.3 ± 0.9*	7.4 ± 1.3	1995 ± 1	1996 − 2002
TX02-9	3 ± 4	4.8 ± 0.6	4.5 ± 0.5	180 ± 15	5 ± 4	60	0.90 ± 0.05	20 ± 3	17 ± 3	1985 ± 3	1976 − 1989
TX02-11	8 ± 4	4.1 ± 0.3	5.3 ± 0.2	159 ± 5	16 ± 4	55	0.80 ± 0.03	19.8 ± 1.4	25 ± 2	1977 ± 2	1963 − 1996
TX02-13	7 ± 3	4.4 ± 0.3	6.6 ± 0.3	167 ± 6	3 ± 4	55	0.92 ± 0.04	57 ± 3	62 ± 4	1940 ± 4	1896 − 1930
TX02-15	6 ± 3	4.5 ± 0.2	5.7 ± 0.2	164 ± 4	3 ± 4	60	0.89 ± 0.03	12 ± 2	13 ± 2	1989 ± 2	1976 − 1989
TX02-16	6 ± 5	7.8 ± 0.7	12.8 ± 0.7	181 ± 16	3 ± 4	40	1.11 ± 0.05	21.0 ± 1.5	19 ± 1	1983 ± 1	1962 − 1980
TX02-17	10 ± 4	5.5 ± 0.3	9.1 ± 0.3	155 ± 5	3 ± 4	45	0.96 ± 0.04	35 ± 2	36 ± 3	1966 ± 3	1942 − 1960
TX02-18	13 ± 4	9.8 ± 0.3	16 ± 0.4	155 ± 5	3 ± 4	50	1.11 ± 0.04	29.1 ± 1.1	26.2 ± 1.4	1976 ± 1	1925 − 1939
TX02-19	3 ± 4	3.5 ± 0.2	4.8 ± 0.2	163 ± 5	4 ± 4	60	0.85 ± 0.03	136 ± 4	160 ± 9	1842 ± 9	1855 − 1863
TX02-23	3 ± 3	4.2 ± 0.2	4.9 ± 0.2	156 ± 4	3 ± 4	30	0.86 ± 0.03	63 ± 20	73 ± 23	1929 ± 23	2001 − 2002
TX02-28	8 ± 2	4.5 ± 0.4	4.8 ± 1.0	203 ± 10	5 ± 4	55	0.99 ± 0.04	260 ± 10	264 ± 18	1738 ± 18	1738 − 1749
TX02-29	6 ± 3	3.6 ± 0.2	4.4 ± 0.2	211 ± 5	5 ± 4	64	0.98 ± 0.04	236 ± 10	240 ± 14	1762 ± 14	1738 − 1749
TX02-30	7 ± 4	4.0 ± 0.6	5.1 ± 0.5	189 ± 16	5 ± 4	60	0.94 ± 0.04	250 ± 3	266 ± 12	1736 ± 12	1738 − 1749
TX02-31	3 ± 4	3.5 ± 0.3	5.2 ± 0.2	202 ± 6	4 ± 4	60	0.96 ± 0.04	244 ± 9	253 ± 14	1749 ± 14	1738 − 1749
TX02-32	3 ± 4	4.3 ± 0.6	5.4 ± 0.5	173 ± 15	5 ± 4	60	0.89 ± 0.04	240 ± 8	267 ± 15	1735 ± 15	1738 − 1749

[a] Spectral data from high-resolution gamma-spectroscopy converted to activity concentrations and infinite matrix dose rates using the conversion data given by Olley *et al.* (1996). The gamma spectrometry calibration is described in Murray *et al.* (1987).

[b] The natural dose rate was calculated from the infinite matrix dose rate using attenuation factors given by Mejdahl (1979). Cosmic rays contributions are included in the dose rate data following Prescott and Hutton (1994). Attenuation factors given by Zimmerman (1971) were used for calculating the effect of water on the dose rates.

[c] Regenerative doses used in the SAR procedure: 0.1, 0.3, 0.5 , 0, 0.1 Gy (test dose: 0.7 Gy), apart from samples marked with * for which doses of: 0.07, 0.13, 0.2, 0, 0.07 Gy (test dose: 0.7 Gy) were used.

[d] Uncertainties in the ages are total errors, i.e. including both random and systematic uncertainties added in quadrature.

2.4 Results and discussion

2.4.1 Degree of resetting

The OSL ages obtained for the samples are presented in Table 2.1. Based on the depositional environment we expected the easy-to-bleach OSL signal to be completely reset at the time of deposition. Results on the youngest sample from the south coast (TX02-7) confirm this hypothesis. We obtained an OSL age of 6 ± 2 years, while we infer an upper limit to the age of 6 years from maps. Additional information on the degree of bleaching is available from sample TX02-8, taken from a dune ridge formed in the past decade. OSL dating gave an age of 7 ± 1 years, again indicating a maximum offset of a few years. As the depositional environment of the other samples in this study is similar to that of these young samples, we assume that offsets due to poor bleaching amount to < 5 years for all the samples in this study. In future work we will address the complications arising from such offsets for the OSL dating of extremely young samples (< 50 years); here we conclude that such offsets are negligible on the timescale involved here.

The origin of sample TX02-23 is different from the samples discussed above. In spite of being deposited during the previous winter (the sample was taken from a very small dune formed on a path that is regularly frequented in summertime), OSL dating of this sample gave an age of 73 ± 24 years. The large offset in age and the large scatter on equivalent doses obtained (leading to a large uncertainty in the age estimate) both point to poor bleaching of this sample (Li, 1994). This anomaly arises because the source of the majority of the sand grains forming this small dune is nourishment sand dumped on the beach in this area to counteract coastal erosion. The bleaching history of this sand is unusual, in that it did not experience numerous bleaching cycles while being washed on the beach, and in that the aeolian transportation distance was probably shorter for these sand grains as the beach is only a few hundred meters wide in this area. In future work we aim to investigate this sample in depth using the equivalent-dose distribution obtained on single grains of quartz.

2.4.2 Reproducibility and precision

Five samples (TX02-28 to TX02-32) were taken from a single dune ridge to test the reproducibility of our OSL dating results. These multiple independent age estimates (Table 2.1) of a single event allow us to assess our estimates of the uncertainty on the individual measurements. The OSL ages are shown in Fig. 2.4, together with their random and total uncertainties. Random uncertainties include contribution from measurement variability in D_e and radionuclide analysis, but exclude uncertainties in e.g. water content and beta source calibration, which are the same for all measurements. Four out offive results are consistent, within one standard error, with a weighted average of 260 years; we conclude that we have no grounds for doubting our estimates of random uncertainties.

A precision of $\sim 6\%$ on individual age estimates was achieved for the five samples discussed above. For the younger samples uncertainties are slightly larger due to greater scatter in equivalent dose determinations. Precision on age estimates for these younger samples are of the same order as those reported for quartz OSL dating of young samples by Murray and Clemmensen (2001; 36 ± 5 y) and Banerjee *et al.* (2001; 2.0 ± 1.7, 12 ± 13 y) .

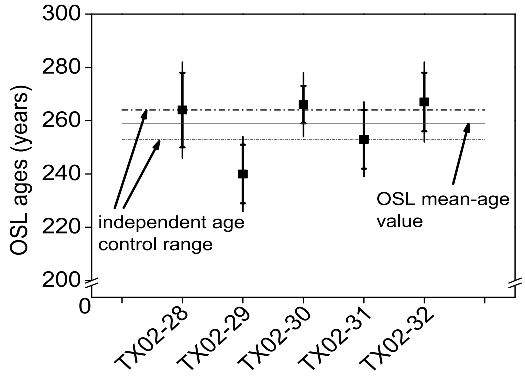

Figure 2.4: OSL ages for five samples taken from a single dune ridge. The uncertainties arising from random errors (i.e. spread in equivalent doses obtained on single-aliquots, and dose rate uncertainties) are plotted as thick error bars; the thin error bars include both random and systematic (i.e. uncertainties in γ-source calibration, internal dose rate, water content) errors. The solid horizontal line represents the OSL mean-age, while the two dashed lines show the independent-age constraints for the dune ridge.

Using the IR-OSL signal from feldspar, ages of 5 ± 30 y (Ollerhead *et al.*, 1994) and 50 ± 7 y (Van Heteren *et al.*, 2000) have been obtained on young dune sands.

2.4.3 Comparison with independent age control

OSL and independent ages are presented in Table 2.1. For all five samples (TX02-28 to TX02-32) from the dune ridge formed between AD 1738 and 1749, the OSL age is consistent with the known age range 2.4. The weighted mean OSL age obtained for the five samples suggests formation in AD 1742 ± 11, which is in excellent agreement with the known age of formation.

Fig. 2.5 presents the OSL ages plotted against the known age range, using the total uncertainties in the OSL ages (see Table 2.1). The weighted mean of the ratios of OSL to independent ages (as presented in Fig. 2.5b) is 0.90 ± 0.02 (sample TX02-23 is not included for this calculation since it is a special case as discussed in section 2.4.1). The ratio is greatly influenced by the underestimation of the OSL age for sample TX02-18, which is likely caused by reactivation of the dune after formation. If this sample is omitted from the calculations, the weighted average ratio of OSL to independent ages is 1.03 ± 0.03, i.e. indistinguishable from unity. In future work we plan to use aerial photographs to identify reactivation of dune ridges. From the comparison of OSL and independent ages we conclude that (i) our OSL ages are accurate, in that the weighted-mean ratio of OSL age to independent age is indistinguishable from unity, and (ii) the precision on our OSL ages is correctly assessed, in that for 13 out of 18 samples (72%) OSL and independent ages agree within one standard error. For all but one sample (TX02-13) they agree within two standard errors.

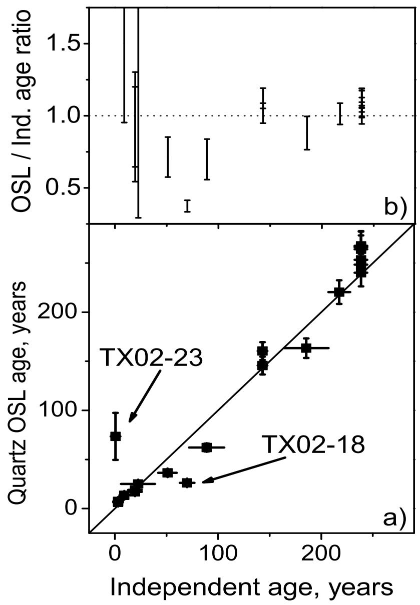

Figure 2.5: OSL ages versus independent ages (a) and OSL-independent age ratio (b).

2.5 Conclusions

We have successfully applied quartz OSL dating to a sequence of coastal dune ridges formed on the south-west coast of the island of Texel over the last 300 years. Offsets due to poor bleaching in modern samples are shown to be < 5 years, indicating that light exposure prior to deposition is sufficient to remove nearly all trapped charge from the OSL traps used for dating. Indistinguishable ages were obtained for five samples from a single dune ridge formed around AD 1743, highlighting the reproducibility of our measurements. The OSL ages obtained on 18 samples taken from eight dune ridges are entirely consistent with the age of formation of the ridges as determined from historical maps and documents. Two samples gave unexpected results, but both are explicable from a consideration of their deposition environment. We have demonstrated that accurate and precise ages are obtained for these deposits, despite their low values and very weak natural OSL signals. Our study highlights the potential of using quartz OSL dating as a chronometric tool for reconstructing coastal evolution and for providing information essential for proper coastal management.

Acknowledgements

We would like to thank all the Risø-National Laboratories stafffor the possibility of using the readers and for the useful advices kindly given. Similar thanks to all the PhDs, post-docs and students for the stimulating conversations even during the cigarette break. Thanks are extended to J. van Groenigen and M.C. Stoepker (Dutch National Forestry Service) for permission to collect samples in the study area, H.J.A. Berendsen (Utrecht University) for providing a GPS, and W. de Wilde and H. Zwaan (TNO-NITG) for providing coring devices.

Bibliography

Banerjee, D, Murray, AS and Foster, IDL (2001). Scilly Isles, UK: optical dating of a possible tsunami deposit from the 1755 Lisbon earthquake. *Quaternary Science Reviews*, 20, 715–718.

Bøtter-Jensen, L and Murray, AS (1999). Developments in optically stimulated luminescence techniques for dating and retrospective dosimetry. *Radiation Protection Dosimetry*, 84, 307–315.

Li, SH (1994). Optical dating: insufficiently bleached sediments. *Radiation Measurements*, 23, 563–567.

Mejdahl, V (1979). Thermoluminescence dating: beta dose attenuation in quartz grains. *Archaeometry*, 21, 61–72.

Murray, AS and Clemmensen, LB (2001). Luminescence dating of Holocene aeolian sand movement, Thy, Denmark. *Quaternary Science Reviews*, 20, 751–754.

Murray, AS, Marten, R, Johnston, A and Marten, P (1987). Analysis for naturally occurring radionuclides at environmental concentrations by gamma spectrometry. *Journal of Radioanalytical Nuclear Chemistry*, 115, 263–288.

Murray, AS and Olley, JM (2002). Precision and accuracy in the optically stimulated luminescence dating of sedimentary quartz: a status review. *Geochronometria*, 21, 1–16.

Murray, AS and Wintle, AG (2000). Luminescence dating of quartz using an improved single-aliquot regenerative-dose protocol. *Radiation Measurements*, 32, 57–73.

Ollerhead, J, Huntley, DJ and Berger, GW (1994). Luminescence dating of sediments from Buctouche Spit, New Brunswick. *Canadian Journal of Earth Sciences*, 18, 419–432.

Olley, JM, Murray, AS and Roberts, RG (1996). The effects of disequilibria in the uranium and thorium decay chains on burial dose rates in fluvial sediments. *Quaternary Science Reviews*, 15, 751–760.

Prescott, JR and Hutton, JT (1994). Cosmic ray contributions to dose rates for luminescence and ESR dating: large depths and long-term time variations. *Radiation Measurements*, 23, 497–500.

Rhodes, EJ (2000). Observations of thermal transfer OSL signals in glacigenic quartz. *Radiation Measurements*, 32, 595–602.

Sha, LP (1990). Sedimentological studies of the ebb-tidal deltas along the West Frisian Islands, the Netherlands. *Geologica Ultraectina*, 64, 159.

Stokes, S, Bray, HE and Blum, MD (2001). Optical resetting in large drainage basins: tests of zeroing assumptions using single-aliquot procedures. *Quaternary Science Reviews*, 20, 879–885.

Ter Wee, MW (1962). The Saalian Glaciation in the Netherlands. *Mededelingen Geologische Stichting, N.S.*, 15, 57–76.

Van Heteren, S, Huntley, DJ, van de Plassche, O and Lubberts, RK (2000). Optical dating of dune sand for the study of sea-level change. *Geology*, 28, 411–414.

Wallinga, J, Duller, GAT, Murray, AS and Törnqvist, TE (2000a). Testing optically stimulated luminescence dating of sand-sized quartz and feldspar from fluvial deposits. *Radiation Measurements*, 32, 691–695.

Wallinga, J, Murray, AS and Duller, GAT (2000b). Underestimation of equivalent dose in single-aliquot optical dating of feldspars caused by preheating. *Earth and Planetary Science Letters*, 193, 617–630.

Wintle, AG and Murray, AS (2000). Quartz OSL: Effects of thermal treatment and their relevance to laboratory dating procedures. *Radiation Measurements*, 32, 387–400.

Zimmerman, DW (1971). Thermoluminescent dating using fine grains from pottery. *Archaeometry*, 13, 29–52.

Chapter 3

Optical dating using single grains of quartz - A review

To be submitted

M. Ballarini[a] and G.A.T. Duller[b]

[a]*Netherlands Centre for Luminescence Dating, Delft University of Technology, Faculty of Applied Sciences, Mekelweg 15, NL-2629 JB Delft, The Netherlands*

[b]*Institute of Geography and Earth Sciences, University of Wales, Aberystwyth, Ceredigion SY23 3DB, UK.*

Abstract

Luminescence dating has been demonstrated to be an invaluable tool for obtaining absolute age estimates in Quaternary Geology. Within this method, the assumption is that the light-sensitive signal of the grains to be dated has been zeroed by sunlight exposure. Such a bleaching process occurs during erosion, transport and sedimentation before the grains are buried. Insufficient exposure to daylight may lead to age overestimation. In recent years, the development of new instrumentation and procedures made it possible to investigate the luminescence signal from individual mineral grains. The major advantage of this method is that populations of differently bleached grains within a sample can be recognized. In this paper, the first attempts of investigating heterogeneously bleached materials with the modern single-grain method are reviewed and results are discussed.

3.1 Introduction

Optically stimulated luminescence (OSL) dating techniques are widely used in Quaternary research as an important tool for obtaining absolute age estimates for sedimentary deposits. These methods provide a means of determining burial ages for materials that have been exposed to sunlight before deposition (Aitken, 1998; Huntley *et al.*, 1985). In order to determine an age of mineral samples by means of luminescence dating, two quantities have to be measured. These are the amount of ionizing radiation received by a sample since burial (palaeodose) and the rate at which this dose was absorbed (dose rate). The final age is given by the ratio of the two:

$$Age(a) = \frac{equivalent\ dose\ (Gy)}{dose\ rate\ (Gy/a)}$$

What is measured through luminescence methods is an estimate of the palaeodose (equivalent dose, D_e).

OSL dating is applicable to sedimentary deposits for which the light-sensitive signal has been removed (zeroed) by sunlight during erosion and transportation. Since the OSL signal is very quickly zeroed by light exposure (much faster than the thermoluminescence (TL) signal previously used for dating), this allows dating of materials that have been exposed to light only for a short time, as may happen in fluvial or marine environments. However, although the signal is reset rapidly, this does not imply that it is always fully reset before deposition. Light exposure may be too short or too weak, depending on the environmental and weather conditions. If part or all of the grains are not completely zeroed before burial, then the effective dose (known as the equivalent dose, D_e) absorbed by such grains is the sum of a certain pre-depositional dose and that acquired after deposition. Depending on the percentage of grains that have been incompletely reset and on the extent of bleaching experienced, different scenarios of grain mixture are possible, with consequences for correct estimation of the burial dose. In the ideal case, all the grains have been fully bleached - we refer to such a sample as "well bleached" sample. In a situation where a sample has been exposed to a very limited amount of light, but where all the grains have been equally bleached to the same percentage of their pre-existing trapped charge population, the kind of bleaching is called "partial bleaching" (Duller, 1994b). This type of partial resetting is very unusual in nature, where it is more likely that any given deposit will contain grains which have been bleached to different extents (heterogeneous bleaching). If there is a small proportion of grains which have had 100% of their signal bleached then that is an incompletely bleached sample, but one which could be feasibly dated. If a sample contains a mixture of grains which had been reset to differing amounts, but none of which had had their entire luminescence signal removed, then only a maximum age can be obtained.

Before Duller (1991), dose measurements were made using a large number of sub samples (aliquots) with the assumption that the luminescence characteristics were identical for all the aliquots. Methods based on such an assumption, known as multiple aliquot methods, can be used on homogenously bleached samples in which indeed all the grains show similar luminescence features. In practice, samples consist of grains that were bleached to different extents prior deposition, and would produce highly scattered ages if the multiple aliquot method is used (Huntley and Berger, 1995). An overview of such methods can be found in Wallinga (2002a).

Development of new methods within the last 15 years (Duller, 1991; 1994a; Murray *et al.*, 1995; 1997; Murray and Wintle, 2000) made it feasible to measure the palaeodose from a single aliquot. The best estimation of the palaeodose received by a sample is then calculated as the average of the equivalent doses measured on several aliquots. If all the grains of a deposit have been completely bleached before burial, then the effective absorbed dose is entirely given by the subsequent post-depositional dose received by the grains. In such a case, aliquots randomly selected within a sample would contain grains that have been equally zeroed and thus give similar D_e values. Equivalent doses calculated in this way will be symmetrically spread around a central value, following a tight Gaussian distribution. The best estimate of the "true" palaeodose is then given by the mean calculated from this distribution. Many authors could obtain consistent D_e estimation simply by taking the mean of their distributions from aeolian and coastal dune deposits (Ballarini *et al.*, 2003; Duller, 1996; Huntley *et al.*, 1985; Ollerhead *et al.*, 1994; Stokes, 1992).

On the other hand, if grains have been differently zeroed before deposition, aliquots would contain a mixture of well- and poorly-bleached grains. Since the proportion of such a mixture of grains is likely to be different between aliquots, a non-Gaussian distribution of D_e values will be produced rather than a number of equivalent doses consistent with one another. This effect is more evident when small aliquots are used (Li, 1994). Several methods have been proposed in the literature to obtain the most meaningful palaeodose estimate from such distributions, but which one of those (if any) represents the best approach to the problem has still to be proved.

The most straightforward method would be to calculate the mean of the observed D_e values. However, this simple method can be only applied to normal distributions and is not suitable for asymmetric or multiple-modal distributions. Usually, when the palaeodose is estimated by taking the mean value from such distributions, an overestimation will result. An example of equivalent dose overestimation is given by Duller *et al.* (1995), who showed that a glacio-fluvial deposit from Scotland yielded an OSL age that was at least five times older than independent age estimates. Murray *et al.* (1995) measured equivalent dose distributions from Australian fluvial sediments of known age. They all were clearly asymmetric and positively skewed. The arithmetic mean resulted in the overestimation of the true age in all the cases but one. However, in this last case the three largest D_e values were discarded.

It must be pointed out that poor-bleaching is not the only cause for spread in D_es determined within the same sample. Murray and Roberts (1997) ascribed distributions of equivalent doses to heterogeneity in the beta microdosimetry. In this scenario, grains of a sample received after deposition a non-uniform beta dose from the surroundings. This has the consequence of inducing different D_e values for different grains. An additional element that may cause spread in paleodoses is the post-depositional modification of buried deposits. Mixing of grains with different ages or turbation as well as reworking of the soil may produce inclusions of grains belonging to different environments with different beaching histories (e.g. Heimsath *et al.*, 2002). This will result in a mixed population of grains carrying different equivalent doses. In such a case, D_e distributions with multiple modes may be produced.

The challenge of dating mixed-population materials is to distinguish grains that have experienced bleaching to different degrees and the selection of only those that are representative of the depositional event of interest. It has been demonstrated that this kind of investigation is more significant when small aliquots and ultimately individual grains are used. This paper is a review starting from the first attempts at recognizing partially bleached materials using small aliquots to the most recent analysis of single grain distributions.

3.2 Single Aliquot methods

Results from small aliquots

Usually, in optical dating procedures small samples (aliquots or sub-samples) are taken as representatives of the whole deposit that has to be dated. A typical sample disk contains as much as ~5 mg of material, which amounts to ~1000 grains when grains of 150 μm in diameter are used. When such an aliquot is measured, the total OSL signal is the sum of the luminescence contribution of all the grains contained in the aliquot. Olley *et al.* (1999); Wallinga (2002b) demonstrated that small aliquots are more suitable for heterogeneous bleaching investigations than large ones. In particular, they showed that in a mixture of grains the probability of selecting only well-bleached grains decreases as the size of the aliquot increases (i.e. the number of grains loaded onto an aliquot increase). Fig. 3.1 shows the probability of selecting only well bleached grains in aliquots containing a mixture of well and poorly bleached grains as a function of the fraction of "contaminating" grains in a sample. For example, if a sample has a concentration of unbleached grains of 7%, the probability of selecting a sub-sample (aliquot) made up of 60 well-bleached grains only is practically zero. It is shown that by decreasing the number of grains per aliquot, the probability of selecting only well bleached grains from a mixed sample increases. In this study, all the grains were supposed to give a measurable luminescence response, which is however not true in reality.

One of the first attempts at recognizing poorly-bleached materials aimed at finding a pattern between the D_e values calculated for different aliquots and the respective OSL signal intensities (Li, 1994; Stokes *et al.*, 2001). In this case, D_es of aliquots plotted against their respective OSL intensities should display along a straight line parallel to the x-axis, meaning that the equivalent dose is independent of the signal intensity. If larger D_e values are obtained for aliquots with larger OSL signal intensities, then this is interpreted as poor-bleaching (Duller, 1994b; Li, 1994). Examples of identification of poorly-bleached materials using small aliquots containing 100 grains are presented in Fig. 3.2. The difference in palaeodoses between small aliquots containing ∼100 grains is accentuated when compared to larger aliquots. Plots such the one showed in Fig. 3.2 are used as a visual indication for poor bleaching. However, it has been demonstrated that this method is reliable only for homogeneously bleached materials, which is quite an exceptional scenario for natural samples (Wallinga, 2002b).

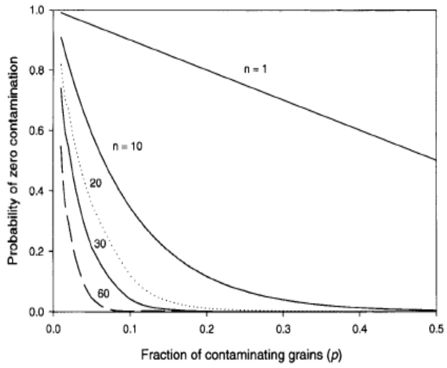

Figure 3.1: Mathematical model that predicts the probability of selecting only well bleached grains from aliquots consisting of n grains (n=1 to 60). This is shown as a function of the proportion of insufficiently bleached grains in a sample. It is evident that by decreasing the number of grains per aliquot, there is an increase in the probability of selecting only well bleached grains from a mixed sample (Olley *et al.*, 1999). In this model it is assumed that all the grains contribute to the total OSL signal.

The work of Li (1994) and Duller (1994b) was undertaken using luminescence measurements on potassium-rich feldspars. The use of feldspars for luminescence dating may be problematic because of difficulties associated with signal instability known as anomalous fading (Wintle, 1973), and thus quartz is more commonly used. However, quartz grains show great variation in their luminescence sensitivity, which means that the OSL response to the same laboratory dose is grain-dependent and may greatly vary. This issue will be discussed later in more detail.

Wallinga (2002b) studied the scatter in equivalent doses as a function of the number of grains contained in one aliquot. His computer simulations indicate that a correlation of natural OSL intensities versus equivalent dose should be expected for poorly-bleached grains (Li, 1994) only when the luminescence sensitivity of the grains is relatively uniform. The absence of such a correlation does not necessarily indicate that the sample was well bleached. He also pointed out that if skewed dose distributions are an indication of poor bleaching, non-skewed distributions indicate either that the sample was well bleached or that the sample contains a large proportion of insufficiently bleached grains. He concludes that

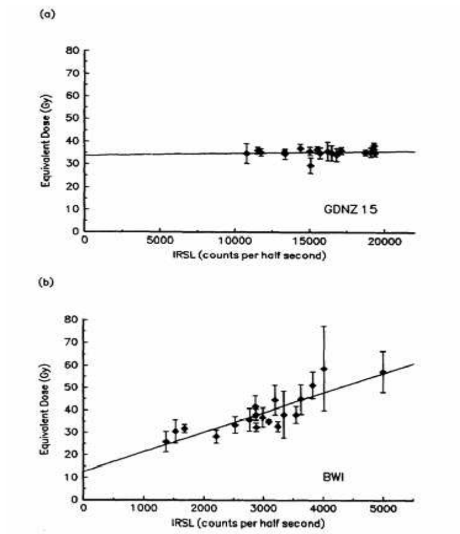

Figure 3.2: Palaeodoses of glaciofluvial samples from Scotland plotted against the intensity of the natural signal (Duller, 1994b). D_es from well-bleached samples are independent of the signal intensity and plot on a straight line (a), while poorly-bleached samples plot on a positively sloped line. The single-aliquot additive dose protocol was applied on feldspar grains to obtain the data.

"the best method to check whether the equivalent dose of a sample might be overestimated as a consequence of poor-bleaching is to use small aliquots (ultimately consisting of a single grain)".

Another way of detecting poorly-bleached materials is to inspect the D_e distribution produced by the aliquots. A tight and symmetric distribution reflects a deposit not (or only slightly) affected by poor bleaching or heterogeneous dosimetry. Skewed distributions indicate insufficient bleaching or/and heterogeneous dosimetry. Fig. 3.3 shows dose distributions obtained from measurements of fluvial and aeolian samples using small aliquots, containing $\sim 60 - 100$ grains per aliquot Olley *et al.* (1998). Equivalent dose distributions from fluvial deposits are skewed and the range of palaeodoses is wider. For aeolian samples the degree of bleaching at deposition is generally higher, so that palaeodoses estimated from different aliquots are similar and the spread is low. Authors suggested that for this fluvial sample the best estimate of the palaeodose is given by taking the last 5% of the aliquots with the lowest equivalent dose. This can be justified with the assumption that grains with the lowest D_e are those that have been best bleached and thus may be expected to give the closest estimation of the "true" palaeodose. This is true when grains with the lowest palaeodose estimates are representative of the depositional event that has to be dated. However, if younger grains (i.e. grains with lower D_es) may have intruded from a different environment, maybe due to bioturbation, or heterogeneous micro dosimetry occurred, then this assumption is not valid. Thus, taking the average of the lowest 5% aliquots will result in underestimation of the palaeodose. The authors do not justify the use of the lowest 5% level, other than noting that it worked for their (limited) number of samples in their study.

This method, besides being arbitrary, is also site dependent.

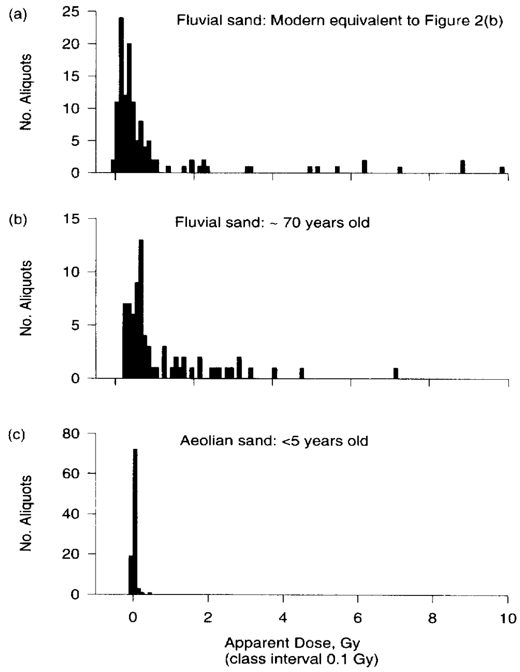

Figure 3.3: Palaeodoses obtained from 116, 78 and 96 small aliquots, (a), (b) and (c) respectively. Broader and more skewed distributions are observed for the two fluvial samples, which reflect that they were insufficiently bleached before deposition. For the aeolian sample the degree of bleaching before burial was higher and results in a tight distribution (Olley *et al.*, 1998).

A similar but more rigorous approach to determine palaeodoses from insufficiently bleached materials was suggested by Lepper *et al.* (2000) and Lepper and McKeever (2002). They state that any distribution of equivalent doses is the sum of two distributions, one arising from natural sedimentary process and the other one from experimental errors. After removing uncertainties introduced during measurements, they applied the "leading edge" method for estimating the true palaeodose related to the last depositional event. This leading edge method consists of fitting a Gaussian to the leading edge (largest positive slope) of the deconvolved distribution to determine the palaeodose D_e (Fig. 3.4). The implicit assumption, common to all methods based on distribution analysis, is that in a skewed distribution of doses the best estimate for the palaeodose is to be sought in the lower dose part. Stratigraphically consistent results were found with this approach but they were not validated by any independent age control.

Fuchs and Lang (2001) and Fuchs and Wagner (2003) proposed a method for recognizing insufficiently bleached samples based on the relative error on the D_e. Fuchs and Wagner (2003) measured the equivalent doses of colluvial and colluvial/torrential samples on aliquots containing different numbers of grains. The statistical parameter ν (defined as the percentage standard error) indicates the precision with which D_e values from different ali-

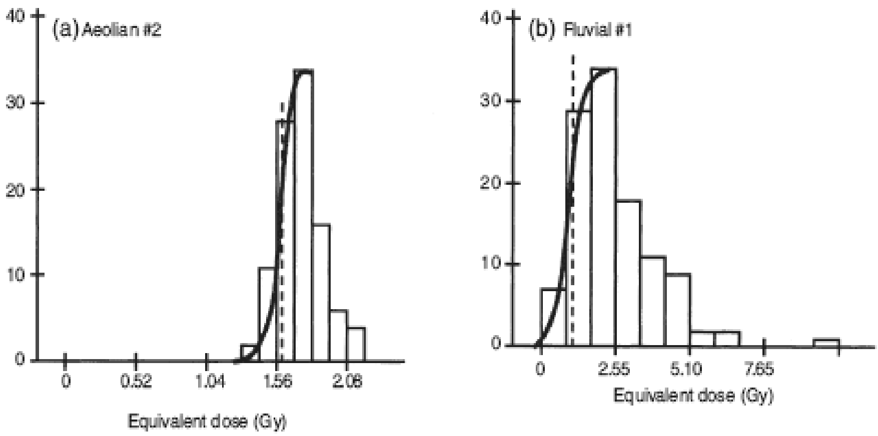

Figure 3.4: Examples of dose distributions from (a) an aeolian dune sand and (b) a sand sample isolated from a floodplain deposit. The true dose is determined by projecting the inflection point of the Gaussian distribution fitted to the leading edge calculated for the original dose distribution (Lepper and McKeever, 2002).

quots were measured and was used to judge whether samples were well- or poorly-bleached. They proposed that aliquots with relative standard errors greater than 10% are likely to consist of poorly bleached grains. The threshold of 10% is justified by the fact that even well-bleached and homogeneously dosed samples show a scatter $< 8\%$, while insufficiently bleached samples show values of ν greater than 10%. They also suggest that this method performs better with aliquots composed of 200-500 grains, in contrast to Olley *et al.* (1998) who suggest the use of aliquots containing 60-100 grains to identify insufficient bleaching.

Zhang *et al.* (2003) used a different approach based on the difference in scatter between the sensitivity-corrected natural and the first regenerated OSL signals during a SAR procedure. Their assumption is that these two kinds of scatter should be similar. If they are not, then the difference is due to poor bleaching before deposition. The relative standard deviation on the first regenerated OSL signals is calculated (RSD_1). The aliquots are then ranked from higher to lower values of their natural OSL and the corresponding RSD compared to the RSD_1. Aliquots with RSDs lower than RSD_1 were retained for D_e calculation (a simple average is used), while the others are discarded. OSL ages calculated with this method were consistent with a single independent archaeological age.

Another method that makes use of the comparison between internal and external variance of a dose distribution was proposed by Spencer *et al.* (2003). If doses are normally distributed, it is expected that the F-ratio of the variance in the D_e distribution and the variance from uncertainties in D_e measurements will approach unity. F-values are calculated for the first, first and second, and the whole distribution over n observations as shown below in eq. 3.1:

$$F_1 = \frac{\sigma^2_{D_{e1}}}{\Delta^2_{D_{e1}}}, \quad F_{\{1,2\}} = \frac{\sigma^2_{\{D_{e1}D_{e2}\}}}{\Delta^2_{D_{e1}} + \Delta^2_{D_{e2}}}, \ldots, \quad F_{total} = \frac{\sigma^2_{D_e\ total}}{\sum_{i=1}^{n} \Delta^2_{D_{ei}}} \tag{3.1}$$

If this method is applied to a mixed distribution of doses, one would expect high F-values, and F-values near unity for single-dose distributions. Individual dose estimated to be used for D_e calculations are those that lie in a plateau where F-values are plotted versus D_es. This method aims at determining the leading edge of a dose distribution and is similar to that proposed by Lepper *et al.* (2000) and Lepper and McKeever (2002). Authors "cautiously suggest that F-ratios at or approaching unity may indicate the part of a D_e distribution dominated by a single dose component".

3.3 Luminescence measurements of individual grains

3.3.1 Initial results from individual sand-sized grains

The methods proposed in the preceding paragraph were aimed at determining the best estimation of the palaeodose in the presence of a mixed population of grains. The crucial point is the ability to separate grains that have been well bleached from those that have poorly bleached. This is best achieved when small aliquots are taken and ultimately measurements on individual grains are carried out.

A review of the first attempts at dating individual grains is given in Duller and Murray (2000). Here we say only that both single grain (SG) measurements on feldspars (Lamothe *et al.*, 1994) and on quartz (Murray and Roberts, 1997) gave broad and asymmetric distributions, in the first case overestimating the true palaeodose by 700% to 70%. Roberts *et al.* (1999) measured a variety of dose distributions from an important archaeological site (Jinmium rock shelter in north-west Australia), the results reflecting the mixed nature of grains of these samples. In the companion paper (Galbraith *et al.*, 1999) theoretical models were developed for interpretation of dose distributions from single grains. This will be discussed later in this review.

3.3.2 Single grain facilities

The single grain measurements cited in the previous section were performed using a conventional TL/OSL Risø reader where optical stimulation was used either a filtered halogen lamp or light emitting diodes, delivering a few tens of milliwatts per square centimetre (Lamothe *et al.*, 1994; Murray and Roberts, 1997). The advantage is that conventional equipment and protocols can be used. The disadvantage is that each mineral grain has to be manually placed onto a stainless-steel disk and then measured. This procedure is complex and time consuming. Other approaches to single grain measurements are reviewed in Duller and Murray (2000).

More recently, Bøtter-Jensen *et al.* (2000) developed an attachment that was specifically designed for single grain measurements that can be mounted on a conventional Risø TL/OSL reader. This new feature allows practical and quick measurements of a large number of individual grains. The new system (Fig. 3.5) is based on a 10 mW Nd:YVO_4 solid-state diode-pumped laser (532 nm) delivering 50 Wcm^{-2} to a spot of about 20 μm in diameter. Mineral grains are mounted onto a special aluminum disk with 100 holes drilled in a ten by ten grid (Fig. 3.6) with each hole being 300 μm wide and 300 μm deep. It should be noted that more than a single grain can find a place in one hole if the grain dimensions are too small (Feathers, 2003). In practice, using grains that are dry sieved between 180-210 μm results in most holes containing a single grain.

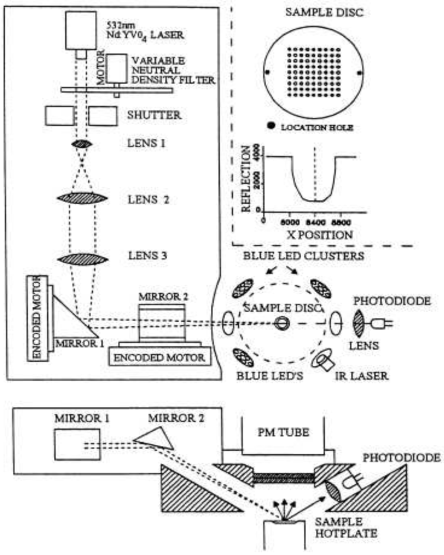

Figure 3.5: Schematic diagram of the single grain system. Details are given in Bøtter-Jensen *et al.* (2000).

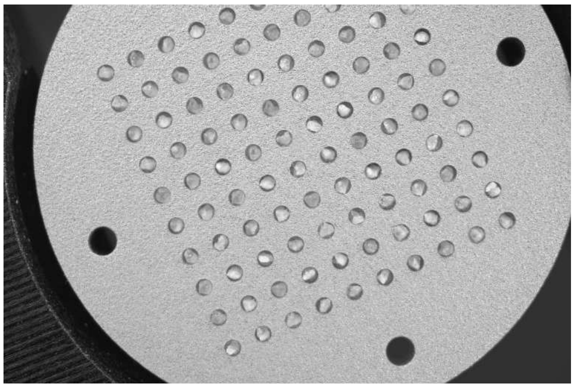

Figure 3.6: Single-grain disk (photograph kindly provided by the Risø National Laboratories).

The most important requirement for a single grain system is the capability of repeating accurate measurements on the same grain. Using a Risø single grain laser luminescence system Duller *et al.* (1999a) were able to recover a known beta dose administered to Al_2O_3:C grains with an uncertainty of 6%. The same experiment was repeated using quartz grains extracted from a modern dune sand in Australia. Of the 320 grains measured, only 80 gave a detectable luminescence signal to allow OSL analysis. The mean value of the absorbed dose was consistent with the administered dose, but the uncertainty was double that calculated for the Al_2O_3:C grains. The authors stated that "this increased uncertainty is thought to relate primarily to counting statistics", as natural quartz is far less bright than Al_2O_3:C. Truscott *et al.* (2000) investigated in more detail the reproducibility of OSL measurements on individual grains using a single grain Risø TL/OSL reader. They found that the laser beam could be repositioned on the same grain with accuracy better than 30 μm and the reproducibility of measurements using both artificial and natural material was $\sim 3.5\%$. Thomsen *et al.* (2005) have repeated this measurement using the latest version of the single grain system. They also took a more sophisticated approach than Truscott *et al.* (2000), removing the impact of counting statistics, and compensating explicitly for changes in sensitivity. Thomsen *et al.* (2005) made repeated measurements of the OSL signal from annealed quartz following irradiation with the same dose, and calculated that the scatter on each OSL measurement was $2.5 \pm 0.3\%$. A similar value was also derived by Jacobs *et al.* (2006).

3.3.3 Procedures for single grain measurements

The single aliquot regenerative dose (SAR) protocol proposed by Murray and Wintle (2000) for quartz samples is the most widely used method for determining equivalent doses from individual grains. This protocol allowed a reliable measurement of D_e on a single aliquot, while earlier procedures required many tens of sub-samples, or aliquots, from which the dose received during burial could be estimated. These last methods rely on the assumption that all the aliquots needed to measure a single equivalent dose have the same luminescence characteristics. As mentioned earlier in this review, this is true only for perfectly bleached samples and homogeneous dosimetry after deposition. If not, D_e values measured with multiple aliquot methods will be inaccurate and imprecise. The SAR protocol, on the other hand, bypasses this problem because in principle only one aliquot is required to estimate D_e. A typical SAR procedure used for OSL measurements on quartz aliquots and, with minor modifications, of individual quartz grains, is summarized in Table 3.1. A test dose D_t is administered after the signal of the natural dose and each of the regenerative cycles is measured. The luminescence response to this test dose (T_i) is used to monitor any sensitivity change that occurred during a measurement. This is caused by the heating and irradiation treatment to which each aliquot is subjected before optical stimulation. Three OSL responses to as many laboratory doses ("regenerative" doses, $D_i, i = 1, 2, 3$) are needed to build a dose-response curve, from which the palaeodose can be estimated. These are usually known as R_i (given by the ratio of L_i and T_i, Table 3.1). In order to test the reliability of the protocol, the OSL response of the quartz is measured at the end of the sequence when no regenerative dose is given (R_4) and is expected to be zero. This check is known as the recuperation test. Thermal transfer (see below) is very likely to be the cause of high recuperation of an OSL signal that is not produced by a laboratory dose. The ability of the protocol to re-measure the same dose is tested in the last step of the protocol. The first of the regenerative doses

Table 3.1: Typical SAR procedure (Murray and Wintle, 2000)

Step	Treatment[a]	Observed[d]
1	Give dose, D_i	-
2	Preheat[b] (160-300°C for 10 s)	-
3	Stimulate[c] for 100 s at 125°C	L_i
4	Give test dose, D_t	-
5	Heat[b] to 160°C	-
6	Stimulate for 100 s at 125°C	T_i
7	Return to 1	-

[a] For the natural sample $i = 0$, and $D_0 = 0$ Gy.

[b] Aliquot cooled to $< 60°$ C after heating. In step 5, the TL signal from the test dose can be observed, but it is not made use of in routine applications.

[c] The stimulation time is dependent on the stimulation light intensity.

[d] L_i and T_i are derived from the initial OSL signal (0.3 or 0.8 s) minus a background estimated from the last part of the stimulation curve.

(D_1) is administered again and the OSL signal measured (R_5). If the ratio R_5/R_1 (known as recycling ratio) is close to the unity, then the protocol gives reproducible results on that aliquot and sensitivity changes are successfully corrected for.

When dating extremely young samples, the SAR protocol as explained above may be impractical. If the expected doses to be measured are too small, then regenerative doses $D_i > D_e$ have to be administered in order to obtain measurable OSL responses. Ballarini *et al.* (submitted) used a single regenerative dose of 5 Gy for dating young aeolian samples with an expected equivalent dose of ~ 0.25 Gy. These authors have shown that the use of such a single regenerative dose is feasible and that equivalent doses are not significantly affected by interpolation methods rather than by using three-point regeneration curves.

The SAR procedure is rather simple, although parameters like pre-heat temperature, test dose and stimulation time can be customized in order to optimize the sequence for a particular sample. For example, a pre-heat-plateau test should be carried out to select the correct pre-heat (PH) temperature to be used within the procedure for D_e determination. In this test, equivalent doses are plotted as a function of the PH temperatures used (usually from 160 to 300°C). The aim is to select a PH temperature for which the transfer of charge induced by heating (step 2 and 5 in Table 3.1) from light-insensitive to light-sensitive traps remains negligible. This effect is called thermal transfer (TT) and leads to measurements of non-zero OSL signals even in the absence of administered doses (Murray and Wintle, 2000; Rhodes, 2000). This thermally induced charge transfer can seriously affect dating of young materials, where the contribution to the apparent dose due to thermal transfer is of the same order of the burial dose.

Jain *et al.* (2002; 2004) have studied the thermal transfer seen in single quartz grains extracted from unheated poorly-bleached mortar samples. A total of 8400 grains ranging in size from 212 to 250 μm were first bleached by green laser stimulation at 125°C, preheated and finally the OSL response measured. Only 48 grains were sufficiently bright to be studied. This measurement was repeated for a range of pre-heat temperatures and Jain *et al.* (2004) found that different D_e distributions as a function of the thermal transfer (measured in Gy) are observed for a range of preheat temperatures (Fig. 3.7). Distributions originating with a preheat temperature of 180°C are skewed but relatively narrow. At this temperature the proportion of grains that contribute to TT is minimized. Broader distributions are observed at higher temperatures (280°C). Authors noticed that grains whose test dose response signal was small gave the major contribution to the total TT (e.g. for the data taken after a 300°C preheat; Fig. 3.8). No correlation between TT and the extent of OSL bleaching of poorly-bleached light-insensitive traps was found. The dose contribution due to thermal transfer from the test dose was also studied and found to be insignificant for a large range of temperatures (Jain *et al.*, 2002).

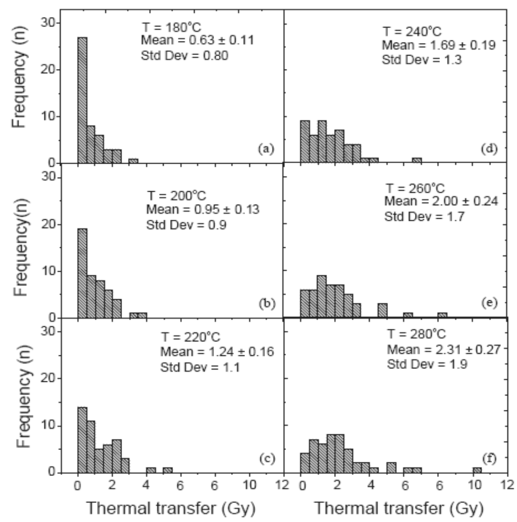

Figure 3.7: Histograms of thermal transfer from the same set of single grains. Only those grains that passed preliminary checks (48 out of 8400, i.e. 0.57%) are shown. These checks consisted of a) relative uncertainty on the test dose and b) test dose OSL signal > 30 counts/0.1 s (Jain *et al.*, 2004).

From these experiments it is concluded that the TT contribution to the measured equivalent dose is minimized at low pre-heat temperatures. The optimal temperature for preheating should be investigated for each sample used with a SAR protocol. It should be pointed out that TT investigations on single grains differ from those on aliquots with multiple grains. For the latter, the assumption is that all the aliquots taken from a sample are representative of that sample. In other words, they all have the same luminescence characteristics (which is not necessarily true). A few aliquots are then used for TT analysis as explained above. When

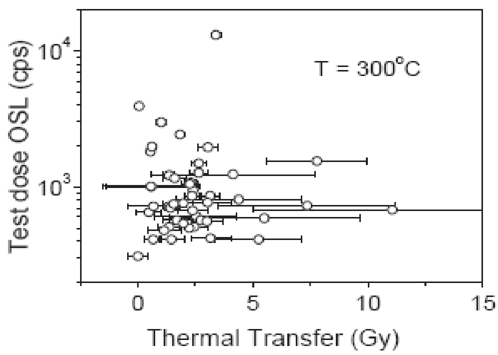

Figure 3.8: The first test dose OSL response is plotted against the cumulative thermal transfer at 300°C for a set of single grains. Large thermal transfer values (converted to dose values, Gy) are associated to grains with low sensitivity (Jain *et al.*, 2004).

the optimal PH temperature is detected, other aliquots, which make use of that temperature for preheating, are used to estimate the equivalent dose. In single grain measurements this assumption is no longer valid. On an individual basis each grain is different from the other, with different intrinsic characteristics that result in different OSL responses to external stimulation like heating or illumination. Thus, the optimal PH temperature estimated from a set of grains, as presented in Fig. 3.7, is not exactly representative for each grain used for D_e determination. Adamiec (2000); McFee (1995); Miallier *et al.* (1985) have clearly shown that thermoluminescence characteristics greatly vary between single grains within a deposit. Hashimoto *et al.* (1996) measured the thermoluminescence emitted by quartz slices cut from single quartz crystals. They found that there is a variation in luminescence even within the same crystal. On the other hand, since a pre-heat test performed on one grain would erase any natural OSL signal, a D_e can not be measured on the same grain where the TT test was carried out. Thus, although not formally correct, this is the only applicable method for TT analysis on single grains.

3.3.4 Single grain decay curves

Bailey *et al.* (1997), Bulur *et al.* (2000) and McKeever (2001) showed that OSL decay curves from quartz consist of different components. Each component originates from different centers in the crystal and contributes in a different proportion to the total signal. Three components have been distinguished in the majority of the grains, and have been termed the fast, the medium and the slow component (Bailey *et al.*, 1997). Electrons that are easily and quickly detrapped during stimulation will produce a steep exponential decay curve dominated by the fast component. Hard-to-bleach traps will give rise to a slower exponential decay curve. The measured OSL decay of a grain is the sum of two or more components and can be fitted with a number of exponential decays that equals the number of components. Adamiec (2000) studied the relationship between TL peaks and OSL decay curves in single grains. He found that grains extracted from the same sample display a wide range of glow and decay curves, and no relationship was found between the different components of a decay curve. Grains that have a fast component (initial signal) can have a dim slow component (late light) and vice versa. In Fig. 3.9 a variety of decay curves from single grains of sensitized quartz are shown.

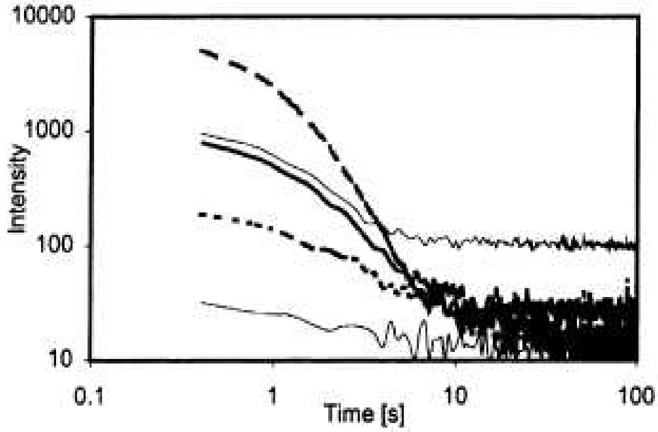

Figure 3.9: Decay curves (log-log scale) from single quartz grains sensitized with five cycles of heating at 500°C and 20 Gy irradiation. Shape and background level of the curves differ from grain to grain (Adamiec, 2000).

Decay curves from single grains are usually of low intensity, unless they were extracted from old deposits or given a high regenerative dose. In Fig. 3.10 the natural OSL decay curves of two grains from a coastal-dune sample are shown. This dune is estimated to be 265 ± 18 years old (Ballarini *et al.*, 2003).

3.3.5 Signal intensity

Analysis of a large number of grains has shown that the luminescence response to a fixed laboratory dose greatly varies from grain to grain. Only a small percentage of grains give rise to a signal when optically stimulated, while the rest of the grains show very little luminescence response or not at all. Duller *et al.* (2000) proposed a method to display the proportion of grains that actually contribute to the total OSL signal (light sum expressed as a percentage) measured from a number of grains (Fig. 3.11). From the two upper curves it can be seen that less than 5% of the grains produce 90% of the total OSL signal. The proportion of bright grains that give the same amount of luminescence increases to 40-45% for the other samples. An ideal sample, whose grains all emit the same luminescence signal, would plot as a diagonal line from the origin. This luminescence variability can be ascribed to the intrinsic properties of each grain and has some implications for luminescence dating. Firstly, it affects the number of grains that can be used for equivalent dose estimation. Grains whose signal is not well distinguishable from the background noise ("dim" grains) should be discarded. Secondly, where a sample contains only few bright grains, multiple grain analysis will be dominated by the characteristics of these very few grains. In contrast,

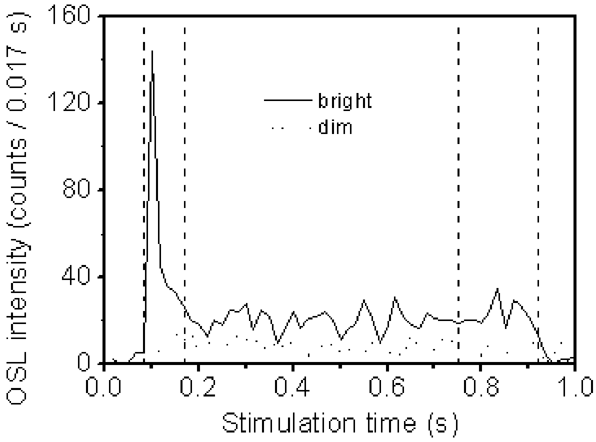

Figure 3.10: Decay curves from two untreated natural quartz grains from Texel (The Netherlands) with an expected burial dose of 260 ± 10 mGy.

multiple grain analysis on samples with a larger proportion of bright grains will mask any grain-to-grain variability (Duller *et al.*, 2000; Wallinga, 2002b).

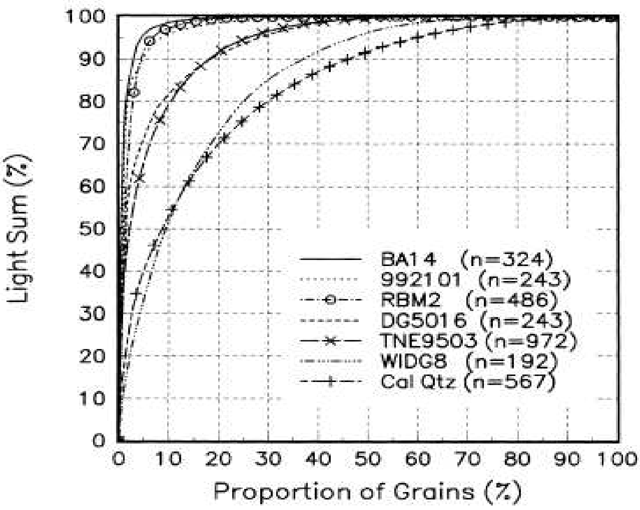

Figure 3.11: The percentage light sum from single grains is plotted against the proportion of grains that contribute to the total OSL signal. Samples with grains evenly contributing to the total light sum would produce a diagonal line. In reality, a small percentage of grains in one aliquot is responsible for the majority of the total OSL signal. The sensitized quartz sample (bottom curve) lies closest to the ideal diagonal line (Duller *et al.*, 2000).

3.3.6 Rejection criteria

Rejection criteria are needed to select only grains that can meaningfully characterize the sample they represent. Grains with poor sensitivity from which a reproducible OSL signal cannot be measured should be discarded, as well as non-quartz grains and grains that show anomalous behavior. The more severe the rejection criteria the more meaningful the data set of selected grains, but at the price of a smaller number of grains to use for calculations. A compromise is needed between these two issues in order to select the largest possible and meaningful data set of grains for D_e determination.

Feldspar contamination

Prior to any measurement, samples go through a number of chemical treatments (Mejdahl and Christiansen, 1994; Wintle, 1997) in order that mineral grains other than quartz are removed. Carbonates and organic matter are dissolved in HCl and H_2O_2 respectively, while HF treatment is needed to eliminate feldspar grains, and density separation to remove zircons. However, samples obtained after such a treatment are not always made up of pure quartz, and often inclusions of feldspars grains can be observed (Baril, 2004). Duller (2003) discusses several methods for distinguishing quartz and feldspar grains in a sample. The most efficient of those consists of taking the ratio of the OSL response to a fixed dose when measured with and without prior infrared stimulation. If this ratio is distinguishable from unity, then there is very likely feldspar contamination (Fig. 3.12). This OSL IR depletion ratio is measured by introducing one extra measurement step on each grain at the end of an SAR run (see for details: Duller, 2003; Olley *et al.*, 2004). Jacobs *et al.* (2003b) stressed the importance of rejecting unwanted grains in the case of feldspar inclusions. Using the above method, Jacobs *et al.* (2003b) were able to identify 22 feldspar grains out of the 56 that gave a reproducible signal from the 1892 grains analyzed. The overdispersion (dispersion in calculated doses that does not arise from counting statistics and/or instrumental reproducibility) of unfiltered data sets was $\sim 36\%$ compared with $\sim 12\%$ after the rejection criterion was applied.

Olley *et al.* (2004) considered feldspar contamination the cause of underestimation of the burial dose measured by Spooner *et al.* (2001). They used the OSL IR depletion method for effectively rejecting the contribution to the OSL signal of feldspar grains from D_e data set. Once this method was applied, good agreement with the independent carbon-14 age was found.

Grain sensitivity

When performing single grain measurements, it would ideal if all grains gave a luminescence signal of sufficient intensity for a D_e to be estimated. However, McFee and Tite (1998) and Duller *et al.* (2000) showed that there is a great variability in luminescence brightness from individual quartz grains in a sample, and usually only a small percentage of grains show a high enough sensitivity to produce a detectable OSL signal. This percentage very much depends on what criteria are used to separate grains that give a detectable signal from grains whose signal is indistinguishable from the background noise ("dim" grains). Obviously

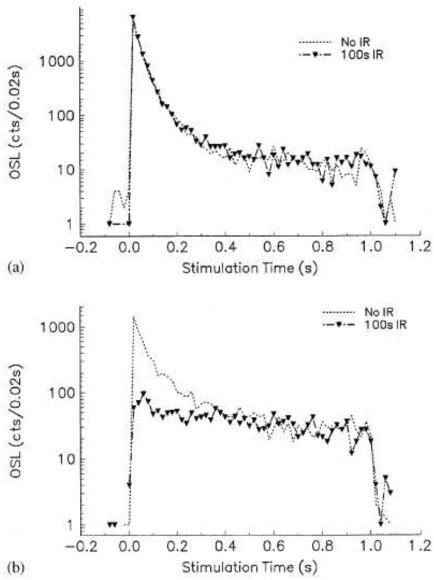

Figure 3.12: OSL decay curves from (a) quartz and (b) feldspar grains. The OSL response was measured twice, with and without prior IR stimulation for 100 s (Duller, 2003).

a rigorous definition of what "detectable" means is needed. There is still no consensus of what criterion should be used for grain selection and often it was arbitrarily applied. Some authors do not even specify what criteria they used for grain selection other than saying that discarded grains showed no detectable OSL signal (Duller *et al.*, 2000; 1999a; Jacobs *et al.*, 2003b; Olley *et al.*, 2004; Roberts *et al.*, 1999).

Murray and Roberts (1997) selected and measured 120 quartz grains, each mounted on a separate 10 mm diameter stainless-steel disk. They accepted 33 grains for further additive-dose single-aliquot measurements on the basis of the OSL natural counts observed, which had to be at least ten times greater than the background level. This criterion is based on the signal-to-noise ratio (S-N) calculated on the luminescence response of the natural dose. More recently, authors have used more than a single criterion for accepting grains, and considerations on sensitivity are made by looking at the OSL response (i.e. number of counts) of the first test dose after the natural signal is measured. The relative standard error (RSE) on this signal is calculated (Banerjee *et al.*, 2000; Galbraith, 2002) and compared to a fixed value that is usually fixed at 30% or less (Bush and Feathers, 2003; Jain *et al.*, 2004; Thomsen *et al.*, 2002; 2003). Ballarini *et al.* (submitted) used a stricter criterion and applied the RSE check on all the test-dose responses.

Since this criterion is based on counting statistics, bright grains (high OSL signal) will produce small RSEs. In contrast, dim grains for which the OSL signal is low will produce a large RSE. Grains with RSE greater than the fixed value are discarded, while the others are accepted for further checks before the equivalent dose is calculated.

Ballarini *et al.* (submitted) showed that the use of test doses hundred times larger than the expected equivalent dose is feasible. This has the advantage of producing higher OSL responses, which results in lower associated RSEs. The benefit of using large test doses is that more individual grains can be accepted after the RSE check is performed.

Dose response curves

Within the SAR procedure, dose response curves (or “growth"” curves) are measured on all the grains. After the natural signal is measured, different laboratory doses that regenerate the OSL signal can be administered. A graph of the measured OSL responses corrected for sensitivity changes (R_i) against the given doses (D_i) characterizes the way that the OSL signal increases with the radiation dose in a particular grain. This is known as the single aliquot regenerative dose (SAR) dose protocol described in Murray and Wintle (2000) and summarized in Table 3.1. Examples of single grain dose response curves are shown in Fig. 3.13.

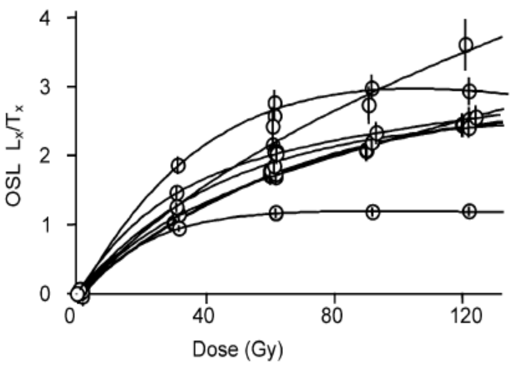

Figure 3.13: Examples of dose response curves measured with the SAR protocol on seven different grains (Jacobs *et al.*, 2003b).

An expectation within the SAR protocol is that increasing laboratory doses produce increasing L_i/T_i ratios. If this does not occur then equivalent doses cannot be calculated since the luminescence behavior of those particular grains cannot be uniquely characterized. Such grains should be immediately discarded for subsequent analysis. A few cases for which the growth decreases after saturation have been reported (Jacobs *et al.*, 2003b; Roberts *et al.*, 1999). However, this effect has not been explained yet.

A few authors apply an additional criterion for rejecting grains based on the recycling ratio (Bush and Feathers, 2003; Feathers, 2003; Jacobs *et al.*, 2003b; Roberts *et al.*, 1999). While for aliquots with multiple grains it is required that the ratio of R5 and R1 (the recycling ratio) should be within 10% of unity, for single grains a less severe criterion is commonly used. As with the choice of the maximum acceptable RSE, the choice of threshold for the recycling ration is arbitrary. Setting severe limits on these rejection criteria allow on the one hand selection of grains with the most desirable luminescence characteristics, but on the other hand the number of grains for which the palaeodose can be determined is restricted.

Murray and Wintle (2003) have recently pointed out that a previously administered dose can be recovered with acceptable precision even when a poor recycling ratio is obtained and vice versa. This indicates that "the recycling ratio is not a particularly sensitive measure for the suitability of the measurement protocol". Also it means that unknown doses may be measured with high accuracy even if poor recycling ratios are observed. Thus, a reasonable threshold for this rejection criterion should not be too severe, since there is no evidence of direct benefit from discarding grains based on the recycling ratio.

Some authors also discard grains that show final D_e values known with poor precision. Feathers (2003) rejected grains with an error on the equivalent dose greater than 30%, though he did not apply this criterion to young samples (expected age $\sim$ 1000 years). However this criterion becomes increasingly impossible to apply as the D_e approaches 0 Gy (Bush and Feathers, 2003).

In some particular circumstances grains were rejected on the base of common sense, rather than a specific criterion. Jacobs *et al.* (2003b) found that for two samples 6 out of 170 and 4 out of 124 grains that passed all the rejection tests, had an equivalent dose consistent with 0 Gy, while the expected age was $\sim$ 65 ka. These anomalous "modern" grains were discarded since it was thought that they had been exposed to light accidentally during sampling. The same authors also found that for 14 to 26% of the grains that remained after application of the rejection criteria, no D_e could be calculated. Surprisingly, the dose response curve of these grains did not attain the sensitivity corrected natural OSL (L_n/T_n). Similar behavior was reported by Roberts *et al.* (2000) for single quartz grains and by Armitage *et al.* (2000) for one aliquot from samples taken in South Africa ("Class 3" grains). Yoshida *et al.* (2000) indicate that the problem seems "to lie with the regenerated signals, which never achieve the same intensity as the natural OSL"". However, no explanation of this effect is currently available.

3.4 Equivalent dose distributions

The procedure of determining a palaeodose begins with informative representation of the data in a graph. The goal of whichever data representation used is to highlight the characteristics of a distribution and provide useful information for further data analysis. This information aims to determine whether a distribution follows normality or not, how many populations there are that form a distribution and what the skewness of the distribution is. It is also informative to display the uncertainty in the D_e value for each data point.

The first step for a meaningful D_e estimation consists of recognizing whether a dose distribution is Gaussian or follows a more complicated pattern. This is the same as determining whether the measured grains were poorly bleached, experienced different dosimetry after burial, or both. If such a distinction is possible, the task of identifying and rejecting poorly-zeroed grains from well-bleached grains used for palaeodose estimation can be tackled. However, it is worth to note that a few authors observed that signal intensities from many individual grains closely follow a log-normal distribution (Galbraith *et al.*, 2005; McCoy *et al.*, 2000).

The most commonly used methods for displaying single grain distributions are discussed below. Methods differ from each other in the particular aspect of the data set that one wants to highlight, but they all aim to determine what kind of D_e distribution is observed for a particular sample and at suggesting a plausible way for palaeodose estimation.

3.4.1 Histograms

Histograms allow a quick visual inspection of the range of burial doses associated with the grains (Bush and Feathers, 2003; Feathers, 2003; Jain *et al.*, 2002; 2004; Roberts *et al.*, 1999; Thomsen *et al.*, 2003). A simple way to determine whether a distribution is normal is to make use of the symmetry properties of Gaussian curves, which means that for a normal distribution the mean, median and mode coincide.

The disadvantage of histograms is that the precision with which D_e values are known is not displayed. Since histograms give meaningful information on distributions only when all the displayed data have similar uncertainties, this method is inadequate for displaying most single grain distributions. A way of circumventing this problem is to include grains that show absolute and relative standard errors on the D_e below a certain threshold (Roberts *et al.*, 1999; Thomsen *et al.*, 2003).

A second problem with histograms is that if not properly built, they can be subjective and lead to misinterpretations. In fact, distribution shapes that arise using this method are very sensitive to the criterion used for binning data. Lepper *et al.* (2000) suggested that an objective bin width could be chosen equal to the median of the σD_e distribution (distribution of errors with which D_e values are known).

3.4.2 Probability density function (PDF)

An alternative method of displaying histograms was proposed by Duller *et al.* (2000), in which uncertainties on each measurement are incorporated in histograms. Here each equivalent dose estimate is represented and fully described by a normal curve whose mean is the D_e and whose height is inversely proportional to the precision of the D_e. The sum of the each distribution produces a probability density function (PDF). It is useful to plot data points (defined by the mean D_e and the standard deviation) together with the relative PDF and the sequence of the D_e estimates and associated errors in ranked order (Fig. 3.14, top figures). Such comparison aims at visualizing non-normality behaviors of data masked by visual inspection of histograms.

3.4.3 Radial plots

Galbraith (1990) proposed a different method based on radial plots for displaying data points having remarkably different uncertainties (Fig 3.14, bottom figures). In this kind of graph a straight line passing horizontally through the origin of the standard estimate (y-axis on the left hand) and intersecting the right hand axis represents an arbitrary palaeodose taken as reference. This value is usually chosen to be close to the expected burial dose. All grains with doses equal to the reference value will fall on this line, while grains with different doses will display above or below this line. The y-axis on the left hand of Fig. 3.14 (bottom figures) shows how many standard deviations away the log D_e is of a particular grain from the reference dose, while on the x-axis, at the bottom, is the associated precision.

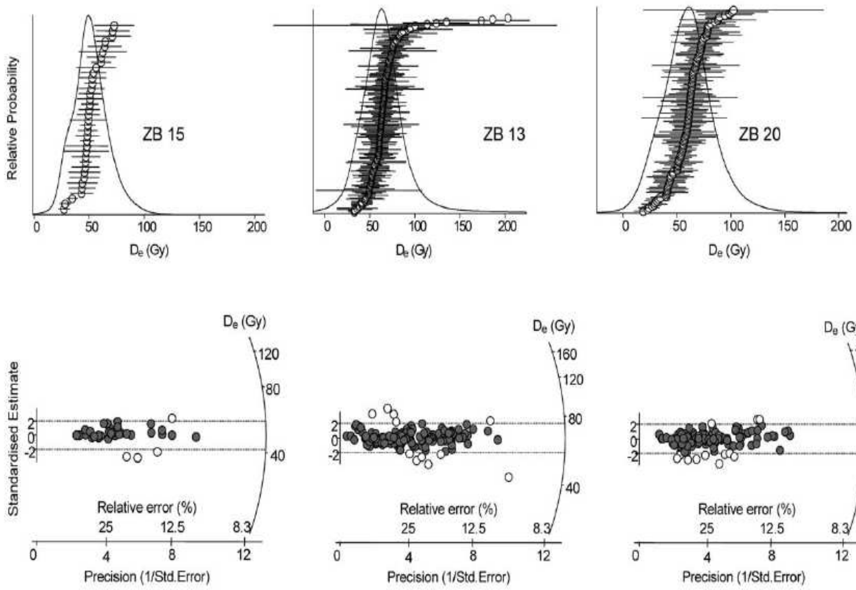

Figure 3.14: Probability density functions (together with ranked individual D_e values and uncertainty estimates) and radial plots are used to display the same data from individual grains (Jacobs *et al.*, 2003b). The reference value for the radial plots was obtained from single aliquot measurements.

An indication of normality can be obtained by adjusting the radial graph to maximize the number of grains that fall within two standard deviations of some reference value. If the distribution is normally distributed, 95% of the D_e values should fall within this 2-σ band.

This kind of graph is particularly convenient when the uncertainties on the grains vary considerably. The precision with which D_e values from single grains are known can be read on the x-axis: the precision of a measurement increases from left to right.

3.5 Palaeodose determination

There is still little consensus on how a palaeodose (i.e. the average dose received since burial by grains in the sediment) should be estimated from D_e distributions. In the simplest case, where equivalent doses are normally distributed, grains are expected to have been well bleached before deposition. The arithmetic (or weighted) mean is then the best estimation of the palaeodose. For non-Gaussian distributions the analysis is usually far more complex.

Although heterogeneity in microdosimetry can be responsible for skewed distributions of equivalent doses (Murray and Roberts, 1997), it is usually assumed that within a sediment all the grains receive the same amount of ionizing radiation (McFee, 1998; Olley *et al.*, 1999). Therefore, asymmetric distributions are usually considered as an indication of incompletely-bleached materials. Different methods have been developed for distinguishing and selecting well-bleached grains from such asymmetric distributions in order to estimate the true palaeodose. These techniques assume that the dose distribution in a well-bleached sample is Gaussian and that there is no intrusion of grains from other layers carrying equivalent doses lower than those representing the last deposition event that has to be dated. With these premises it is clear that attention should be paid to the lowest part of the distribution, which leaves the decision of which grains to include in the palaeodose calculation as the main problem.

3.5.1 Cumulative frequencies and probability plots

Jain *et al.* (2002; 2004) proposed a method of distinguishing well-bleached grains based on the cumulative frequency of D_e values that is plotted against the dose. In such a graph (probability plot) a normal distribution appears as a straight line. Mixed-grain populations can be identified by breaks in the slope, which reflect the asymmetric shape of the distribution (Fig. 3.15). The lowest dose population represents the most well-bleached grains. The advantages of this method are that, unlike histograms, the shape of the probability plot is not very sensitive to the bin width and several different data sets can be represented on the same graph. Equivalent doses are calculated by taking the weighted mean of values identifying the first slope of probability plots. The limit of this method is the lack of reliability when the overlap of the distributions is not strong and changes in the slope are not easily recognizable.

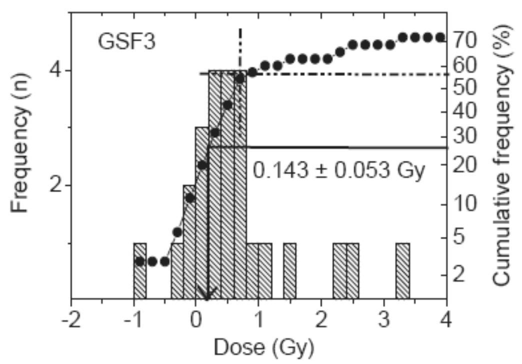

Figure 3.15: Histograms and cumulative frequency for individual grains from untreated mortar are plotted. The probability plot method uses the lowest normal population in the distribution identified by changes in the slope (dashed line). Grains selected in such a way are used for palaeodose estimation (Jain *et al.*, 2004).

3.5.2 The common, the central and the minimum age model

Galbraith *et al.* (1999) proposed three statistical methods that model the burial dose received by individual grains.

In the common age model, the ideal case of grains that all receive the same dose is analyzed. The measured equivalent doses from n grains will then be consistent with a common value. This can be written as

$$\hat{\delta}_i = \delta + \epsilon_i \tag{3.2}$$

where δ is the true burial log dose and $\hat{\delta}_i$ the equivalent log doses measured for each grain that are normally distributed around the true burial dose δ. The (known) deviation ϵ_i between the true and estimated palaeodose is assumed to be a random quantity with expected mean 0 and variance ${\sigma_i}^2$. The best estimate of the burial dose is the weighted average of the measured $\hat{\delta}_i$s from all the grains. However, this method is inadequate when the estimated log doses are not consistent with a common value.

The central age model assumes that the true palaeodoses δ_i are not equal but a random sample from a normal distribution with mean δ and standard deviation σ. Thus, D_e values are measured from grains that received different burial doses. This is written

$$\hat{\delta}_i = \delta_i + \epsilon_i \tag{3.3}$$

The unknown parameters that need to be estimated are δ and σ, which are interpreted as the mean of the true log palaeodoses and the standard deviation of these log palaeodoses. There is no simple procedure for estimating these two quantities and numerical methods are required (see Galbraith *et al.*, 1999; for details). This model also assumes that grains belong to the same population and that unknown effects may induce random deviations from the previous model (e.g. microdosimetry).

A model developed to take account of poor bleaching is the minimum age model. This is a generalization of the central model and takes into account the possibility that some quartz grains may have been fully bleached before deposition while some others may have been only partially bleached. Thus, grains do not necessarily belong any longer to the same population but to a mixed one. The model is again based on equation (2) but now the true log palaeodoses δ_i are a random sample from a mixed truncated normal distribution. The meaning of this truncation is to leave out of the calculation poorly-bleached grains, which show larger doses. With this model one is able to estimate the proportion of insufficiently bleached grains (taken as unknown), the minimum log palaeodose received by each grain and the mean and standard deviation of the truncated distribution. Again, no simple equations for the unknown parameters are available, and these must be estimated by using some optimization software (see Galbraith *et al.*, 1999; for details).

3.5.3 The finite mixture model

A method for distinguishing dose populations within a distribution made of sediment mixtures was proposed by Roberts *et al.* (2000). They constructed a series of synthetic mixture samples made of grains individually bleached by sunlight exposure that received different laboratory doses (0, 5, 10 and 20 Gy, respectively). The advantage of synthetic mixtures is that the applied dose is known for each grain, whereas this information is lost using physical mixtures. Finite mixture models were fitted to each sample to estimate the number of dose components, the corresponding doses and the relative proportion of each component. Within this model, doses are regarded as a random sample from a mixture of k normal component populations with a common standard deviation (σ) and different means (μ_i) and mixing proportions (π_i). Although no method is currently available for estimating the exact number of components in a finite mixture, the *smallest* number of components that are necessary to explain the data can be inferred informally. The finite mixture model reduces to the central age mode (Galbraith *et al.*, 1999) for a one-component sample ($k = 1$).

3.5.4 The leading edge (LE) method

The methods above have been criticized by Lepper and McKeever (2002) with the argument that the assumption of Galbraith *et al.* (1999) that precision and accuracy of a D_e value are linked is not necessarily true. Weighted means are used for palaeodose estimation, implying that more precise D_e values are also more accurate. However, the precision of an equivalent dose does not reflect the accuracy of a measurement. "A grain with low precision (low sensitivity) is equally as likely to be well reset by sedimentary processes as a grain with high precision (high sensitivity)". Thus, precision and accuracy are not necessarily linked (Lepper, personal communication).

The leading edge method was first proposed by Lepper *et al.* (2000) and it has already been discussed for single aliquots. As for the lowest 5% method, it can also be applied to single-grain distributions. It is an objective method used to determine a representative palaeodose from a (asymmetric) distribution made of differently bleached grains. The observed distribution of equivalent doses is the convolution of a natural sedimentary process with an experimental error distribution. Deconvolution of the experimental error distribution from the observed D_e distribution should reveal the natural sedimentary process distribution. In the case of a perfectly bleached sample, all the grains have a zero dose before deposition and receive the same amount of ionizing radiation (no microdosimetry variations are assumed). The normal distribution that arises is then caused only by experimental uncertainties and a deconvolution will produce a distribution that is zero for all D_e values other than for the true burial dose value ("delta" function). If the as-measured distribution is not Gaussian, the deconvolved distribution would be similar to the one shown in Fig. 3.16. A steep edge will occur because during erosion and transportation no bleaching process can reset a luminescence signal to a value less than zero, while a "tail" extends towards larger D_e values. They hypothesize that the leading edge represents the true palaeodose. Their objective method for calculating the burial dose begins with a proper presentation of the data with histograms. Once data are properly binned, a Gaussian curve is fitted to the rising limb of the distribution and the palaeodose is determined as the value of D_e that puts to zero the second derivative of the Gaussian equation. The corresponding uncertainty is given by the standard error calculated on the estimated true D_e.

3.5.5 Comparison of internal and external uncertainties (IEU)

Another method for discerning well- from poorly-bleached grains based on statistics was proposed by Jain *et al.* (2002). This method relies on the fact that the variance of a variable (such as the D_e) normally distributed tends to σ^2 for large number of measurements. We can check whether extra sources of error other than the individual uncertainties σ_i are contributing to the total uncertainty on the D_e. This can be done by estimating the value of α_e and α_i defined in this way

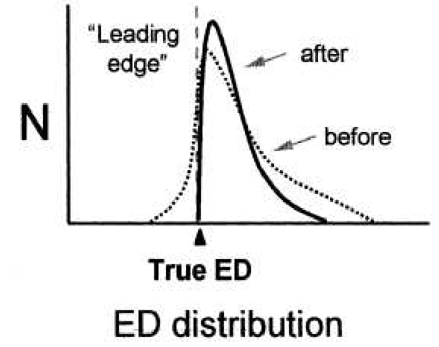

Figure 3.16: Each measured D_e distribution (dashed) is the convolution of an experimental error and a depositional distribution (solid). The leading edge of the deconvolved distribution is thought to represent the best estimation of the true burial dose (Lepper *et al.*, 2000).

$$\alpha_e = \frac{\sum_{i=1}^{n}(x_i - \bar{x})/\sigma_i}{(n-1)\sum_{i=1}^{n} 1/{\sigma_i}^2} \qquad \alpha_i = \frac{1}{\sum_{i=1}^{n} 1/{\sigma_i}^2} \tag{3.4}$$

where x_i are the individual dose estimates, $\bar{x}$ is the weighted average, σ_i the uncertainties on x_i. The first estimate α_e combines information on both individual estimates of uncertainty (σ_i) and the deviation from the weighted mean ($x_i - \bar{x}$). If there is no additional source of variance in the data other than σ_i, then α_e reduces to α_i for large n and the ratio α_e/α_i approaches the unity. The uncertainty on this ratio is $(2(n-1))^{-0.5}$. In a population where additional variance is caused by poor bleaching, the ratio α_e/α_i can be used to select the lowest part of the distribution that contains only well-bleached grains. This is done by first sorting doses in increasing order and then calculating α_e and α_i for all the grains beginning with the smallest dose. The process stops when $\alpha_e/\alpha_i = 1 \pm (2(n-1))^{-0.5}$, and grains on which this calculation was performed are assumed to be well bleached.

3.6 Case studies of the analysis of single grain dose distributions

As previously mentioned, the simple mean is not a realistic palaeodose estimate for poorly-bleached samples. Also the use of the weighted mean has been criticized for biasing towards the most precise D_e values, which are not necessarily the most accurate (Lepper and McKeever, 2002). Feathers (2003) was able to determine precise and accurate palaeodose estimations using the simple mean from a fluvial sample, named UW479, whose D_e distribution was close to normal (skewness value ~ 0, Fig. 3.17). It is interesting to note that symmetric and narrow distributions do not always reflect good bleaching. Feathers (2003) observed for a dune sample a relatively narrow Gaussian distribution (compared to sample UW479, considered well-bleached and taken as reference). However, the mean value overestimated the expected age given by radiocarbon methods by a factor of four. This is the case of a poorly bleached sample giving rise to a Gaussian-like distribution.

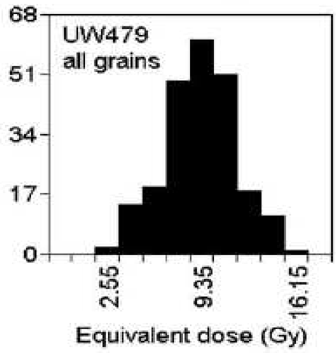

Figure 3.17: Histogram of single-grain D_e values from sample UW479 (Feathers, 2003). For this alluvial-sand sediment the burial dose was estimated by means of the simple average.

For non-normal distributions, it has been suggested that the lowest part contains well-bleached grains of a sample and is representative of the last depositional event. Positively skewed distributions indicate that the majority of the grains of a sample have been sufficiently bleached before deposition, while a small fraction did not experience sufficient bleaching. A distribution with negative asymmetry reflects the opposite situation. In the unfortunate circumstance in which none of the grains were sufficiently bleached before burial, the palaeodose will be necessarily overestimated.

Olley *et al.* (1998) proposed the lowest 5% method to determine the true dose from asymmetric distributions. However, this method has not been validated by comparison with some independent age control and did not provide reliable D_e estimates when applied in other studies. Jain *et al.* (2004) compared four methods for determining the best possible dose estimates for three mortar samples that showed skewed D_e distributions. These were the simple average, the first 5% method, probability plots and the IEU method. The average nearly always overestimated the expected dose, while the first 5% method gave poor precision results and often not in agreement with other methods. Probability plots and the IEU method returned identical results in good agreement with the expected dose. They also found that coarser grains (180-212 and 250-300 μm) were slightly better bleached than finer grains (90-112 μm). Zhang *et al.* (2003) found that even well bleached fluvial samples might show considerable D_e scatter and concluded that "the lowest D_e dose does not always necessarily represent the true burial dose". In this case the lowest 5% method is not reliable.

The leading edge (LE) approach to the problem of asymmetric distributions is more analytical than the first 5% method. The attention is again focussed on the lowest part of the distribution. However, the assumption is that a measured distribution is the sum of an experimental distribution and a depositional distribution. The first one is subtracted from the measured distribution before estimating the burial dose. In this way the "lowest" tail of the distribution is eliminated. This correction makes this method suitable for determining

D_es also from well-bleached grains (normal distributions), where the lowest 5% would fail. This last method approaches the leading edge for extremely skewed distribution, where the experimental errors give a little contribution in the lowest part of the distribution. Bush and Feathers (2003) applied the leading edge method in an anthropogenic soil profile study. Good agreement was found between OSL ages and the ages given by retrieved ceramics and C-14 from charcoal. Feathers (2003) used the LE method for dating two slopewash deposits that showed positively skewed distributions. The ages estimated with this method were considered "reasonable", being also the D_es calculated with the simple mean and not inconsistent with the radiocarbon data.

The central and the minimum age models have been extensively applied in the last years in a variety of environments, always with satisfactory results. Although mathematically rigorous, these methods have been criticized by Lepper and McKeever (2002) for the assumptions they are based on. Jacobs *et al.* (2003b) have used the common and central age model for dating dune sand samples from South Africa. The agreement between small aliquots and single grain measurements suggested the lack of disturbance of the sand layer. Olley *et al.* (2004) used the minimum age model for dating Holocene fluvial, aeolian and marine sediments. OSL estimates were compared with independent ^{14}C and ^{137}Cs ages and the minimum age model gave the most accurate estimates compared to other methods. The weighted mean provided consistent ages only in the case of sufficiently bleached materials, while overestimated the age by to 200% in the case of a poorly-bleached young aeolian sediment. The spread in measurements (σ) for this sample was calculated to be 42%, indicating incomplete bleaching although aeolian sediments are usually considered to be very well bleached materials. For a marine sediment (σ value of 27%) the expected radiocarbon age was 3640-4420 years. The minimum age model predicted a burial age of 4300 ± 380 years, which falls in the expected range, while other methods produced substantial age underestimates: 1880 ± 240 years using the technique of Zhang *et al.* (2003); 2150 ± 290 years using the method of Fuchs and Lang (2001) and 2500 ± 300 years using the lowest 5%. The leading edge method produced an overestimated age of 5200 with a large uncertainty of 3200 years. Olley *et al.* (2004) conclude that the minimum age model is the best available method to determine reliable burial ages of Holocene sediments using the lowest D_e population. However, this method may not be appropriate when the spread in dose distributions is not due to partial bleaching but to other factors. One of these can be post-depositional reworking with inclusion of grains from younger strata. In this case, the dose distribution will be negatively skewed and the lowest part is not representative of the last depositional event. Feathers (2003) observed such distributions for one alluvial sediment with aeolian components and from a sample from a massive homogeneous aeolian sand unit (shown in Fig. 3.18a and 3.18b respectively). In the first case the source of the skewness was uncertain and attributed perhaps to some turbation process. When the values from the lowest bins in the histograms were removed, the asymmetry seemed to disappear. The mean of this truncated histogram was assumed to represent the best estimate of D_e. In the second case, the lack of structure of the sand dune suggested a high degree of mixing by various turbation processes. The trailing edge (analogous to Lepper's leading edge) was used for D_e estimation. In both cases good agreement with the independent control was found. Mixing of grains was considered the cause of the broad but non-skewed distribution from an alluvial sample shown in Fig.

3.18c. The mean value was used to estimate the equivalent dose from this deposit, which resulted in good agreement with the expected age.

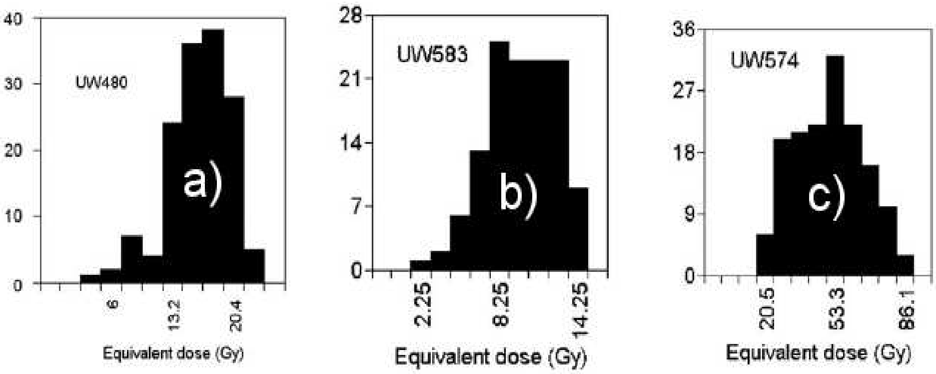

Figure 3.18: Distributions of Holocene single grains of quartz from (a) paludal mud/loam, (b) aeolian sand and (c) dune sand (Feathers, 2003). Broadness and negative skewness of these distributions indicate that very likely these samples experienced post depositional turbation and grain mixing.

3.7 Determining the palaeodose: which is the most reliable method?

Various methods have been applied for single grain D_e estimation from samples of different environments. There is so far no method that is universally applicable in all circumstances. The choice of a particular method rather than another is strongly dependent on the type of D_e distribution, which is a function of the geological history of the deposit. Methods like the leading edge, the central/minimum age model and the cumulative plots work with the assumption that the lowest part of the distribution is the most representative of the last depositional event. This is true in the case of poorly-bleached material that did not experience post-depositional reworking. However, if asymmetric distributions arise from differences in dosimetry and not from insufficient bleaching, these methods cannot be applied. In this scenario all the equivalent doses that build a distribution are representative of the last burial event provided the corresponding dose rate is known. Since in principle insufficient bleaching and microdosimetry heterogeneity may produce similar distributions, it cannot be established in advance with no extra geological information which method is most suitable for D_e estimation. For example, the IEU method only considers whether some external source other than counting statistics is causing a certain spread in the equivalent doses. It cannot be assessed whether poor bleaching or heterogeneity in microdosimetry caused this anomalous spread.

Usually a situation of "good" poor bleaching is assumed when positive asymmetric distributions are observed. This means that in most of the environments it is expected that the majority of the grains will be well bleached and a small fraction to be insufficiently bleached. If there are no differences in microdosimetry between grains, the minimum age model is probably the method of choice, being validated in a variety of environments.

Two possible explanations can be given when negatively skewed distributions are observed. The first one is that only a small fraction of the grain population of a sediment was sufficiently bleached while the majority of the grains were poorly bleached. In such a case the lowest region of the distribution is still representative of the last burial event. The second explanation takes into account inclusion of grains from younger deposits responsible of the first part of the distribution. In this case attention should be focussed on the latter part of the distribution. A possible approach for D_e determination could be discarding the first bins of such a histogram and than taking the mean value or applying the trailing edge method (Feathers, 2003).

More complicated distributions may arise when several "inconvenient" effects occur at the same time, like inclusion of grains and poor bleaching. In such cases reliable D_e estimations can be determined only with extra information from geological evidence. "Such geological modelling will be probably required to understand better single-grain distributions" (Feathers, 2003).

3.8 Improving the quality of single grain measurements

Although single grain measurements are nowadays quick and reproducible, a large number of grains have to be measured in order to gather sufficient data to generate a reliable dose distribution. This is due to the fact that usually only 2-3% of the measured grains shows detectable OSL sensitivity and represents one of the biggest challenges in measurements of individual grains. Moreover, not all the OSL sensitive grains show the necessary characteristics (such as consistent dose-response curves) to be used for used for D_e determination, but a generous fraction is rejected during the accepting criteria process. Efforts should be put into increasing the number of accepted grains for further analysis.

One of these criteria is based on the measurement of the OSL intensity after a laboratory dose is administered. Only grains with a background-corrected OSL signal above a certain threshold are accepted. Thus, one might in principle increase this number by improving the light efficiency of the SG system. This can be done in several ways; Ballarini *et al.* (2005) investigate the use of alternative detection filters with a higher luminescence transmission.

Other criteria are based on the reproducibility of the SAR protocol. This protocol can be made more reliable by preventing some effects that alter its performance like thermal transfer. Murray and Wintle (2003) proposed a supplementary step to be added at the end of each SAR step to prevent the recuperation of an undesired OSL signal. For the same purpose, longer OSL stimulation should be investigated. The choice of pre-heat temperatures has been demonstrated to play an important role in the thermal transfer production and some investigations have already been carried out (Jain *et al.*, 2004).

Clear and detailed measurement procedures together with plausible reasoning for the choice of parameters and rejection criteria should be reported in future publications, especially concerning single grain studies for which a definitive protocol is not yet established.

3.9 Summary and conclusions

Equivalent dose overestimation using small aliquots of quartz grains has suggested the need for the investigation of individual-grains in order to produce reliable D_e values. These kinds of studies are now feasible with the development of single grain equipment that allows quick and precise measurements. Different dose distributions are observed depending on the degree of bleaching before deposition, individual sensitivity, difference in microdosimetry, instrumental errors and mixture of different grain populations. The main challenge is to recognize and select only those grains that have been sufficiently bleached before deposition to determine the burial dose. Several methods have been developed for displaying data, each one highlighting particular characteristics of dose distributions. Histograms represent the more intuitive way of displaying the dose occurrences within a sample, but they do not provide information on the uncertainties associated with each D_e estimate. Probability and radial plots are more informative in this sense and are usually preferred to simple histograms.

Palaeodose estimations based on the D_e values obtained for a number of grains from a sedimentary sample are in general not straightforward, unless the grains are well bleached. In this case the simple mean is in general the best estimate of the burial dose. For poorly bleached samples, skewed distributions are observed. It is advisable to use more than one method for dose estimation when no age control is available, and check whether the same results are obtained with different approaches. In any case, single grain distributions are more significant when supported by geological evidence that corroborates statistical interpretations.

Bibliography

Adamiec, G (2000). Variations in luminescence properties of single quartz grains and their consequences for equivalent dose estimation. *Radiation Measurements*, 32, 427–432.

Aitken, MJ (1998). *An introduction to optical dating.* Oxford University Press.

Armitage, SJ, Duller, GAT and Wintle, AG (2000). Quartz from southern Africa: sensitivity changes as a result of thermal pretreatment. *Radiation Measurements*, 32, 571–577.

Bailey, RM, Smith, BW and Rhodes E.J. (1997). Partial bleaching and the decay form characteristics of quartz OSL. *Radiation Measurements*, 27, 123–136.

Ballarini, M, Wallinga, J, Bos, AJJ and Wintle, AG (submitted). A modified SAR protocol for optical dating of individual grains from young quartz samples. *Radiation Measurements.*

Ballarini, M, Wallinga, J, Duller, GAT, Brouwer, JC, Bos, AJJ and Van Eijk, CWE (2005). Optimizing detection filters for single-grain optical dating of quartz. *Radiation Measurements*, 40, 5–12.

Ballarini, M, Wallinga, J, Murray, AS, Van Heteren, S, Oost, AP, Bos, AJJ and Van Eijk, CWE (2003). Optical dating of young coastal dunes on a decadal time scale. *Quaternary Science Reviews*, 22, 1011–1017.

Banerjee, D, Bøtter-Jensen, L and Murray, AS (2000). Retrospective dosimetry: estimation of the dose to quartz using the single-aliquot regenerative-dose protocol. *Applied Radiation and Isotopes*, 52, 831–844.

Baril, RM (2004). Emission and excitation spectra of feldspar inclusions within quartz. *Radiation Measurements*, 38, 87–90.

Bøtter-Jensen, L, Bulur, E, Duller, GAT and Murray, AS (2000). Advances in luminescence instrument systems. *Radiation Measurements*, 32, 523–528.

Bulur, E, Bøtter-Jensen, L and Murray, AS (2000). Optically stimulated luminescence from quartz measured using the linear modulation technique. *Radiation Measurements*, 32, 407–411.

Bush, DA and Feathers, JK (2003). Application of OSL single-aliquot and single-grain dating to quartz from anthropogenic soil profiles in the SE United States. *Quaternary Science Reviews*, 22, 1153–1159.

Duller, GAT (1991). Equivalent dose determination using single aliquots. *Nuclear Tracks and Radiation Measurements*, 18, 371–378.

Duller, GAT (1994a). Luminescence dating using single aliquots: new procedures. *Quaternary Geochronology (QSR)*, 13, 149–156.

Duller, GAT (1994b). Luminescence dating of poorly bleached sediments from Scotland. *Quaternary Geochronology (QSR)*, 13, 521–524.

Duller, GAT (1996). Recent developments in luminescence dating of quaternary sediments. *Progress in Physical Geography*, 20, 127–145.

Duller, GAT (2003). Distinguishing quartz and feldspar in single grain luminescence measurements. *Radiation Measurements*, 37, 161–165.

Duller, GAT, Bøtter-Jensen, L and Murray, AS (2000). Optical dating of single sand-sized grains of quartz: sources of variability. *Radiation Measurements*, 32, 453–457.

Duller, GAT, Bøtter-Jensen, L, Murray, AS and Truscott, AJ (1999a). Single grain laser luminescence (SGLL) measurements using a novel automated reader. *Nuclear Instruments and Methods B*, 155, 506–514.

Duller, GAT and Murray, AS (2000). Luminescence dating of sediments using individual mineral grains. *Geologos*, 5, 87–106.

Duller, GAT, Wintle, AG and Hall, AM (1995). Luminescence dating and its application to key pre-late Devensian sites in Scotland. *Quaternary Science Reviews*, 14, 495–519.

Feathers, JK (2003). Single-grain OSL dating of sediments from the Southern High Plains, USA. *Quaternary Science Reviews*, 22, 1035–1042.

Fuchs, M and Lang, A (2001). OSL dating of coarse-grain fluvial quartz using single-aliquot protocols on sediments from NE Peloponnese, Greece. *Quaternary Science Reviews*, 20, 783–787.

Fuchs, M and Wagner, GA (2003). Recognition of insuficient bleaching by small aliquots of quartz for reconstructing soil erosion in Greece. *Quaternary Science Reviews*, 22, 1161–1167.

Galbraith, RF (1990). The radial plot: graphical assessment of spread in ages. *Nuclear Tracks and Radiation Measurements*, 17, 207–214.

Galbraith, RF (2002). A note on the variance of a background-corrected OSL count. *Ancient TL*, 20, 49–51.

Galbraith, RF, Roberts, RG, Laslett, GM, Yoshida, H and Olley, JM (1999). Optical dating of single and multiple grains of quartz from Jinmium rock shelter, northern Australia: Part I, Experimental design and statistical models. *Archaeometry*, 41, 339–364.

Galbraith, RF, Roberts, RG and Yoshida, H (2005). Error variation in OSL palaeodose estimates from single aliquots of quartz: a factorial experiment. *Radiation Measurements*, 39, 289–307.

Hashimoto, T, Notoya, S, Arimura, T and Konishi, M (1996). Changes in luminescence color images from quartz slices with thermal annealing treatments. *Radiation Measurements*, 26, 233–242.

Heimsath, AM, Chappell, J, Spooner, NA and Questiaux, DG (2002). Creeping soil. *Geology*, 30, 111–114.

Huntley, DJ and Berger, GW (1995). Scatter in luminescence data for optical dating - some models. *Ancient TL*, 13, 5–9.

Huntley, DJ, Godfrey-Smith, DI and Haskell, EH (1985). Optical dating of sediments. *Nature*, 313, 105–107.

Jacobs, Z, Duller, GAT and Wintle, AG (2006). Interpretation of single grain D_e distributions and calculation of D_e. *Radiation Measurements*, 41, 264–277.

Jacobs, Z, Wintle, AG and Duller, GAT (2003b). Optical dating of dune sand from Blombos cave, South Africa: II – single grain data. *Journal of Human Evolution*, 44, 613–625.

Jain, M, Bøtter-Jensen, L, Murray, AS and Jungner, H (2002). Retrospective dosimetry: Dose evaluation using unheated and heated quartz from a radioactive waste storage building. *Radiation Protection Dosimetry*, 101, 525–530.

Jain, M, Thomsen, KJ, Bøtter-Jensen, L and Murray, AS (2004). Thermal transfer and apparent-dose distributions in poorly bleached mortar samples: results from single grains and small aliquots of quartz. *Radiation Measurements*, 38, 101–109.

Lamothe, M, Balescu, S and Auclair, M (1994). Natural IRSL intensities and apparent luminescence ages of single feldspar grains extracted from partially bleached sediments. *Radiation Measurements*, 23, 555–561.

Lepper, K, Larsen, N.A. and McKeever, SWS (2000). Equivalent dose distribution analysis of Holocene eolian and fluvial quartz sands from Central Oklahoma. *Radiation Measurements*, 32, 603–608.

Lepper, K and McKeever, SWS (2002). An objective methodology for dose distribution analysis. *Radiation Protection Dosimetry*, 101, 349–352.

Li, SH (1994). Optical dating: insufficiently bleached sediments. *Radiation Measurements*, 23, 563–567.

McCoy, DG, Prescott, JR and Nation, RJ (2000). Some aspects of single-grain luminescence dating. *Radiation Measurements*, 32, 859–864.

McFee, CJ (1995). *The use of an imaging photon detector for luminescence dating.* Ph.D. thesis, Research Laboratory for Archaeology and History of Art, Oxford University. Unpublished.

McFee, CJ (1998). The measurement of single grain IRSL EDs using an imaging photon detector. *Quaternary Science Reviews*, 17, 1001–1008.

McFee, CJ and Tite, MS (1998). Luminescence dating of sediments - The detection of high equivalent dose grains using an imaging photon detector. *Archaeometry*, 40, 153–168.

McKeever, SWS (2001). Optically stimulated luminescence dosimetry. *Nuclear Instruments and Methods in Physics Research B*, 184, 29–54.

Mejdahl, V and Christiansen, HH (1994). Procedures used for luminescence dating of sediments. *Quaternary Science Reviews*, 13, 403–406.

Miallier, D, Fain, J and Sanzelle, S (1985). Single-quartz grain thermo-luminescence dating - An approach for complex materials. *Nuclear Tracks and Radiation Measurements*, 10, 163–168.

Murray, AS, Olley, JM and Caitcheon, GG (1995). Measurement of equivalent doses in quartz from contemporary water-lain sediments using optically stimulated luminescence. *Quaternary Geochronology (QSR)*, 14, 365–371.

Murray, AS and Roberts, RG (1997). Determining the burial time of single grains of quartz using optically stimulated luminescence. *Earth and Planetary Science Letters*, 152, 163–180.

Murray, AS, Roberts, RG and Wintle, AG (1997). Equivalent dose measurement using a single aliquot of quartz. *Radiation Measurements*, 27, 171–184.

Murray, AS and Wintle, AG (2000). Luminescence dating of quartz using an improved single-aliquot regenerative-dose protocol. *Radiation Measurements*, 32, 57–73.

Murray, AS and Wintle, AG (2003). The single aliquot regenerative dose protocol: potential for improvements in reliability. *Radiation Measurements*, 37, 377–381.

Ollerhead, J, Huntley, DJ and Berger, GW (1994). Luminescence dating of sediments from Buctouche Spit, New Brunswick. *Canadian Journal of Earth Sciences*, 18, 419–432.

Olley, JM, Caitcheon, GG and Murray, AS (1998). The distribution of apparent dose as determined by optically stimulated luminescence in small aliquots of fluvial quartz: Implications for dating young sediments. *Quaternary Geochronology (QSR)*, 17, 1033–1040.

Olley, JM, Caitcheon, GG and Roberts, RG (1999). The origin of dose distributions in fluvial sediments, and the prospect of dating single grains from fluvial deposits using optically stimulated luminescence. *Radiation Measurements*, 30, 207–217.

Olley, JM, Pietsch, T and Roberts, RG (2004). Optical dating of Holocene sediments from a variety of geomorphic settings using single grains of quartz. *Geomorphology*, 60, 337–358.

Rhodes, EJ (2000). Observations of thermal transfer OSL signals in glacigenic quartz. *Radiation Measurements*, 32, 595–602.

Roberts, RG, Galbraith, RF, Olley, JM, Yoshida, H and Laslett, GM (1999). Optical dating of single and multiple grains of quartz from Jinmium rock shelter, northern Australia: Part II, Results and implications. *Archaeometry*, 41, 365–395.

Roberts, RG, Galbraith, RF, Yoshida, H, Laslett, GM and Olley, JM (2000). Distinguishing dose populations in sediment mixtures: a test of single-grain optical dating procedures using mixtures of laboratory-dosed quartz. *Radiation Measurements*, 32, 459–465.

Spencer, JQ, Sanderson, DCW, Deckers, K and Sommerville, AA (2003). Assessing mixed dose distributions in young sediments identified using small aliquots and a simple two-step SAR procedure: the F-statistic as a diagnostic tool. *Radiation Measurements*, 37, 525–531.

Spooner, NA, Olley, JM, Questiaux, DG and Chen, XY (2001). Optical dating of an aeolian deposit on the Murrumbidgee flood-plain. *Quaternary Science Reviews*, 20, 835–840.

Stokes, S (1992). Optical dating of young (modern) sediments using quartz - results from a selection of depositional environments. *Quaternary Science Reviews*, 11, 153–159.

Stokes, S, Bray, HE and Blum, MD (2001). Optical resetting in large drainage basins: tests of zeroing assumptions using single-aliquot procedures. *Quaternary Science Reviews*, 20, 879–885.

Thomsen, KJ, Bøtter-Jensen, L, Murray, AS and Solongo, S (2002). Retrospective dosimetry using unheated quartz: a feasibility study. *Radiation Protection Dosimetry*, 101, 345–348.

Thomsen, KJ, Jain, M, Bøtter-Jensen, L, Murray, AS and Jungner, H (2003). Variation with depth of dose distributions in single grains of quartz extracted from an irradiated concrete block. *Radiation Measurements*, 37, 315–321.

Thomsen, KJ, Murray, AS and Bøtter-Jensen, L (2005). Sources of variability in OSL dose measurements using single grains of quartz. *Radiation Measurements*, 49, 47–61.

Truscott, AJ, Duller, GAT, Bøtter-Jensen, L, Murray, AS and Wintle, AG (2000). Reproducibility of optically stimulated luminescence measurements from single grains of Al_2O_3:C and annealed quartz. *Radiation Measurements*, 32, 447–451.

Wallinga, J (2002a). Optically stimulated luminescence dating of fluvial deposits: a review. *Boreas*, 31, 303–322.

Wallinga, J (2002b). On the detection of OSL age overestimation using single-aliquot techniques. *Geochronometria*, 21, 17–26.

Wintle, AG (1973). Anomalous fading of thermoluminescence in mineral samples. *Nature*, 245, 143–144.

Wintle, AG (1997). Luminescence dating: laboratory procedures and protocols. *Radiation Measurements*, 27, 769–817.

Yoshida, H, Roberts, RG, Olley, JM, Laslett, GM and Galbraith, RF (2000). Extending the age range of optical dating using single 'supergrains' of quartz. *Radiation Measurements*, 32, 439–446.

Zhang, JF, Zhou, LP and Yue, SY (2003). Dating fluvial sediments by optically stimulated luminescence: selection of equivalent doses for age calculation. *Quaternary Science Reviews*, 22, 1123–1129.

Chapter 4

Spatial variation of dose rate from beta sources as measured using single grains

Ancient TL, submitted

M. Ballarini[a], Wintle, A.G.[b], Wallinga, J.[a]

[a] *Delft University of Technology, Faculty of Applied Sciences, Mekelweg 15, NL-2629 JB Delft, The Netherlands*

[b] *Institute of Geography and Earth Sciences, University of Wales, Aberystwyth, Ceredigion SY23 3DB, UK.*

Abstract

Dose rates across the centre of a 1 cm diameter aluminium disc were measured using a 10x10 array of single grains of quartz held in holes drilled with 600 μm separation. The dose rates were obtained by measuring the OSL signals from quartz grains that previously had been given a known gamma those measured following increasing doses given by a beta source held 5 mm above the disc surface. The patterns of dose rate were obtained for four $^{90}Sr/^{90}Y$ beta sources. Two were found to produce a non-uniform dose rate at the disc surface, with one showing a factor of two across the 7.6 mm diameter of the area containing the 10x10 array. The implications for both single grain and multiple grain measurements are discussed.

4.1 Introduction

There has been an increasing number of publications relating to the use of Risø readers that have a special attachment for the measurement of the OSL signals from individual sand-sized grains using a focussed laser for optical stimulation (Duller and Murray, 2000). The main applications have been to the dating of sand related to archaeological sites (e.g. Jacobs *et al.*, 2003b), fluvial deposits (e.g. Thomas *et al.*, 2005), glacial deposits (e.g. Glasser *et al.*, 2006) and dosimetry studies of concrete blocks (Thomsen *et al.*, 2003) and mortar (Jain *et al.*, 2004) . The prototype of Duller *et al.* (1999b;a) used an 8x8 array of holes drilled into the surface of a 0.97 cm diameter aluminium disc. More recently a 9x9 array (Bøtter-Jensen *et al.*, 2000) and then a 10x10 array (Bøtter-Jensen *et al.*, 2003) have been used. The most commonly used discs have holes that are ∼300 μm in diameter and 300 μm deep with their centres being 600 μm apart; they are designed to receive single grains with diameters ranging from 180 to 250 μm, a common size used in environmental and dosimetric studies.

The reproducibility of measurements made with the single grain system has been reported by Truscott *et al.* (2000) who used both Al_2O_3:C grains and thermally annealed quartz grains. By making repeated measurements using the same dose, they demonstrated the precision and accuracy of the laser stimulation system. This resulted in a standard deviation of $\sim 3.5\%$ for repeated measurements. Thomsen *et al.* (2005) found similar results in another study of repeated paired measurements, though they noted that the standard deviation could be decreased by increasing the signal integration time; similar findings were reported by Jacobs *et al.* (2006).

The experiments described above have established the reproducibility of the measurement procedure. A crucial part of using such a system is calibration of the beta source. This can be undertaken using individual grains that have previously been sensitised and stabilised by heating, and then been given a known gamma dose. The SAR protocol (Murray and Wintle, 2000) can then be used to determine the dose rate. Measurements of such gamma-irradiated quartz, should provide a distribution of doses that has a standard deviation that is similar to that of the grains given repeated beta doses. However, it has been shown that the scatter in dose rate is much larger (Thomsen *et al.*, 2005). Thomsen *et al.* (2005) also presented evidence that using individual dose rates for each grain position, rather than an average dose rate for the whole disc, caused a reduction in the error term. Their results indicated that for their source, non-uniformity of dose rate did not contribute more than about 5% to the variability observed. However, given the different methods of source construction, it is possible that other sources may be more variable, and that is what this paper explores.

Although the grains are individually optically simulated with the laser, both irradiation and heating of all 100 grains on a disc is carried simultaneously. The heating of the grains will be very similar as aluminium is a good conductor. The uniformity of irradiation will depend upon the source-sample distance and the homogeneity of the source. For older versions of the Risø TL/OSL reader, the source-sample distance is 7 mm, as reported by Mauz and Lang (2005). For more recent readers, this distance has been reduced to 5 mm (Bøtter-Jensen *et al.*, 2000). It might be assumed that this geometry would provide uniform irradiation across the 7.6 mm diameter of the area occupied by the holes in the special single grain disc. However, this should not be assumed given recently reported spatial variations in dose rate reported when using a source with a ceramic substrate in a stand-alone irradiator with the sources at distances of 15 to 25 mm from a radioluminescent probe made of CaF_2 (Spooner and Allsop, 2000).

It is particularly important to take account of all laboratory-derived sources of error in the measurement of single grains before obtaining dose distributions for naturally-irradiated sand grains. Thus it is important to investigate the dose rate for each position across a single grain disc. In this study, we investigate the uniformity of the dose rate at each grain position for discs irradiated in a Risø TL/OSL reader.

4.2 Equipment

The Risø TL/OSL DA-15 reader employed in the study was purchased in 2002 and has a source-sample distance of 5 mm (Bøtter-Jensen *et al.*, 2000). The carousel used to carry the sample discs has 48 positions. Single grain discs were placed on the carousel of the reader with alternate positions left empty in order to avoid cross-talk during irradiation (Bøtter-Jensen *et al.*, 2000; Markey *et al.*, 1997) and optical stimulation (Bray *et al.*, 2002). The discs were carefully aligned so that they were identically oriented.

Four $^{90}Sr/^{90}Y$ sources are assessed, one original SIP silver plaque type source and three, more recent, SIF ceramic-substrate type sources manufactured by AEA Technology (Germany). The relative merits of these different types of source have been discussed by Aitken (1985) and by Spooner and Allsop (2000). In particular, it was reported that the active area of the SIP source has a diameter of 12 mm, whereas the equivalent diameter for the SIF source is only 5 mm (Spooner and Allsop, 2000). The sources were moved to the single grain reader. Each source was mounted in turn in the rotating stainless steel wheel, which is built into a lead castle to provide shielding (Markey *et al.*, 1997). The laboratory code and nominal activity for each source is given in Table 4.1.

4.2.1 Experimental procedure

The sources were calibrated using two batches of quartz (grain size of 180-212 μm) that had received doses of 5.00 and 3.18 Gy, respectively, using a ^{60}Co γ-source at the Risø National

Table 4.1: Source used, source activity, number of grains (n) investigated, percentage of grains that fail a series of quality control tests (dose response curve, recycling ratio and recuperation; Murray and Wintle, 2000), average min, max and final dose rate. R are normalized luminescence values (L/T) for cycles 1 to 5 in the SAR protocol. R_5/R_1 is the recycling ratio. $R_1 < R_2 < R_3$ indicated that the dose response curve grows systematically.

Source	Activity	n	$R_1 < R_2 < R_3$	R_5/R_1	Recuperation (% of R_1)	Min	Max	Average dose rate
5583	74 MBq	600	4	30	4	1.81	3.39	2.66 ± 0.04 mGy/s
5626	24.1 MBq	1600	15	38	6	1.02	1.44	1.236 ± 0.003 mGy/s
6100	1.48 GBq	1200	1	15	1	0.064	0.142	0.103 ± 0.002 Gy/s
6088	1.48 GBq	2000	1	21	1	0.117	0.166	0.147 ± 0.002 Gy/s

Laboratory. This quartz has been heat treated in the Risø National Laboratory and is used by them for beta source calibrations. For all the quartz grains used in this study an OSL signal could be measured. For source 5626, quartz with a calibration dose of 3.18 Gy was used; for the other sources, quartz with 5.00 Gy was used. A SAR protocol was applied using a 10 s preheat at 240°C prior to the OSL measurement that was made for 1 s at 125°C, and a cut heat to 220°C after the delivery of the test dose. L_i and T_i are derived from the initial OSL signal (0.1 s) minus a background estimated from the last part of the stimulation curve (0.2 s). The SAR protocol used three regenerative beta doses to build up the dose-response curve, with $R = L/T$.

The reliability of the protocol within a measurement was assessed through three checks. First, the dose-response curves were tested for consistency; i.e. that larger doses gave larger OSL signals ($R_1 < R_2 < R_3$). Second, the ratio between the two sensitivity-corrected OSL responses generated from the same regenerative dose (R_5/R_1, recycling ratio) is within 10% of unity. Third, the OSL response when a zero regenerative dose is administered, expressed as a percentage of the corrected natural OSL signal L_n/T_n, is small (recuperation test of Murray and Wintle, 2000). The percentage of grains that failed the above checks, and thus were rejected, are listed in Table 4.1.

4.3 Results

The results of the experiment are plotted in 3-D graphs where on the x - and y-axis is the ten-by-ten position-grid, and on the z -axis is the estimated dose rate. The spatial distributions of dose rates obtained using single-grain discs are shown in Figs. 4.1-4.4. The data used to obtain the plot shown in Fig. 4.4 are given in Table 4.2. For this source (6100), 12 discs, each carrying 100 grains, were used. Each point in the table is obtained by calculating the mean and standard error (not shown) from the individual measurements. Table 4.3 gives the individual measurements (and the mean and standard error) for two grain positions (1, 10) and (10, 2); these positions correspond to the positions giving the lowest and highest dose rates, respectively. In each case, the dose rate was measured on 8 grains (out of the possible

12 prior to the grain rejection criteria being applied).

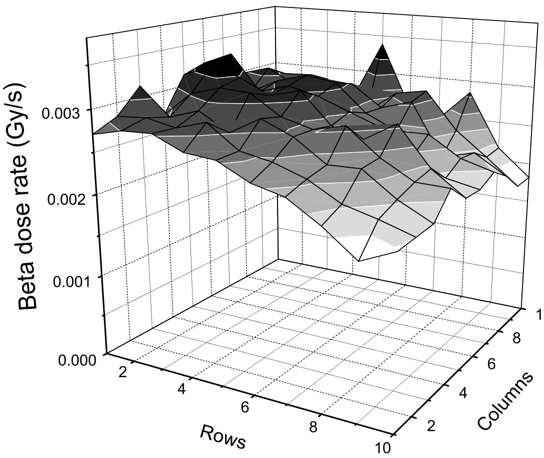

Figure 4.1: 3-D plot of dose rate (z axis) as a function of grain position (x, y) on ten-by-ten grid position for source 5583 (74 MBq SIP silver plaque source).

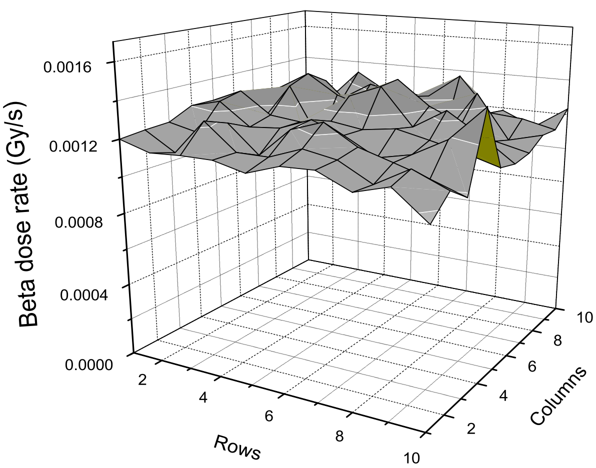

Figure 4.2: 3-D plot of dose rate (z axis) as a function of grain position (x, y) on ten-by-ten grid position for source 5626 (24.1 MBq SIF ceramic source).

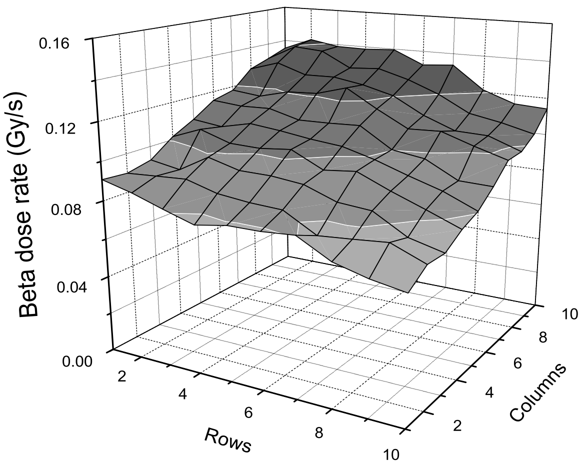

Figure 4.3: 3-D plot of dose rate (z axis) as a function of grain position (x, y) on ten-by-ten grid position for source 6100 (1.48 GBq SIF ceramic source).

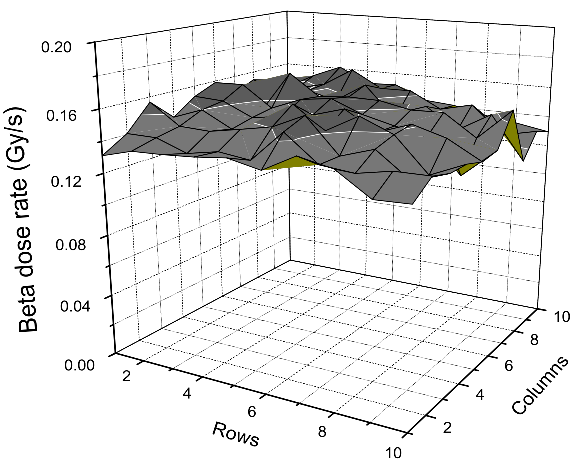

Figure 4.4: 3-D plot of dose rate (z axis) as a function of grain position (x, y) on ten-by-ten grid position for source 6088 (1.48 GBq SIF ceramic source).

Table 4.2: Source 6100: Average individual single-grain dose-rate estimates (Gy/s) calculated for each position on the disc (100 grains are measured on each of 12 discs). In bold are the minimum and maximum dose rate values

	1	2	3	4	5	6	7	8	9	10
1	0.090	0.087	0.081	0.076	0.078	0.080	0.078	0.071	0.067	**0.064**
2	0.090	0.091	0.092	0.087	0.087	0.084	0.075	0.076	0.078	0.073
3	0.091	0.089	0.098	0.095	0.094	0.091	0.086	0.084	0.076	0.071
4	0.102	0.108	0.102	0.101	0.103	0.095	0.094	0.089	0.083	0.076
5	0.108	0.106	0.108	0.108	0.105	0.103	0.099	0.093	0.088	0.080
6	0.116	0.114	0.114	0.110	0.110	0.111	0.101	0.098	0.089	0.088
7	0.118	0.116	0.120	0.121	0.123	0.118	0.108	0.108	0.102	0.098
8	0.128	0.133	0.128	0.127	0.125	0.120	0.110	0.105	0.104	0.097
9	0.131	0.140	0.138	0.131	0.132	0.126	0.121	0.112	0.105	0.104
10	0.136	**0.142**	0.139	0.137	0.140	0.133	0.134	0.121	0.115	0.111

Table 4.3: Source 6100: Dose rate measurements for 8 discs for two positions

Position	Individual dose rate estimates (Gy/s)								Mean and s.e.
(1,10)	0.136	0.147	0.142	0.132	0.149	0.150	0.137	0.142	**0.142± 0.002**
(10,2)	0.065	0.060	0.071	0.060	0.054	0.060	0.063	0.085	**0.064± 0.003**

For determination of the dose rate for one grain on one disc, e.g. that at position (1, 1) on the first disc, it is necessary to be sure that the OSL signal is measured reliably. The reproducibility of the OSL signal measurement through a SAR run can be assessed by looking at the recorded position of the laser beam during successive measurements. An example of this is shown in Fig. 4.5, where for the first grain the position of the measurement of the gamma dose is shown at the centre of a circle drawn to represent the size of a 300 μm diameter hole. The co-ordinate centres for each subsequent beta dose measurement (irradiation with source 6100) are shown. There is a slight movement (< 20 μm) for the second measurements and the remaining six are clustered at $\sim$ 100 μm from the initial position. This shows that no further relative measurement has occurred as a result of the movement of the disc whilst in the reader.

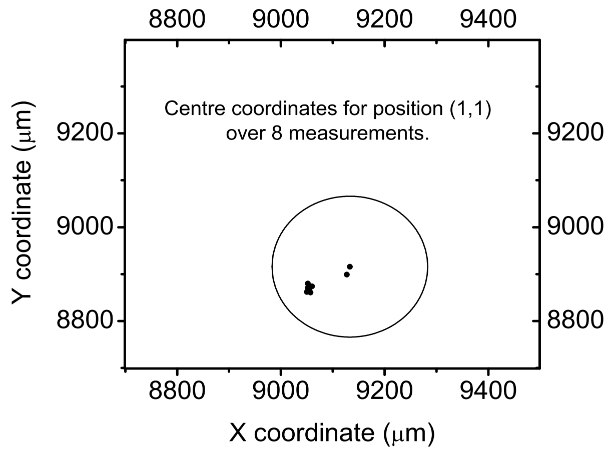

Figure 4.5: Plot of centre co-ordinates for position (1, 1) as obtained over 8 OSL measurements made in a SAR cycle. Circle drawn to show size of hole with its centre at the first measurement position.

The fact that the disc is not moving far relative to the laser beam, implies that it is not moving far relative to the beta source either. This will allow for the dose response curve for each grain in that position to be well defined. However, for it to be meaningful for the mean dose rate for a grain position, the discs should be placed in a similar position relative to the source. That this has been accomplished in this study, can be seen by plotting the recorded co-ordinates for four consecutively measured discs. In Fig. 4.6 these positions are shown for both the first (i.e. related to the gamma dose) and the last (i.e. related to the final beta dose). From this plot it is inferred that the dose rate is being measured at positions relative to the source that are within 500 μm.

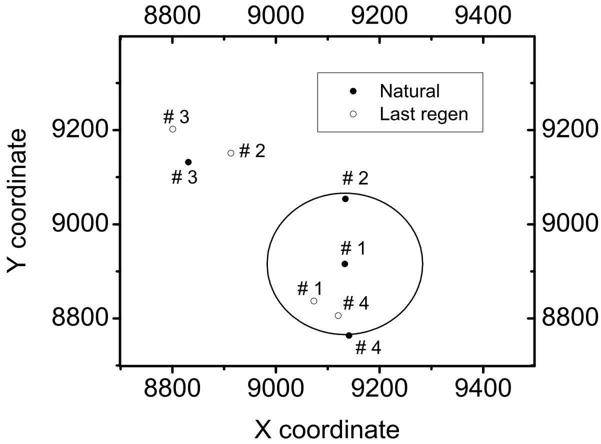

Figure 4.6: Plot of centre co-ordinates for first and last measurements of SAR run for position (1, 1) on each of four discs (#1, #2, #3 and #4). Circle drawn to show size of hole.

4.4 Discussion

A source's homogeneity can be assessed by visual inspection of the 3-D plots. Flat surfaces indicate spatial homogeneity of irradiation and such a surface is found for sources 5583 and 6088. If a non-flat surface is observed, this indicates that irradiation does not occur uniformly, and these are found for sources 5626 and 6100. The results shown in Figs 4.1-4.4 indicate that two of the sources result in a steep gradient in the dose rate across the 10x10 array of grains. In Fig. 4.1, showing the data obtained using the SIP type source (5583), the dose rate varies from 3.39 mGy/s to 1.81 mGy/s. In Fig. fig:6100, showing the data obtained using the SIF type source 6100, the dose rate varies from 0.142 Gy/s to 0.064 Gy/s (Table 4.1). For the other two SIF type sources, 5626 (Fig. 4.2) and 6088 (Fig. 4.4), the dose rate is much more uniform, and the maximum and minimum values for each source are given in Table 4.1. The ratio of the maximum to minimum values for the latter two sources is 1.41.

Non-uniform irradiation could be cause by non-uniform distribution of radioactive material on the source face. The method of manufacture of both types of sources employs the dropping of a liquid containing ^{90}Sr onto a surface. In the case of SIP sources, the liquid is evaporated from the silver plate that forms the front of the source (Aitken, 1985). In the manufacture of SIF sources, the liquid is dropped onto a ceramic surface, into which it can penetrate; this may result in it not being uniformly distributed prior to evaporation. There appears to be no immediate solution to this problem with source construction, though it has been suggested that a mini X-ray generator may provide an alternative (but uniform) irradiation source (Andersen *et al.*, 2003).

An alternative interpretation of the results is that the steep gradient in dose rate for sources 5626 and 6100 is caused by a mis-alignment of the source and the aperture through which the electrons pass. This possibility is supported by the high and low points in the plots being in the same position for both sets of irradiation. The experiment was not repeated with the sources in different orientations.

For single grain measurements, it is possible to obtain individual dose rates for each hole in a single grain disc and, indeed, it is essential to do this to avoid incorrect dose evaluation. However, it should be pointed out that there is likely to be a problem if these poorly-performing sources are used for measurement of aliquots made up of several thousand grains. It would still be possible to measure an average dose rate for a non-uniform source, using the uniformly bright calibration quartz spread over a 9 mm diameter area in the centre of the disc. However, in the case of un-sensitised sand-sized quartz grains, it has been demonstrated that only a small percentage of grains produce almost all the OSL signal (e.g. Duller *et al.*, 2000; Jacobs *et al.*, 2003b). These bright grains would be randomly distributed amongst the thousand or so grains on a sample disc. The value of the equivalent dose that would be calculated would depend upon exactly where the bright grains were situated. For a non-uniform source such as 6100, this could result in a previously unconsidered source of scatter in the distribution of the values of the equivalent dose. In contrast to the case for single grains, it is not possible to obtain an appropriate calibration and this will result in meaningless D_e distributions or, at the very least, prevent using overdispersion measurements to obtain information on bleaching history. For laboratories without access to a single grain reader, or equipment of the type used by Spooner and Allsop (2000), a simple test can be applied. A quartz grain can be placed several mm from the centre of a regular sample disc and given a dose. The disc should then be rotated by 180ř and the SAR protocol applied. If the number of seconds of irradiation required to match the first irradiation time is identical, then the disc may be considered to be uniformly irradiated.

4.5 Conclusions

Using OSL signals from highly-sensitised quartz grains that had been given a laboratory gamma dose, we have demonstrated that two of the four $^{90}Sr/^{90}Y$ sources in the Netherlands Centre for Luminescence Dating in Delft give non-uniform dose rates across the inner area of a standard 10 mm diameter sample disc. The measurement used single grains mounted in a 10x10 array within an area of 7.6 mm diameter.

Of the two sources that resulted in a uniform dose rate, both were of the SIF type. Of the two sources that showed poor uniformity, one was of the SIP type and one of the SIF type. This study has shown that it is essential to make a calibration for each hole position when using the single grain facility. The gradient across the 7.6 mm diameter area would make it inappropriate for use in regular dosimetry measurements in which grains of variable sensitivity are randomly distributed across a 9 mm diameter area of the 10 mm diameter aluminium disc.

It is not clear whether the strong non-uniformity of the measured dose rate is the result of non-uniformity of the radioactive material on the source face or the mis-alignment of the source and the aperture.

Bibliography

Aitken, MJ (1985). *Thermoluminescence dating.* Academic Press, London.

Andersen, CE, Bøtter-Jensen, L and Murray, AS (2003). A mini X-ray generator as an alternative to a ^{90}Sr/^{90}Y beta source in luminescence dating. *Radiation Measurements*, 37, 557–561.

Bøtter-Jensen, L, Andersen, C.E., Duller, GAT and Murray, AS (2003). Developments in radiation, stimulation and observation facilities in luminescence measurements. *Radiation Measurements*, 37, 535–541.

Bøtter-Jensen, L, Bulur, E, Duller, GAT and Murray, AS (2000). Advances in luminescence instrument systems. *Radiation Measurements*, 32, 523–528.

Bray, HE, Bailey, RM and Stokes, S (2002). Quantification of cross-irradiation and cross-illumination using a Risø TL/OSL DA-15 reader. *Radiation Measurements*, 35, 275–280.

Duller, GAT, Bøtter-Jensen, L, Kohsiek, P and Murray, AS (1999b). A high-sensitivity optically stimulated luminescence scanning system for measurement of single sand-sized grains. *Radiation Protection Dosimetry*, 84, 325–330.

Duller, GAT, Bøtter-Jensen, L and Murray, AS (2000). Optical dating of single sand-sized grains of quartz: sources of variability. *Radiation Measurements*, 32, 453–457.

Duller, GAT, Bøtter-Jensen, L, Murray, AS and Truscott, AJ (1999a). Single grain laser luminescence (SGLL) measurements using a novel automated reader. *Nuclear Instruments and Methods B*, 155, 506–514.

Duller, GAT and Murray, AS (2000). Luminescence dating of sediments using individual mineral grains. *Geologos*, 5, 87–106.

Glasser, NF, Harrison, S, Ivy-Oches, S, Duller, GAT and Kubik, PW (2006). Evidence from the Rio Bayo valley on the extent of the North Patagonian Icefield during the Late Pleistocene-Holocene transition. *Quaternary Research*, 65, 70–77.

Jacobs, Z, Duller, GAT and Wintle, AG (2006). Interpretation of single grain D_e distributions and calculation of D_e. *Radiation Measurements*, 41, 264–277.

Jacobs, Z, Wintle, AG and Duller, GAT (2003b). Optical dating of dune sand from Blombos cave, South Africa: II – single grain data. *Journal of Human Evolution*, 44, 613–625.

Jain, M, Thomsen, KJ, Bøtter-Jensen, L and Murray, AS (2004). Thermal transfer and apparent-dose distributions in poorly bleached mortar samples: results from single grains and small aliquots of quartz. *Radiation Measurements*, 38, 101–109.

Markey, BG, Bøtter-Jensen, L and Duller, GAT (1997). A new, flexible system for measuring thermally and optically stimulated luminescence. *Radiation Measurements*, 27, 83–89.

Mauz, B and Lang, A (2005). The dose rate of beta sources for optical dating applications: A comparison between fine silt and fine sand quartz. *Ancient TL*, 22, 45–48.

Murray, AS and Wintle, AG (2000). Luminescence dating of quartz using an improved single-aliquot regenerative-dose protocol. *Radiation Measurements*, 32, 57–73.

Spooner, NA and Allsop, A (2000). The spatial variation of dose-rate from ^{90}Sr/^{90}Y beta sources for use in luminescence dating. *Radiation Measurements*, 32, 49–56.

Thomas, PJ, Jain, M, Juyal, N and Singhvi, AK (2005). Comparison of single-grain and small-aliquot OSL dose estimates in $<$ 3000 years of river sediments from South India. *Radiation Measurements*, 39, 457–469.

Thomsen, KJ, Jain, M, Bøtter-Jensen, L, Murray, AS and Jungner, H (2003). Variation with depth of dose distributions in single grains of quartz extracted from an irradiated concrete block. *Radiation Measurements*, 37, 315–321.

Thomsen, KJ, Murray, AS and Bøtter-Jensen, L (2005). Sources of variability in OSL dose measurements using single grains of quartz. *Radiation Measurements*, 49, 47–61.

Truscott, AJ, Duller, GAT, Bøtter-Jensen, L, Murray, AS and Wintle, AG (2000). Reproducibility of optically stimulated luminescence measurements from single grains of Al_2O_3:C and annealed quartz. *Radiation Measurements*, 32, 447–451.

Chapter 5

Optimizing detection filters for single grain optical dating of quartz

Radiation Measurements, 40 (2005) 5-12

M. Ballarini[a], J. Wallinga[a], G.A.T. Duller[b], J.C. Brower[a], A.J.J. Bos[a], C.W.E. van Eijk[a]

[a] *University of Technology, IRI, Radiation Technology Group, Netherlands Centre for Luminescence Dating, Mekelweg 15, NL-2629 JB Delft, The Netherlands.*

[b] *Institute of Geography and Earth Sciences, University of Wales, Aberystwyth, Ceredigion SY23 3DB, UK.*

Abstract

We investigate the use of different optical detection filters for single-grain optically stimulated luminescence (OSL) measurements of quartz samples with a Risø TL/OSL single-grain reader. We selected three filter combinations that considerably improve the light detection efficiency when compared with the 7.5 mm U340 filters that are routinely used. These are the UG1+BG4 filter combination, the 2 mm UG1 and the 2.5 mm U340 filters, which allow a greater transmission in the quartz emission band. This leads to two benefits: 1) more grains can be accepted for equivalent dose analysis, and 2) OSL responses on individual grains are determined with a greater precision. While these three alternative filter combinations perform equally well if compared to each other, we suggest the 2.5 mm thick Hoya U340 to be the filter of choice as it allows the use of blue-diode and IR-diode stimulation sources for bleaching purposes and feldspar detection.

5.1 Introduction

Recent developments in luminescence measurement facilities (Bøtter-Jensen *et al.*, 2000) allow rapid measurement of individual sand-sized grains of a sample. A number of studies have shown that the optically stimulated luminescence (OSL) intensity of quartz varies considerably from grain to grain (Duller *et al.*, 2000; Murray and Roberts, 1997), and that only few grains show OSL signals that are bright enough to allow equivalent dose (D_e) determination. A criterion widely used to select grains that can be used for further investigation is based on counting statistics (e.g. Bush and Feathers, 2003; Thomsen *et al.*, 2003); data are rejected if the relative error on the test dose response is greater than 10-30%.

The number of grains accepted for D_e analysis might in principle be increased by improving the luminescence detection efficiency, for example by a better choice of detection filters. Detection filters are used for blocking light transmission in the region where the stimulation source emits, while transmission in the quartz emission band is allowed.

A cemented Hoya U340 filter of 7.5 mm thickness is commonly used in conventional Risø TL/OSL readers (Bøtter-Jensen *et al.*, 2003; Bush and Feathers, 2003; Feathers, 2003; Yoshida *et al.*, 2003) that make use of blue diodes (470 ± 30 nm) for stimulation. This filter has a high peak transmission (~60% at 340 nm; Fig.5.1) but allows a relatively low proportion of the quartz OSL to be transmitted because its window is not centered on the quartz emission band (peak at ~365 nm at room temperature, Huntley *et al.*, 1991). Risø single-grain OSL readers are equipped with a green laser for stimulation of sand-sized grains and also use a 7.5 mm U340 filter. However, since the emission of the laser (532 nm) is of a much longer wavelength than the blue diodes, blocking transmission in the blue region is no longer such an important point of concern. This allows us to use filters better centered on the quartz emission wavelength, even if their transmission band slightly extends into the blue region.

Here we investigate whether the OSL light collection for single-grain OSL measurements of quartz can be improved by using different detection filters. The aim of this paper is

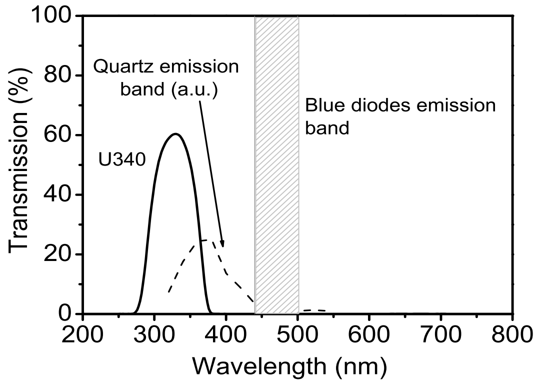

Figure 5.1: Transmission curve of a 7.5 mm thick Hoya U340 filter, the spectral distribution of quartz OSL emission (after Huntley *et al.*, 1991) and the emission characteristics of the blue-diodes used in this study.

to investigate whether more efficient light collection results in a larger number of accepted grains for further equivalent dose analysis.

5.2 Filter selection criteria

Besides the standard 7.5 mm thick U340, we tested five filter configurations (Table 5.1). Preliminary studies were carried out to check whether these filters fulfilled two basic requirements. Firstly, filters should have a high transmission in the quartz emission band and secondly, no transmission in the region where the green laser emits (i.e. negligible background as a consequence of light leakage from the stimulation source). Filters that showed satisfactory transmission characteristics were subsequently used in a number of experiments to select the most suitable filter configuration for OSL measurements of single grains of quartz.

Previous investigations used the highest signal-to-noise (S-N) ratio as a criterion for filter selection (Bøtter-Jensen and Duller, 1992). In OSL, but especially in single grain measurements, the decision of whether to accept grains for further calculations is based on the precision with which the OSL signal is determined. This too will be related to the relative magnitude of the signal and noise, but in a more complex manner than used by Bøtter-Jensen and Duller (1992). A commonly used parameter to estimate the uncertainty on an OSL signal is the relative standard error (RSE). For the calculation of the RSE we follow the definition given in Galbraith (2002) equation (7), (given below as equation 5.1):

$$RSE(\mu) = \sqrt{1 + \frac{\sigma^2}{Y}} \frac{\sqrt{Y_0 + Y/k}}{Y_0 - Y} \tag{5.1}$$

Table 5.1: Filters investigated in this paper

		Transmission	Instrumental BG (cps)[3]				OSL BG	OSL
Manufacturer	Filter combination	peak (nm)	T[2]	Green laser	Blue diodes	IR diodes	(cps)[4]	Transmission[5]
Hoya	7.5 mm U340	~ 340	1 (23)	27	40	50	87	1
Schott	1mm UG1 + 2mm BG4[1]	~ 360	2 (46)	111	5E+06	2E+06	682	2.4
Hoya	2.5 mm U340	~ 340	1.7 (38)	48	5E+03	1E+04	450	2.3
Schott	2 mm BG4	330-390	3.6 (83)	3E+05	–	–	–	–
Schott	1 mm UG1	~ 360	2.2 (51)	1E+06	–	–	–	–
Schott	2 mm UG1	~ 360	1.7 (39)	65	5E+03	5E+05	343	2.1

[1] In the text we refer to this filter combination as UG1+BG4 combination.

[2] Expected transmission of the quartz OSL signal through a filter combination (after Huntley *et al.*, 1991) normalized to the theoretical transmission of the 7.5 mm U340 filter. In brackets the expected transmission is given as percentage (see text for details).

[3] Instrumental background measured in counts per second on an empty disk with the green laser (532 nm), blue diodes or IR diodes on. The stimulation power was 90, 50 and 50% respectively.

[4] Average background measured on 800 untreated grains. Values refer to the last 10 channels of the luminescence signal stimulated by a green laser (see text and Table 5.2 for experimental details). This background includes the contribution of both instrumental noise and remaining OSL signal at the end of the stimulation.

[5] Experimental OSL transmission. Values are calculated by normalizing the total light sum for 800 untreated grains of each alternative filter (Fig. 5.5) to that of the 7.5 mm U340 filter.

where μ is the net signal calculated by subtracting the background from the initial signal; Y_0 the initial signal measured in the first n channels and Y the background measured in the last m channels; k is defined as m/n. The parameter σ^2 is calculated from the experimental results (Galbraith, 2002; equation (5)); and takes into account that the background counts, or the signal counts, may not follow a Poisson distribution but are over-dispersed. In the case of no over-dispersion σ^2 equals zero and the above formula reduces to its simplest form given in equation (3) in Galbraith (2002).

A commonly used procedure for determining the equivalent dose in quartz is the single-aliquot regenerative-dose protocol (Murray and Wintle, 2000). In such a situation, the RSE of the signal obtained from the test-dose response following the natural stimulation is commonly calculated and compared with a fixed threshold. The smaller the RSE the better the precision with which the OSL signal of a grain is known. Grains that show RSE values below this fixed threshold are selected for equivalent dose estimations, while the others are discarded. The threshold is usually fixed between 10 and 30% (Bush and Feathers, 2003; Feathers, 2003; Jain *et al.*, 2004; Thomsen *et al.*, 2002; 2003).

In this paper we investigate the dependency of the RSE on the detection filter used. In particular, we want to determine with which filter a) more grains can be accepted for further analysis, and b) the OSL signal of accepted grains is known with the highest precision.

5.3 Characterization of detection filters

Transmission characteristics of the filters listed in Table 5.1 were measured with a diode array spectrophotometer (Hewlett Packard 8452A) with a wavelength resolution of 2 nm.

5.3.1 First criterion - high OSL transmission

The transmission characteristics of the standard 7.5 mm U340 are presented in Fig. 5.1, together with the OSL quartz emission spectrum measured at room temperature (after Huntley *et al.*, 1991) and the blue-diode emission band (470 ± 30 nm; Bøtter-Jensen *et al.*, 2000). Note that the blue diodes have very broad emission tails, but that these are suppressed by short pass filters (GG420) in front of the diodes which cut emissions below 420 nm. The U340 filter allows transmission in the quartz emission band, while no transmission is possible in the blue diode emission band. Franklin *et al.* (1995) pointed out that the emission spectrum from the traps associated with the 325°C TL peak, which are related to the source traps that gives the OSL signal (Kaylor *et al.*, 1995; Smith *et al.*, 1986), is temperature dependent and moves to longer wavelengths as the temperature of the sample increases. A similar process is thought to occur for the OSL emission spectrum and this is likely to make the mismatch between the U340 transmission and the quartz emission spectrum worse when the sample is kept at elevated temperatures during stimulation (e.g. 125°C), as is commonly done (Murray and Wintle, 2000).

The transmission curves for the alternative filters studied here are plotted in Figs. 5.2 and 5.3. The proportion of the quartz OSL signal transmitted through the filter can be calculated by combining the transmission data for each filter with the emission characteristics from Huntley *et al.* (1991) (Table 5.1). The UG1+BG4 combination is very well centered on the quartz emission band and calculations give a detection efficiency of about 46% for this combination, which is double that of the 7.5 mm U340 (23%). The U340 filter of 2.5 mm thickness shows high transmission efficiency but it is less well centered on the quartz emission peak (5.3). The quartz OSL detection efficiency through this filter is about 38%. All the alternative filters listed in Table 5.1 show higher detection efficiency in the quartz emission window compared to the standard 7.5 mm U340 filter.

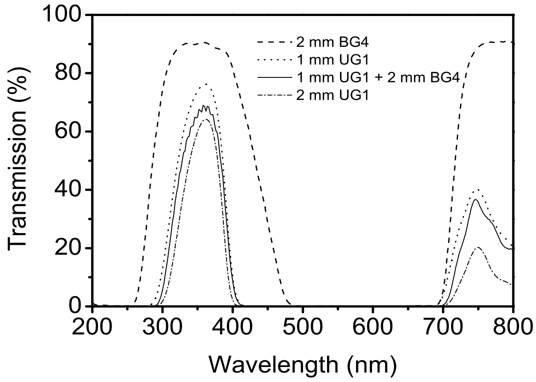

Figure 5.2: Transmission spectra of some alternative filter combinations.

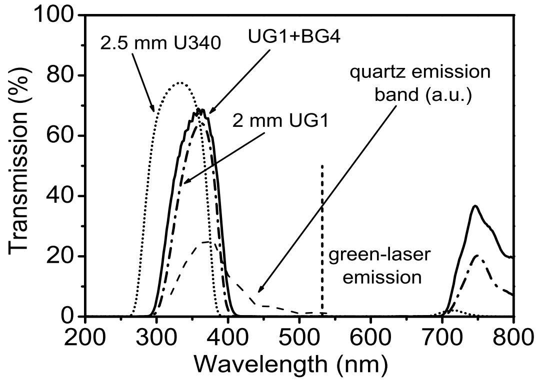

Figure 5.3: Transmission spectra of the Schott UG1+BG4 filter combination, a 2 mm Schott UG1 and of a 2.5 mm Hoya U340 filter. The quartz emission spectrum (after Huntley *et al.*, 1991)) and the green laser emission at 532 nm are shown as well.

5.3.2 Second criterion - low background noise

We tested whether the filters listed in Table 5.1 blocked the stimulation light sufficiently. Measurements on an empty single grain disk were made to quantify the background noise due to leakage of the 532 nm stimulation light with different filter combinations. An average background signal calculated over 100 empty single-grain holes is shown in Table 1. Using either 1 mm of UG1 or 2 mm of BG4 results in a high background signal arising from the stimulation source (Fig. 5.4). We conclude that used on their own, the 1 mm thick UG1 filter and the 2 mm BG4 filter are not suitable for single grain OSL measurements; these filters were discarded in further experiments.

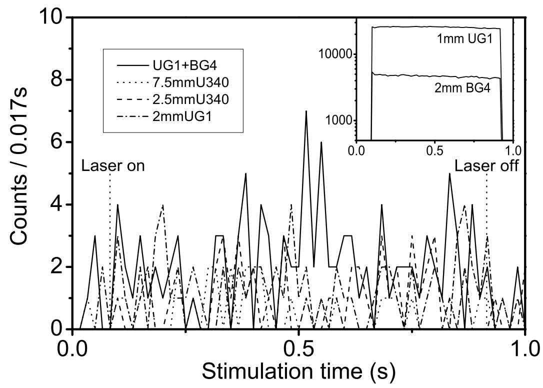

Figure 5.4: Typical background levels due to light leakage from the 532 nm laser measured on an empty disk for different filters (see also Table 5.1). The vertical dotted lines show when optical stimulation began and stopped.

Additionally, the background signal detected by the PM tube due to leakage of IR diodes was measured for these last three filter combinations. Even though the PM tube is not very sensitive in the IR region, this may cause problems when IR-lasers or IR-diodes are used to check for feldspar contamination (Duller, 2003). To test the effect of leakage from the IR-diodes on the PM tube, measurements at different stimulation power were undertaken on an empty single grain disk for each filter combination. A similar kind of check was carried out with the blue diode stimulation source. Results are presented in Table 5.1.

Since the UG1+BG4 filter combination, the 2 mm thick UG1 and the 2.5 mm thick U340 show high transmission in the quartz emission band, and at the same time provide sufficient light suppression at 532 nm (Fig. 5.4), further investigations are focussed on these three alternative filter configurations.

Table 5.2: Protocol applied to measure the OSL signal of single grains of quartz

Step	Treatment
1	0.83 s green OSL at 240°C
2	20 Gy β dose
3	10 s pre-heat at 200°C
4	0.83 s green OSL at 125°C (90% stim. power; 60 data points per sec.)
5	Back to 1

5.4 Experimental comparison

5.4.1 Samples and experimental details

We used untreated and sensitized quartz for our investigation (the word ŞuntreatedŤ used in this paper indicates quartz material that passed through the standard laboratory procedures to concentrate quartz but that was not sensitized by heating or dosing prior to measurements). The untreated quartz is from a sample taken from a 220-year-old dune ridge (sample TX02-02; Ballarini *et al.*, 2003). The sensitized quartz was provided by the Nordic Laboratory for Luminescence Dating (Denmark) and prepared by heating for one hour at 500°C and dosing with 5 Gy given by a ^{60}Co γ-source. Eight hundred grains of untreated quartz were loaded on eight single-grain disks, and as many grains of sensitized quartz were mounted on eight more disks.

We designed an experiment consisting of: initial bleaching, dosing, pre-heating and green OSL stimulation (experimental details in Table 5.2). The whole cycle was repeated three times on the same disks with each filter to check for any sensitivity change. However, no significant sensitivity change was observed. We used the three sets of measurements on the same grain to calculate σ^2 as shown in Galbraith (2002) and only the first set for RSE calculation. The luminescence response of a grain was calculated as the signal integrated over the first 0.083 s (five channels) with the average background signal integrated over the last 0.17 s (ten channels) subtracted.

5.4.2 Light detection efficiency

We compared the light detection efficiency of different filter combinations following the method proposed by Duller *et al.* (2000). Grains were ranked in order of descending net OSL signal and the cumulative OSL light sum plotted as a function of the proportion of the grains included. Results show that the light sum using the UG1+BG4 combination, the 2 mm UG1 and the 2.5 mm U340 filter, is more than 2 times higher than that using the 7.5 mm U340 filter (Fig. 5.5).

Results on sensitized quartz showed similar trends and the absolute OSL signal intensity was on average 300 times higher than for untreated quartz (data not shown). The absolute

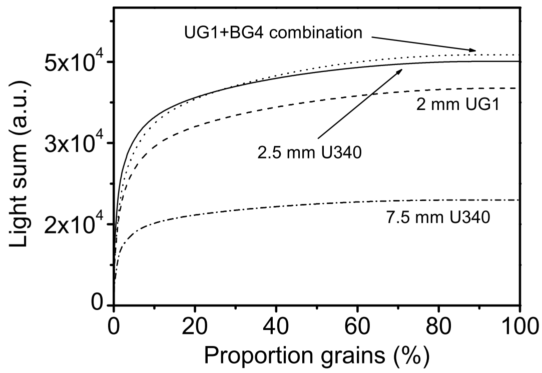

Figure 5.5: Distribution of net OSL signal intensity from 800 grains of untreated quartz using the U340 filters of 7.5 and 2.5 mm thickness, the 2 mm UG1 and the UG1+BG4 filter combination.

light sum for each filter, which gives the total OSL signal transmitted through a filter, is normalized to that of the 7.5 mm U340 filter and reported in Table 5.1. The mismatch between the measured and the expected transmission for the filters is due to the approximations inherent in deducing the parameters needed for the calculation of the expected transmission from the literature (e.g. Huntley *et al.*, 1991). If the relative light sum is plotted as a function of the brightest grains (Fig. 5.6), almost no difference in the four curvesŠ shape can be observed. This confirms that the only effect of using different filters is that more light from the same luminescence centers is detected.

The average background level calculated from the experimental data is also reported in Table 5.1. This is a combination of both the "late light" OSL signal due to slowly decaying components and the instrumental background, which is shown separately in Table 5.1.

5.4.3 Selection of the most suitable filter configuration based on RSE comparisons

Our selection of the optimal filter is based on two factors. Firstly, the number of grains that can be accepted, and secondly, the precision with which the luminescence signal can be determined, expressed as the relative standard error. We used the data from the previous experiment to calculate the RSE on all the 1600 grains measured with each of the different filter combinations.

To assess the impact of using alternative filters upon the proportion of quartz grains that would be accepted for equivalent dose analysis, the number of untreated and sensitized grains that gave RSE values within certain thresholds was calculated. Table 5.3 shows the number of grains with RSE values less than 1, 5, 10, 20, 30 and 50%.

To compare relative standard errors obtained on single grains using different detection filters we plot the RSEs obtained on individual grains against each other. This kind of plot is used to show graphically which of the two applied filters leads to a lower RSE on

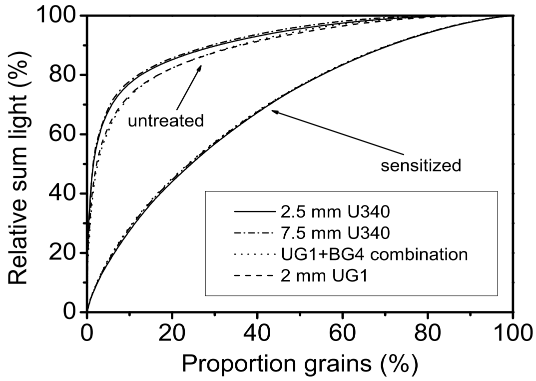

Figure 5.6: Distribution of relative OSL signal intensity from single grains of untreated and sensitized quartz as percentage of the total OSL light sum. The curves measured for the sensitized quartz overlap.

Table 5.3: Percentage of grains below a certain RSE threshold. The number of accepted grains is indicated in brackets. For sensitized quartz all grains are accepted for RSE values greater than 10%

Quartz (800 grains)	RSE threshold (%)	7.5 mm U340		UG1+BG4		2.5 mm U340		2 mm UG1	
a) Untrated	50	33	(260)	42	(336)	40	(323)	46	(367)
	30	15	(123)	20	(159)	20	(161)	23	(181)
	20	9	(70)	14	(109)	13	(101)	13	(107)
	10	3	(22)	6	(50)	6	(45)	6	(48)
	5	1	(10)	2	(17)	2	(13)	2	(14)
b) Sensitezed	10	100	(800)	100	(800)	100	(800)	100	(800)
	1	26	(205)	62	(499)	65	(520)	52	(413)

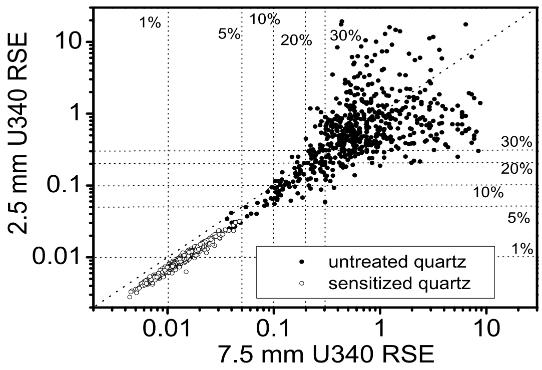

Figure 5.7: RSE comparison between the U340 filters of 7.5 and 2.5 mm thickness. A data point sitting on the one-to-one line indicates that the same RSEvalue was obtained for the two filters. When a grain is displayed below the one-to-one line, then the filter that is indicated on the y-axis gives the lowest RSE, and vice versa. The RSE thresholds of 1, 5, 10, 20 and 30% are also shown.

the same grain (i.e. with which filter the OSL response of a grain is known with a higher precision). In Fig. 5.7 the RSEs calculated for the 2.5mm U340 are plotted against the RSEs calculated for the 7.5 mm U340 filter. Comparing the 7.5 mm U340 filter to the UG1+BG4 combination and the 2 mm UG1 shows similar trends to that of Fig. 5.7 (data not shown). In Fig. 5.8 and 5.9 the RSEs for the UG1+BG4 and the 2 mm UG1 are plotted against the RSEs calculated for the 2.5 mm U340 filter.

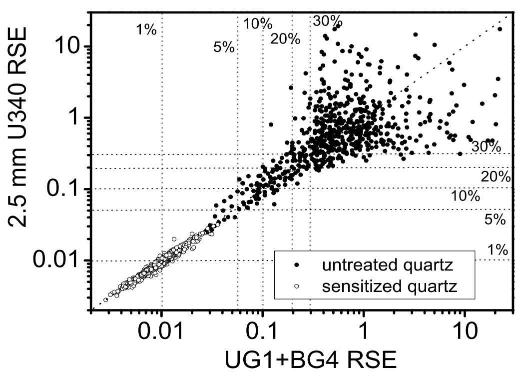

Figure 5.8: RSE comparison between the 2.5 mm U340 filter and the UG1+BG4 filter combination.

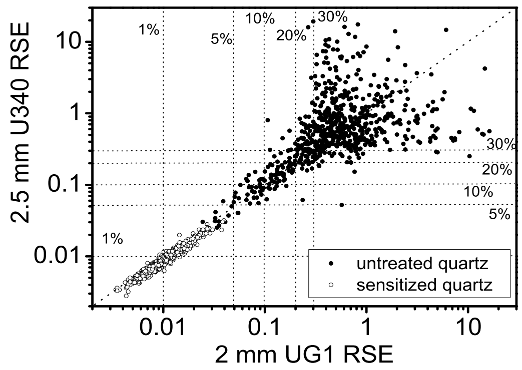

Figure 5.9: *RSE* comparison between the 2.5 mm U340 and the 2 mm UG1 filters.

5.5 Discussion

Table 5.3 shows that when any of the alternative filter combinations are used, a larger number of grains is accepted at any given *RSE* threshold when compared with the data obtained using the standard 7.5 mm U340 filter, reflecting the larger OSL signals obtained. This benefit is also evident from Fig. 5.7. For the dim grains, there is a large scatter in the data points. However, the general trend is for the data points to show lower *RSE* values for the 2.5 mm thick U340 when compared with the 7.5 mm thick U-340. The *RSE*s for the sensitized grains are lower than those for the untreated grains.

The three alternative combinations perform equally well when compared to each other (Figs. 5.8 and 5.9). However, from Table 5.3 it can be concluded that a) a slightly larger number of dim grains (*RSE* of 30-50%) are accepted by using the 2 mm UG1 filter and b) for extremely bright grains the lowest *RSE*s are observed with the 2.5 mm U340 filter (see "sensitized quartz" data set, $RSE < 1\%$).

The UG1+BG4 combination and the 2.5 mm U340 show similar transmission characteristics (difference of $\sim 3\%$, Fig. 5.5), resulting in these two filters having similar behavior in terms of the number of accepted grains for different *RSE* thresholds (Table 5.3). In Fig. 5.8 the *RSE*s of these two filters are compared and no significant differences are observed. A comparison between the 2 mm UG1 and the 2.5 mm U340 filters shows that a larger number of bright grains (sensitized quartz) is accepted when the latter filter is used (Table 5.3). This can be explained by considering the role that the OSL signal and the total background level obtained for the filters plays in the formula for calculating the *RSE*. From equation refeq:rse it can be seen that the *RSE* is a function of these two parameters only. In the extreme case of relatively dim grains the final *RSE* value is mainly dominated by the background, while for particularly bright grains it is dominated by the luminescence signal. Thus, for bright grains the higher the transmission of a filter the lower the *RSE*value. Conversely, lower *RSE* values for dim grains can be obtained with 2 mm UG1 filter, for which the total background is the lowest (Table 5.1).

It must be pointed out that grains with an associated relative uncertainty of 50% on the test dose response are usually discarded and only few untreated grains show RSE values lower than 5%. In practice, the common RSE range that one has to deal with spans from 10 to 30%. For this range we infer that the three alternative filter combinations represent an equal improvement over the standard U340 of 7.5 mm.

The data in Figs. 5.7-5.9 imply that the precision on the single-grain D_e estimates can be improved by using filters with higher transmission efficiency. This might result in more precise final values of D_e. However, in the presence of poorly- or even well-bleached materials, an improved precision on the estimates of D_e obtained from individual grains may not necessarily reduce the dispersion of the D_e dose distribution (Jacobs *et al.*, 2003a;b; Roberts *et al.*, 1999).

Results from measurements of the light leakage from IR and blue diode stimulation sources show a significant breakthrough for the alternative filters that precludes the use of these light sources for single- or multi-grain dating. In particular, the UG1+BG4 combination shows very high background values for these stimulation sources and should be avoided for purposes other than measurement using the green laser. The 2 mm UG1 and the 2.5 mm U340 filter combinations can be used with care with blue and IR diodes on single grain disks for rapid bleaching and feldspar detection, but not for dating purposes. The 2.5 mm U340 filter shows the lowest breakthrough for blue and IR diodes (Table 5.1).

5.6 Conclusions

A number of alternative filter configurations with high transmission efficiency were investigated for optically stimulated luminescence measurements of single grains of quartz. We found that the combination of a Schott UG1 and a BG4 filter, of 1 and 2 mm thickness respectively, the 2.5 mm Hoya U340 and the 2 mm UG1 are more suitable for single-grain OSL measurements than the commonly used 7.5 mm thick Hoya U340 filter. The advantages of these alternative filter configurations are that 1) more grains can be accepted for equivalent dose analysis and 2) single-grain OSL responses are known with a greater precision. Although they represent an equal improvement over the standard 7.5 mm U340 filter in terms of the number of accepted grains, for practical reasons the 2.5 mm thick Hoya U340 filter might be the filter of choice. This filter shows lowest breakthrough if compared to the other alternative filter combinations when blue- and IR-diodes are used, which allows the use of these sources for quick bleaching or feldspar detection.

5.7 Acknowledgements

We thank the reviewers for their valuable comments and A. Murray (Nordic Laboratory for Luminescence Dating, Denmark) for providing the sensitized quartz used in this study. J.W. is grateful for financial support from The Netherlands Organization for Scientific research (NWO VENI Grant 863.03.006).

Bibliography

Ballarini, M, Wallinga, J, Murray, AS, Van Heteren, S, Oost, AP, Bos, AJJ and Van Eijk, CWE (2003). Optical dating of young coastal dunes on a decadal time scale. *Quaternary Science Reviews*, 22, 1011–1017.

Bøtter-Jensen, L, Andersen, C.E., Duller, GAT and Murray, AS (2003). Developments in radiation, stimulation and observation facilities in luminescence measurements. *Radiation Measurements*, 37, 535–541.

Bøtter-Jensen, L, Bulur, E, Duller, GAT and Murray, AS (2000). Advances in luminescence instrument systems. *Radiation Measurements*, 32, 523–528.

Bøtter-Jensen, L and Duller, GAT (1992). A new system for measuring optically stimulated luminescence from quartz samples. *Nuclear tracks and Radiation Measurements*, 20, 549–553.

Bush, DA and Feathers, JK (2003). Application of OSL single-aliquot and single-grain dating to quartz from anthropogenic soil profiles in the SE United States. *Quaternary Science Reviews*, 22, 1153–1159.

Duller, GAT (2003). Distinguishing quartz and feldspar in single grain luminescence measurements. *Radiation Measurements*, 37, 161–165.

Duller, GAT, Bøtter-Jensen, L and Murray, AS (2000). Optical dating of single sand-sized grains of quartz: sources of variability. *Radiation Measurements*, 32, 453–457.

Feathers, JK (2003). Single-grain OSL dating of sediments from the Southern High Plains, USA. *Quaternary Science Reviews*, 22, 1035–1042.

Franklin, AD, Prescott, JR and Scholefield, RB (1995). The mechanism of thermoluminescence in an Australian sedimentary quartz. *Journal of Luminescence*, 63, 317–326.

Galbraith, RF (2002). A note on the variance of a background-corrected OSL count. *Ancient TL*, 20, 49–51.

Huntley, DJ, Godfrey-Smith, DI and Haskell, EH (1991). Light-induced emission spectra from some quartz and feldspars. *Radiation Measurements*, 18, 127–131.

Jacobs, Z, Wintle, AG and Duller, GAT (2003a). Optical dating of dune sand from Blombos cave, South Africa: I – multiple grain data. *Journal of Human Evolution*, 44, 599–612.

Jacobs, Z, Wintle, AG and Duller, GAT (2003b). Optical dating of dune sand from Blombos cave, South Africa: II – single grain data. *Journal of Human Evolution*, 44, 613–625.

Jain, M, Thomsen, KJ, Bøtter-Jensen, L and Murray, AS (2004). Thermal transfer and apparent-dose distributions in poorly bleached mortar samples: results from single grains and small aliquots of quartz. *Radiation Measurements*, 38, 101–109.

Kaylor, RM, Feathers, J, Hornyak, WF and Franklin, AD (1995). Optically stimulated luminescence in kalahari quartz: bleaching of the 325°c peak as the source of the luminescence. *Journal of Luminescence*, 63, 1–6.

Murray, AS and Roberts, RG (1997). Determining the burial time of single grains of quartz using optically stimulated luminescence. *Earth and Planetary Science Letters*, 152, 163–180.

Murray, AS and Wintle, AG (2000). Luminescence dating of quartz using an improved single-aliquot regenerative-dose protocol. *Radiation Measurements*, 32, 57–73.

Roberts, RG, Galbraith, RF, Olley, JM, Yoshida, H and Laslett, GM (1999). Optical dating of single and multiple grains of quartz from Jinmium rock shelter, northern Australia: Part II, Results and implications. *Archaeometry*, 41, 365–395.

Smith, BW, Aitken, MJ, Rhodes, EJ, Robinson, PD and Geldard, DM (1986). Optical dating: methodological aspects. *Radiation Protection Dosimetry*, 17, 229–233.

Thomsen, KJ, Bøtter-Jensen, L, Murray, AS and Solongo, S (2002). Retrospective dosimetry using unheated quartz: a feasibility study. *Radiation Protection Dosimetry*, 101, 345–348.

Thomsen, KJ, Jain, M, Bøtter-Jensen, L, Murray, AS and Jungner, H (2003). Variation with depth of dose distributions in single grains of quartz extracted from an irradiated concrete block. *Radiation Measurements*, 37, 315–321.

Yoshida, H, Roberts, RG and Olley, JM (2003). Progress towards single-grain optical dating of fossil mud-wasp nests and associated rock art in northern Australia. *Quaternary Science Reviews*, 22, 1273–1278.

Chapter 6

A modified SAR protocol for optical dating of individual grains from young quartz samples

Radiation Measurements, submitted

M. Ballarini[a,b], J. Wallinga[b], A.J.J. Bos[a], Wintle, A.G.[c]

[a]*Delft University of Technology, Faculty of Applied Sciences, Mekelweg 15, NL-2629 JB Delft, The Netherlands*

[b]*Netherlands Centre for Luminescence Dating, Delft University of Technology, Faculty of Applied Sciences, Mekelweg 15, NL-2629 JB Delft, The Netherlands*

[c]*Institute of Geography and Earth Sciences, University of Wales, Aberystwyth, Ceredigion SY23 3DB, UK.*

Abstract

We investigate the feasibility of a modified SAR protocol for OSL dating of young samples (< 300 years). Parameters such as pre-heat temperature, test- and regenerative-dose size, additional bleaching step at high temperature and optical stimulation time are optimized for the highest percentage of accepted grains. The optimized protocol makes use of a 50 Gy test dose, two regenerative doses of 5 Gy, an additional bleaching step and an optical stimulation of 10 s. No zero dose measurement is used in the equivalent dose determination. In particular, the use of a large test dose allowed a greater number of grains to be accepted by using a criterion of $< 30\%$ for the relative standard error for each grain. This protocol is validated in the second part of the paper using coastal-dune samples of known age. It is shown that the expected equivalent doses can be successfully retrieved if 1) short integration intervals are used for the natural and regenerated OSL signals as well as the test-dose responses and 2) the background is estimated from the subsequent two channels used for the signal. Conventional signal integration intervals and background subtraction methods resulted in gross D_e overestimation.

6.1 Introduction

Although optically stimulated luminescence (OSL) of individual quartz grains is a relatively young discipline, a number of papers have been published on the subject (e.g. Adamiec, 2000; Feathers, 2003; Jacobs *et al.*, 2003b; Olley *et al.*, 2004; Roberts *et al.*, 1999; Thomsen *et al.*, 2003). The increasing interest in single grain (SG) dating using the OSL signal is justified by its potential for dating poorly-bleached sediments (Roberts *et al.*, 2000). With SG techniques it is possible to determine whether the natural light exposure was sufficient to completely reset (bleach) the OSL signal of all grains, or just some of the grains in a sample. For non-uniformly bleached materials, the distribution of equivalent doses obtained for both single grains and single aliquots are usually wide and skewed, depending on the degree of bleaching (Murray *et al.*, 1995; Olley *et al.*, 1998; 1999; Wallinga, 2002a). It must be noted that factors other than poor-bleaching, such as heterogeneous microdosimentry (Murray *et al.*, 1997) and inclusions of grains in a sample with different depositional history (Jacobs *et al.*, 2003b), may also contribute to the spread observed in equivalent dose (D_e) distributions. Equivalent doses determined for insufficiently-bleached samples obtained using aliquots made up of a large number of grains (in the order of a few thousands) are overestimated by conventional methods (Duller *et al.*, 1995). Although poor bleaching can be recognized by means of SG analysis, determining a meaningful representative of the burial dose from D_e distributions obtained for single grains is not a straightforward process for a number of reasons. In the first instance, several works have shown that only a small percentage of grains shows a measurable luminescence signal (e.g. Duller *et al.*, 2000; Murray and Roberts, 1997; Yoshida *et al.*, 2000). They found that the luminescence brightness within a sample varies greatly from grain to grain and that only a few grains are responsible for most of the signal. Consequently, a large number of grains must be measured in order to obtain enough grains that are sufficiently bright to be used for D_e estimation. Secondly, there are no well-defined criteria for establishing which D_e values within a distribution should be included for calculation of the equivalent dose.

The most common criteria for selecting single grains are adopted from tests built into the single-aliquot regenerative-dose protocol (SAR) developed by Murray and Wintle (2000; 2003) for optical dating of multi-grain aliquots. These criteria are 1) grains for which a regenerative dose-response curve can be calculated, 2) a recycling ratio that is close to unity and 3) low recuperation. In order to select only those grains that show a luminescence response, an extra check is performed on the signal intensity of the first test dose OSL response. The calculated relative standard error (RSE; Banerjee *et al.*, 2000; Galbraith, 2002) must be below a certain threshold, which is usually chosen to be between 10 and 30% (Bush and Feathers, 2003; Jain *et al.*, 2004; Thomsen *et al.*, 2002; 2003). The choice of the RSE threshold is arbitrary. With a severe threshold only very bright grains are accepted; with a lower threshold a larger number of grains is accepted, but grains with low sensitivity to applied doses ("dim" grains) are also included.

Optical dating of individual grains from young deposits is rather problematic because of the very weak natural signals expected for low values of the natural dose. In this paper we aim at developing an appropriate SAR protocol for optical dating of single grains of quartz younger than 300 years. Firstly, parameters used in the SAR protocol such as pre-heat temperature, test- and regenerative-dose size, stimulation time and temperature and duration of the bleaching step will be investigated on quartz grains that have had their natural OSL removed by three separate optical stimulations of 10 s using a green laser. The aim of this investigation is to adjust the experimental parameters so that the percentage of grains accepted by means of the RSE test is maximized, and use these parameters in a new SAR protocol. In the second part, we validate our modified SAR protocol by comparing SG D_e values with those obtained in previous single aliquot (SA) work on very young aeolian samples with good independent age control.

6.2 Development of a modified SAR protocol

The Single-Aliquot-Regenerative dose (SAR) protocol developed by Murray and Wintle (2000) is the most widely accepted method used for single-aliquot OSL dating. Within this protocol, the natural OSL signal of the sample is first recorded (L_n). Subsequent laboratory (regenerative) doses are administered and the luminescence signals (L_i) are used to characterize the OSL dose-response of the sample. The equivalent dose D_e is estimated by projecting the natural OSL signal onto the growth curve and obtaining the D_e value for this point. SAR differs from other dose-regenerative methods in its ability to correct for sensitivity changes due to pre-heating. This is achieved by administering small test doses (D_t) in each measurement cycle and recording the OSL response to these doses (T_i). The sensitivity-corrected regenerative OSL signals are given by the ratio L_i/T_i and are used to construct a sensitivity-corrected dose-response curve. The reliability of the SAR protocol within a measurement sequence, for a particular sample, is usually assessed through two checks. In the first, the ratio between two sensitivity-corrected OSL responses generated from the same regenerative dose (recycling ratio) is determined. If this ratio is within 10%

of unity, the SAR protocol is thought to be reproducible. The second check consists of determining what the OSL response is when a zero regenerative dose is administered and it is usually expressed as a percentage of the corrected natural OSL signal L_n/T_n. Such a signal is expected to be zero, but transfer of charge from deeper traps occurred during previous irradiation, heating and optical stimulation may cause this signal (recuperation) to be greater than zero.

Murray and Wintle (2003) proposed the inclusion of an optical bleach at the end of each SAR cycle with blue diodes at 90% of the power for 40 s at a temperature higher than the one used for pre-heating (in their case 280°C for any preheat from 160 to 260°C). The purpose of this extra optical stimulation at high temperature is to remove charge that is thermally transferred from light-insensitive traps into the main OSL traps during preheat.

Since the SAR protocol as described above performs extremely well on a wide variety of of samples from different depositional environments, it was considered the most suitable protocol to be used for SG purposes. The implicit assumption is that if the SAR is reliable for aliquots containing a large number of grains, then it should also be reliable for aliquots made up of a single grain. However, single-aliquot and single-grain optical dating differ from one another in many aspects. The main difference is that only a tiny fraction of all the individually measured grains shows luminescence sensitivity to a given dose, and thus only a small percentage of the grains can be used for individual D_e estimation.

For SG measurements of young materials there are a few additional complications. Due to the low sensitivity of individual grains and the small natural luminescence signal of young samples, the SAR protocol cannot be applied in its original formulation as stated in Murray and Wintle (2000). Within the SAR protocol the test dose is conventionally chosen to be small compared to the expected dose and the regenerative doses to bracket the expected D_e. However, this procedure is impractical for dating of relatively young sediments because the OSL response to small doses is dominated by instrumental background. In the present paper, we investigate the feasibility of a modified SAR protocol.

The experiments described in this section are devoted to optimizing the SAR protocol for young samples and are summarized in Table 6.1.

6.2.1 Instrumentation

A Risø TL/OSL reader equipped with a single-grain attachment (Bøtter-Jensen *et al.*, 2000) was used for investigating both optically bleached and untreated quartz. With the single grain unit, automated measurements of the luminescence response from a large number of single grains are made possible by a sophisticated positioning system (Truscott *et al.*, 2000). A Nd:YVO4 diode-pumped laser ($\lambda \sim 532$ nm) capable of delivering 50 W/cm^2 to a grain is used for stimulating grains individually. In this study we selected a Hoya U340 filter of only 2.5 mm thickness for OSL signal detection in order to improve light collection efficiency compared to the standard filter thickness of 7.5 mm (Ballarini *et al.*, 2005). One hundred grains were mounted on each aluminium disk which had a grid of ten-by-ten 300 μm holes drilled in its surface to contain individual grains. During OSL measurements the disk was held at 125°C in order to prevent the 110°C TL trap from accumulating charge and subsequently contributing to the OSL signal (Murray and Wintle, 1998).

Table 6.1: Details of the experiments described in section 6.2

Step	Exp. 1 Additional step*	Exp. 2 Thermal transfer*	Exp. 3 Test-dose size*	Exp. 4 Dose response curves*
1	Bleach 10 s OSL at 210°C (x3)	Bleach 10 s OSL at 210°C (x3)	Bleach 10 s OSL at 210°C (x3)	Bleach 10 s OSL at 210°C(x3)
2	Dose = 0, 20 Gy	Dose = 50 Gy	Dose D_n = 10 Gy	Dose = 10, 40, 70, 100, 130 Gy**
3	10 s PH at 180°C	1 s OSL at room temperature	10 s PH at 180°C	10 s PH at 180°C
4	1 s OSL at 125°C	Dose = 20 Gy	1 or 10 s OSL at 125°C	10 s OSL at 125°C
5	Test Dose = 10 Gy	10 s PH at 120, 150, . . . , 300°C	Test Dose = 0.15 to 1000 Gy	Test Dose = 50 Gy
6	Cut Heat 160°C	1 s OSL at 125°C	Cut Heat 160°C	Cut Heat 160°C
7	1 s OSL at 125°C	Test Dose = 5 Gy	1 or 10 s OSL at 125°C	10 s OSL at 125°C
8	0, 1 or 10 s OSL at 210°C	Cut Heat 160°C	0, 1 or 10 s OSL at 210°C	10 s OSL at 210°C
9	Return to 2	1 s OSL at 125°C	Return to 2	Return to 2
10		10 s OSL at 210°C		
11		Return to 4		

* Experiments 1 and 2 use the same set of 800 grains; experiments 3 and 4 use two different set of 100 grains. For all optical stimulations 0.017 seconds per data point were used. The OSL signal and the background were calculated as the integrated counts over the first 5 and over the last 10 channels, respectively.

** The regenerative point of 40 Gy was repeated for the recycling ratio estimation.

6.2.2 Description of the experiments and results

Four experiments were carried out to test the reliability of a modified SAR protocol for OSL dating of quartz from young sediments. A single set consisting of 800 grains was used in the first two experiments, while two sets of 100 grains were used in the third and fourth experiments. Samples are from a coastal dune ridge that was formed about 300 years ago on the island of Texel - The Netherlands (Ballarini *et al.*, 2003). A grain size of 180-212 nm was used. Before each experiment, grains were optically bleached for ten seconds at 210°C using the green laser and this bleach was repeated twice more with a pause of 1000 s in between each bleach. The first stimulation is used to minimize the charge remaining in the main OSL traps, the delay is intended to allow the 110°C trap to empty without heating and the second stimulation empties any transferred charge from the 110°C trap into the OSL traps (Wintle and Murray, in press).

In the experiments that follow, we make use of a dose-recovery test for our investigations. In this test, a surrogate for the natural dose (N) is administered and treated as unknown. Such a dose is retrieved by using the standard SAR protocol, in which a single parameter at a time is studied, and compared to the value of the known dose. The purpose is to optimize the parameters used in the SAR for which a known dose can be retrieved with the best accuracy.

Testing the additional bleaching step (Exp. 1)

The usefulness of an additional bleaching step for our samples is investigated using laser stimulation at 210°C at 90% of the power. The experiment consisted of repeatedly administering and retrieving a dose of either 20 or 0 Gy to monitor possible recuperation effects from one cycle to the other. This was carried out using eight disks each containing 100 grains. A pre-heat temperature of 210°C and a cut-heat of 160°C were applied (the same temperatures were used in a previous single-aliquot work on the same samples; Ballarini *et al.*, 2003). A bleaching step consisting of optical stimulation for 1 or 10 s at 210°C was introduced after each SAR cycle to investigate whether prolonging the exposure time increased the bleaching efficiency. These results were compared with those from a similar experiment where no additional bleaching step was used. The choice of the 210 °C temperature for the bleaching step, follows the suggestion of Murray and Wintle (2003) of using a temperature which is slightly above the preheat temperature.

Results from this experiment (Fig. 6.1) show that although the *measured* recuperation can be reduced (filled circles for zero dose points) from 10% to close to 5% by introducing an additional bleaching step at the end of a SAR cycle, the benefits in terms of reducing the spread in the sensitivity-corrected OSL signals are not evident. In fact, a similar spread in corrected OSL signals is observed through the cycles regardless of the use of the bleaching step. However, it can be seen that the measured recuperation is smaller when 10 instead of 1 s optical bleaching is used (filled squares for the two 0 Gy points). In order to reduce as much as possible recuperation effects induced by the use of high test doses, an extra bleaching step consisting of 10 s OSL stimulation (90% of laser power) at 210°C was introduced at the end of each SAR cycle in all the subsequent experiments in this study.

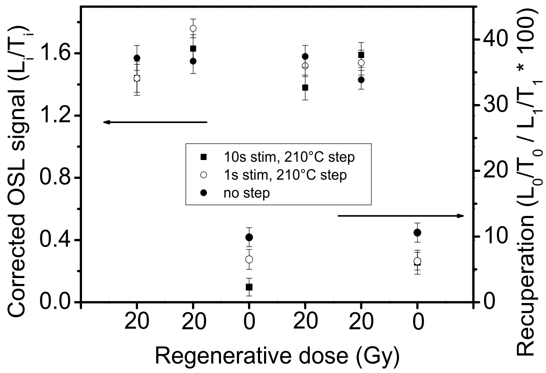

Figure 6.1: Effect of the additional bleaching step at the end of each SAR cycle on the recuperated OSL signal through repeated cycles, giving doses of 20, 20, 0, 20, 20 and 0 Gy in turn. For the 20 Gy doses, values of L_i/T_i are given. For the two cycles for which the administered dose was zero, recuperation is expressed as a percentage of the sensitivity-corrected OSL signal for the 20 Gy dose. Each data point is the average of the grains (about 50 for each recycling cycle) that showed a RSE of less than 30% for the test dose OSL measurement (10 Gy). For the last cycle, the two data points at the bottom overlap.

Dependency on the pre-heat temperature (Exp. 2)

The effect of the pre-heat (PH) temperature on the final equivalent dose has been extensively discussed (Duller, 1991; Jain *et al.*, 2004; Stokes, 1994). Here such a dependency is assessed within a dose-recovery test. In this experiment, a second set of 800 grains was prepared using a different bleaching procedure. This was designated to mimic the bleaching process that grains experience in a natural environment. It consisted of a three-time optical bleaching at a temperature of 210°C, as explained above, giving a dose of 50 Gy that acted as a surrogate for the geological dose received in nature and laser stimulation of each grain for 1 s at room temperature. In this way the thermally unstable traps filled by the laboratory irradiation were not depleted and the influence on the final D_e of thermal transfer during the first OSL measurement can be investigated.

Pre-heat tests cannot be applied for single grains in a sample in the same way that they are normally performed for aliquots made up of multiple grains. For the latter, each aliquot is assumed to be representative of the whole sample and results for pre-heat tests obtained from a few aliquots are applied to those to be used for D_e estimation. However, single grains differ highly from one another in terms of luminescence properties and thus preheat plateaus from individual grains cannot be generalized. The approach adopted here is to investigate the average preheat plateau of 800 individual grains and from these extend the results to other single grains from the same sample.

The use of different parts of a decay curve for aliquots made up of multiple grains and using optical stimulation from blue light-emitting diodes for D_e estimation was studied by

Banerjee *et al.* (2000). They concluded that smallest statistical uncertainty in the net OSL signal was achieved by using the first second(s) of the OSL signal rather than the whole stimulation curve obtained after 60 seconds (Banerjee *et al.*, 2000; Fig. 1). In addition, the use of short integration intervals has the advantage that the signal is dominated by the most light-sensitive component of the OSL signal. In this way, the difficult-to-bleach component that is present when integrating of the whole signal is avoided. The net OSL signal was calculated by subtracting a background based on the signal observed at end of the stimulation period. Here we use a similar approach but for laser stimulation the collection time per channel was 0.017 s. The net OSL response was calculated either by integrating over the first 0.034 or 0.17 s of the decay curve and using the last 0.17 s for late background (LBG) correction, or by integrating the signal over the first 0.034 s and using the subsequent 0.034 s for background subtraction (we refer to this technique as early background (EBG) subtraction; the rationale of this subtraction method will be discussed in detail in section 6.3.

Frequency distributions of the retrieved dose for all the grains measured using different pre-heat temperatures are presented.

For a pre-heat temperature of 180°C, dose recovery ratios (measured/given) could be calculated for 67 grains out of 800 (grains rejected if $RSE < 30\%$). This is shown in inset a) to Fig. 6.2. For a pre-heat temperature of 300°C dose recovery ratios were calculated for 32 grains out of 400 (inset b) to Fig. 6.2). The mean values for the above preheat temperatures are 1.08 ± 0.41 and 2.78 ± 0.99, respectively (the two outliers at 12 and 23 Gy shown in the inset (b) were not included in the calculation). Only in the first case there is consistency with unity.

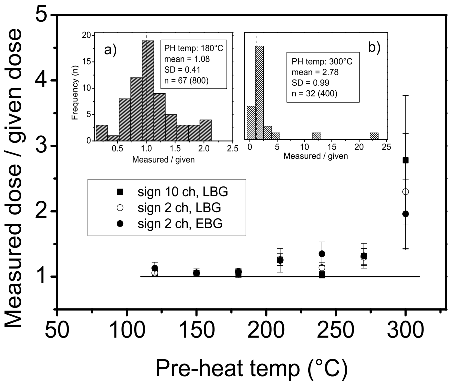

Figure 6.2: Dose-recovery ratios are plotted as a function of the pre-heat temperature. The OSL signal was integrated over the first 0.034 s (open circles) and over the first 0.17 s (filled squares) both using the last five channels for the LBG subtraction (0.085 s), and over the first 0.034 s using the subsequent 0.034 s for EBG subtraction (filled circles). Insets show dose-recovery ratio distributions when pre-heat temperatures of a) 180°C and b) 300°C were used (OSL signal integrated over the first 0.17 s, LBG).

The ratio of the measured dose to the given dose is plotted as a function of the pre-heat temperature (Fig. 6.2). Each data point is the average determined on approximately 50 individual estimates.

The luminescence response was calculated using three different integration intervals for the signal and the background: a) first two channels (0.034 s) and b) first ten channels (0.17 s) for the signal, both with late background (LBG) subtraction of five channels (0.085 s); c) first two channels for the signal and subsequent two channels for the background (EBG). The latter background correction technique will be discussed in detail in the next section. From the main data set in Fig. 6.2, we conclude that for this sample thermal transfer effects are not significant for pre-heat temperatures up to at best 180°C.

Test-dose size (Exp. 3)

We also investigated the effect of the size of the test dose on a) estimation of a laboratory-given known dose N, b) the percentage of grains accepted after rejection criteria have been applied and c) the recuperation.

The use of relatively large test doses is likely to be advantageous when the RSE of the OSL test dose response is used as a rejection criterion. The use of higher test doses is likely to lead to lower RSE values for the test dose OSL signal, as the RSE is inversely proportional to the luminescence response to a given dose. As a consequence, more grains may be accepted when larger test doses are used and individual equivalent dose estimates calculated with a higher precision. Disadvantages of administering large test doses are longer irradiation times and possible recuperation effects due to thermal transfer.

In this study, a dose-recovery test was performed using different test doses ranging from 0.15 to 1000 Gy. Three doses of 10 Gy were given in each SAR measurement sequence (Table 6.1), one (N) that was taken as the unknown, one as the first regenerative dose (R_1) and a third to obtain the recycling point (R_3). The OSL response to a given dose of 0 Gy was also measured (R_2) in order to monitor recuperation effects. The whole experiment was repeated using either 1 or 10 s laser stimulation, with and without the additional bleaching step. In both cases we used a collection time per data point of 0.017 s. The first 0.085 and the last 0.17 s were used for initial signal and background estimation, respectively. The photomultiplier background was estimated to be approximately $\sim$ 118 counts per second.

No clear dependency of the measured-to-given dose response ratio (R_1/N) on the test-dose size was observed (Fig. 6.3a). The two sets of data, obtained for 1 s stimulation with no extra bleaching (open circles) and for 10 s stimulation with extra bleaching (filled circles), show large spread around unity, the expected value. However, the spread was reduced for the second data set (filled circles), as found from a least square calculation. A similar reduction in spread of data is evident when the recycling ratio R_3/R_1 is plotted as a function of the test-dose size (Fig. 6.3b); in addition, for the lower test doses, values obtained using the 1 s stimulation and no extra bleaching are systematically lower than unity. Fig. 6.3c shows that the percentage of grains that are accepted after application of the rejection criteria increases with test-dose size up to 50 Gy. From Fig. 6.3a it can be seen that, even with a test dose as large as 1000 Gy (100 times higher than the given dose), it is possible to recover the administered dose. Regarding this last point, large recuperation was measured when the additional bleaching step was not applied, while recuperation of a few percent was observed after introduction of the additional bleaching step (data not shown).

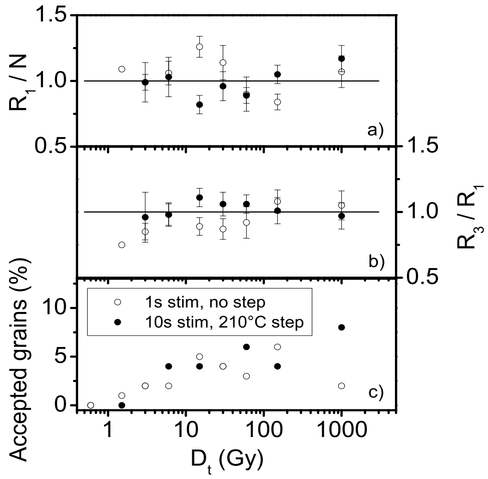

Figure 6.3: Dependency on the test-dose size (D_t) of a) the dose recovery ratio (R_1/N) for a surrogate natural dose of 10 Gy, b) recycling ratio (R_3/R_1) and c) percentage of accepted grains. The experiment was first carried out using a 1 s OSL stimulation and no additional bleaching step (open circles) and then repeated on the same grains using 10 s OSL stimulation and the extra bleaching step at high temperature (filled circles). A single set of 100 grains was used for the two experiments.

Dose-response curves (Exp. 4)

The dose-response curves of several grains obtained using several regenerative doses, but no zero point, were investigated. For young sedimentary grains that are the object of this study, we consider the possibility of using a single regenerative dose chosen to be in the linear region of the growth curve. In this way, equivalent doses could be calculated by projecting the natural OSL response onto the line between the regenerative point (R_1) and the origin, provided that recuperation is negligible. In order to assess the feasibility of such a procedure, which will be used in the next section, we studied the dose-response curves of several single grains. The following equation was used for fitting the OSL dose-response curves constructed with five regenerative dose points:

$$I = I_{sat}(1 - e^{-D/D_0}) \tag{6.1}$$

where I_{sat} is the sensitivity-corrected OSL intensity at saturation, I is the sensitivity-corrected OSL intensity produced by D, the laboratory regenerative dose, and D_0 is a dose parameter indicative of the onset of saturation. The fitted curves were forced through the origin and no evidence of the need for adding a linear term was found.

In Fig. 6.4 six dose-response curves from laboratory irradiated grains are presented. Different types of saturation rates can be observed. Information on the fitted curves obtained for these grains using a saturating exponential function (given as equation 6.1) are presented in the inset table in Fig. 6.4. The majority of the grains show saturation above 100 Gy, while a few saturate at doses as low as 40 Gy. The information presented here for laboratory irradiated quartz will be used in section for measurements of untreated quartz grains.

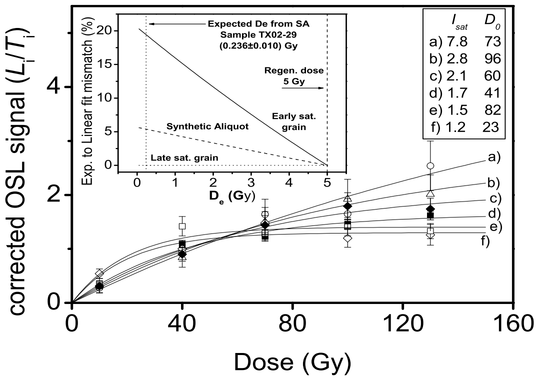

Figure 6.4: Six dose-response curves for single grains of quartz (sample TX02-29) corrected for sensitivity changes using the response to a 50 Gy test dose. In the inset, the percentage mismatch between expected D_e and D_e obtained by linear interpolation between the origin and a point at 5 Gy. Estimates are given for the synthetic aliquot (dashed), for one early-saturating grain (solid) and for a grain whose dose-response curve is almost linear (dotted). Results from the exponential fitting of the curves are also presented (inset table).

6.2.3 Discussion

Murray and Wintle (2003) showed that, for dose-recovery experiments, the measured-to-given dose ratios were closer to unity when an additional high-temperature bleaching step was applied after a SAR cycle. Based on our experiments, we conclude that the additional bleaching step leads to little benefit in terms of accuracy for the recovered-dose estimation (Fig. 6.1 and Fig. 6.3a), but does lead to a remarkable reduction in the measured recuperation (Fig. 6.1). This result suggests that for the measured grains changes in recuperation do not significantly affect the recovered dose. However, it is possible that high recuperation may lead to D_e overestimation for different samples. Therefore, in subsequent experiments for quartz containing a natural depositional dose, an extra optical bleaching for 10 s at 210°C was introduced after each SAR cycle.

In Fig. 6.2 we demonstrated that thermal transfer affects on the recovered dose are negligible in the temperature range of 120-180°C using different regions of the decay curve for signal integration and background subtraction. This is in agreement with our findings for multi-grain aliquots from the same sample (Ballarini *et al.*, 2003) and therefore we selected a PH temperature of 180°C for subsequent measurements on natural samples. A recovered dose ratio consistent with unity was also found by using only the first 0.034 s (instead of 0.17 s) for the OSL signal and when using a background subtracted from either the early or the late part of the decay curve, indicating no dependency of the recovered dose on the integration interval. As already pointed out by Jain *et al.* (2004), the frequency distribution of the equivalent doses measured from single grains becomes broader and more skewed as the pre-heat temperature increases. A similar trend was found for our grains (inset of Fig. 6.2).

Murray and Wintle (2000) previously studied the effect of test-dose size within the SAR protocol and possible influences of it on the final D_e estimation. They showed that the D_es obtained did not vary over a broad range of test doses sizes up to three times the size of the natural dose. In their experiments, Roberts et al. (2000) used a test dose as large as the natural dose (5 Gy) to maximize the OSL signals from single grains. In a broader study, Galbraith *et al.* (2005) examined the error variation on the recycling ratio within a SAR protocol when test doses as large as 0.5 and 5 Gy were administered (expected equivalent doses from 2.74 to 46 Gy). Their results showed that the accuracy for the retrieved dose is not dependent on the test dose size. We obtained similar results, although we studied the effects of test-dose size over a much wider dose range (0.15 - 1000 Gy). The benefit in terms of accepted grains of using relatively large test doses has been demonstrated in Fig. 3c. More grains are accepted when using a larger test dose value for the RSE criterion.

If LBG subtraction is used, almost twice as many grains are accepted when using a fixed RSE percentage acceptance, compared with those when EBG subtraction is used. However, using grains with the LBG subtraction does not give the correct value of the expected dose. The acceptance rate is higher using the LBG because the net number of counts is larger, but that is at the expense of accepting luminescence that had not been bleached at deposition derived from optically sensitive traps other than the fast OSL traps.

It has been demonstrated that a variety of growth curves with different shapes can be observed from grains within a sample (Adamiec, 2000; Jacobs *et al.*, 2003b; Yoshida *et al.*, 2000). These authors found that for their samples the majority of the grains saturated in the range of 100-200 Gy, but a few saturated at doses lower than 50 Gy. Similarly, in our study, we found that most of the grains saturate at doses above 100 Gy, but some saturated at doses well below this. Since the natural samples collected from Texel have expected doses far below 100 Gy , the use of a single regenerative dose chosen in the "linear" region of the dose-response curve is feasible. For samples less than 300 years and with dose rates of < 1 Gy/ka, D_es are expected to be < 1 Gy.

For the new SAR protocol (Table 7.1), a regenerative dose of 5 Gy was chosen and a test dose of 50 Gy was employed for natural quartz. Two regenerative doses of 5 Gy were used, the first for D_e calculation and the second to test for reproducibility (recycling ratio). A zero dose point was measured, but not used either for construction of the dose-response curve or as a rejection criterion. This is because the OSL responses to a zero dose are highly scattered on a single-grain basis, and the measured values (expressed as percentage of R_1) vary from -1000 to 1000. We decided that these recuperation points are not suitable for construction of the dose-response curve.

Test doses were applied and the resulting OSL signals measured after all four measurements in this modified SAR protocol. After the final measurement for construction of the dose response curve, the test dose was repeated and measured after the disk had been exposed to IR for 40 s at room temperature; this was used to check for the presence of feldspar grains on the disk. Equivalent doses were estimated by interpolation between the origin of the axis and the OSL response to the first regenerative dose. The advantages of such a method are the shorter measurement times and the fact that no fitting through the regenerated points is needed. The uncertainty introduced by this modified procedure, rather than using full growth curves, is discussed in the next section.

6.3 Validation of the modified SAR protocol for young natural quartz samples

6.3.1 Samples

We validate our modified SAR protocol using two aeolian samples from a coastal dune ridge developed about 300 years ago on the island of Texel (The Netherlands). These samples have codes TX02-29 and TX02-31, and have expected D_es obtained by SAR using multi-grain aliquots of 0.236 ± 0.010 and 0.244 ± 0.009 Gy, respectively. Ages calculated using these results are in agreement within errors with historical records available for that area. Thus, we infer that these samples experienced sufficient light exposure before deposition. Extensive information on these samples can be found in Ballarini *et al.* (2003). Two thousand single grains from both samples were analyzed for D_e estimation. The modified SAR protocol used for these measurements is explained in Table 7.1.

6.3.2 Experimental details

OSL signal integration and background subtraction

Several different integration regions both for signal and background were investigated (for L_i as well as T_i). These regions are shown in Fig. 6.5. The first 0.034 s of the recorded signal were used for determining the intensity of the OSL response of a grain. With such a short integration interval, we aim at focusing on the fast component of the decay curve. The subsequent 0.034 s were used as an estimate of the early background (EBG), while the last 0.085 s were used for a standard late background subtraction (LBG). Using the EBG subtraction may represent a more appropriate choice regarding our hypothesis of using only the fast component of the signal. In fact, the EBG takes into account the eventuality that the medium and/or slow components present in the natural signal may not have been completely bleached before deposition. If such components are not present in the natural OSL response, the EBG acts in a similar way to the LBG subtraction. We tested this by estimating theoretically the contribution of the medium component to the total OSL signal after the EBG and the LBG (integrated over 0.034 and 0.085 s, respectively) were subtracted from the initial signal (first 0.034 s).

It must be noted that there are two scenarios in which our method based on the calculation of D_es based on the EBG will not work. These are poor-bleaching and/or absence of the fast component (in the first case, no OSL-based method is able to determine a D_e representative of the burial dose).

Table 6.2: Modified SAR protocol used for D_e estimation of natural quartz from very young samples

Step	treatment	Observed
1	Dose, D_i[1] ($i = 1, \ldots, 4$)	–
2	10 s PH at 180°C	–
3	10 s OSL at 125°C[2]	L_i
4	Test dose, $D_t = 50$ Gy	–
5	Cut Heat 160°C	–
6	10 s OSL at 125°C	T_i
7	10 s OSL at 210°C	–
8	Return to 1	–
9	Test dose, $D_t = 50$ Gy[2]	–
10	Cut Heat 160°C	–
11	40 s IRSL at room temperature	–
12	10 s OSL at 125°C	T_{IR}

[1] In the first cycle ($i = 1$) no dose was given and the natural OSL signal recorded. The administered regenerative doses were 5, 0 and 5 Gy.

[2] Decay curves were collected in 600 data points (10 s). For the first and the last 5 channels the laser was switched off. OSL data points were collected each 0.017 s.

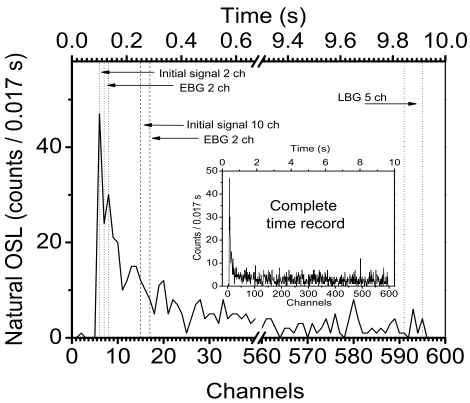

Figure 6.5: Example of the beginning (35 channels) and end (last 35 channels) of a natural OSL decay curve measured over a total of 600 channels (as seen in inset) from a bright grain (sample TX02-31). Different integration intervals for the initial signal and the background are shown (vertical lines). Laser stimulation starts at channel 5 and ends at channel 595; in channels 1-5 and 596-600 only PM tube noise is observed.

In our calculations, the OSL decay curve of a grain was approximated as the sum of three components plus a constant. These are taken to be the fast, the medium and a single slow component. Each component is described by a single exponential decay curve of the form given below:

$$OSL_i(t) = A_i \exp(\lambda_i t) \tag{6.2}$$

where i is indicative of the three components (i = fast, medium and slow), Ai are the maximum intensities and i the decay constants for each component. In particular, fast was taken from Bulur *et al.* (2002), while medium was derived from the photoionization cross-section of the medium component given in Singarayer and Bailey (2004). The total signal is given by $\sum_i OSL_i(t)$. The percentage contribution of each component to the net OSL signal after EBG subtraction is compared to that after LBG subtraction. We assumed a total stimulation time of 10 s (0.017 s per data point), since this is the one applied in the measurements described later in this section. The equation we used is:

$$\frac{OSL_{\mathrm{EBG}_i}}{OSL_{\mathrm{EBG}_i}} = \frac{A_i \left(\int_0^{t_s} \exp\left(\lambda_i t\right) - \int_{t_s}^{t_{\mathrm{EBG}}} \exp\left(\lambda_i t\right) \right)}{A_i \left(\int_0^{t_s} \exp\left(\lambda_i t\right) - \int_{t_{591}}^{t_{595}} \exp\left(\lambda_i t\right) \right)} \tag{6.3}$$

where t_s is the time over which the initial signal was integrated in the first n channels ($t_\mathrm{s} = n \cdot 0.017$ s; $n = 1, 2, 10$); t_{EBG} is time used for integrating the EBG in the subsequent m channels ($t_{\mathrm{EBG}} = m \cdot 0.017$ s; $m = 1, 2$); $t_{591} - t_{595}$ is the time interval used for the LBG and corresponds to the last five channels of the decay curve (for $t_{591} = 9.85$ s; $t_{595} = 9.93$ s).

The results are given in Table 6.3. If the first channel is used for the initial signal and the subsequent channel for the EBG, the contribution of the medium component to the net signal is reduced to 9% compared to that given by using the LBG. However, the fast component is reduced by about 50%. When as many as ten channels are used for the initial signal and two for the EBG, the contribution of the medium component is reduced only to 89%, while the fast component contributes 100% to the net OSL signal. The medium-to-fast ratio is lower when short intervals are used for the signal (thus optimal, with regard to our hypothesis of using only the fast component for D_e calculations); the contribution of the medium component increases with longer intervals. However, the smaller the intervals used for integration, the smaller the intensity of the OSL signal. Hereafter, we chose to integrate the initial signal over the first 0.034 s and to use the subsequent 0.034 s for the EBG. This leads to a reduction of the medium component to 17% on the measured signal, while 78% of the fast component is still contributing to the net signal.

The different contributions of the fast, medium and slow components within a decay curve of a synthetic aliquot made up of 400 grains is shown in Fig. 6.6. For a synthetic aliquot, the sum of the luminescence signals obtained from several individual grains is used, as previously used by Henshilwood *et al.* (2002) and Jacobs *et al.* (2003b). The data have been fitted with a function containing the three exponential components plus a constant background. The decay rates of the fast (45 s^{-1}) and medium (5.52 s^{-1}) component were taken from Bulur *et al.* (2002) and Singarayer and Bailey (2004). The decay rate of the slow component (0.33 s^{-1}) and the background were derived from the curve in the time interval

Table 6.3: Ratio of the percentage contribution to the net OSL signal of the fast medium and slow component using the EBG and the LBG subtraction. The last line shows the size of the medium component (expressed as percentage) within the net OSL signal compared to that of the fast component

	Net signal ratio using EBG and LBG: $(OSL_{\text{EBG}})/(OSL_{\text{LBG}})$ (%)*		
Component	Signal, EBG = 1 ch	Signal, EBG = 2 ch	Signal = 10 ch EBG = 2 ch
Fast	53	78	100
Medium	9	17	89
Slow	0.7	1.2	82
Medium/Fast	17	22	89

* See text for calculation details.

beyond 1 s. The only free parameters in the fit were the amplitudes of the exponentials. From Fig. 6.6 it can be observed that, with these constraints, a very good fit can be obtained.

$$\frac{OSL_{\text{EBG}_i}}{OSL_{\text{EBG}_i}} = \frac{A_i\left(\int_0^{t_s} \exp(\lambda_i t) - \int_{t_s}^{t_{\text{EBG}}} \exp(\lambda_i t)\right)}{A_i\left(\int_0^{t_s} \exp(\lambda_i t) - \int_{t_{591}}^{t_{595}} \exp(\lambda_i t)\right)} \tag{6.4}$$

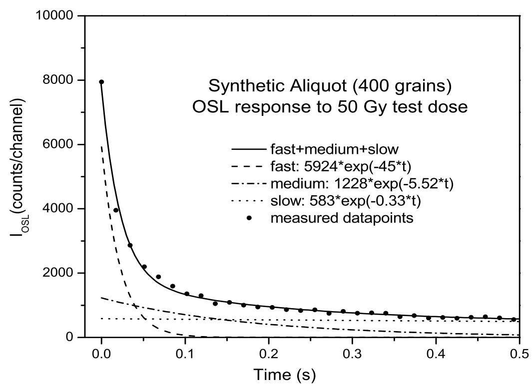

Figure 6.6: OSL decay curve obtained using the laser in response to a 50 Gy test dose for a synthetic aliquot made up of 400 grains. The solid line was obtained using a fitting function made of three exponential decay curves the fast (dashed) medium (dash-dotted) and slow (dotted) components which are also shown. The initial total intensity was $4 \cdot 10^5$ cts/s.

Rejection criteria

Three rejection criteria were applied. These are (a) feldspar contamination, (b) agreement with each other within errors of the first and third regenerated OSL responses, and (c) counting statistics related to the first OSL response to a test dose.

The first rejection criterion applied is that of Duller (2003) related to the presence of feldspars. Quartz grains were checked by observing the OSL response to a dose of 50 Gy recorded with and without IR stimulation prior optical stimulation at the end of the sequence. If the first response is much smaller than the second, feldspar is thought to be present. In this study, we discarded all the grains for which the OSL response after IR stimulation was less than 30% of the OSL response to the same dose when no IR stimulation was applied. Values $< 30\%$ were found by Duller (2003) in his measurements on potassium-rich feldspars separated from a dune sand. This criterion resulted in discarding 8 and 2 grains for samples TX02-29 and TX02-31, respectively.

Murray and Wintle (2000) suggested the use of the recycling ratio to check the reliability of the SAR protocol within a measurement. If this ratio is within 10-30% of unity, the SAR protocol is thought to be reproducible. For SG measurements, this approach is too strict; instead, we have checked whether the two responses are consistent with each other within one standard error. For the two samples, all the grains successfully passed the recycling test (i.e. no grains were discarded after this check was performed). This is due to the large uncertainties associated to the individual estimates, which makes two apparently inconsistent recycling responses being consistent within errors.

The most common criterion for selecting individual grains for equivalent dose estimation is based on counting statistics analysis. A reasonable assumption is that grains with little or no luminescence sensitivity should not be included for D_e estimation. A measure of the sensitivity of a grain is given by the relative standard error (RSE) with which the OSL response from the first test dose is known. In this paper we follow the definition for the RSE given in Galbraith (2002), equation (3):

$$RSE(\mu) = \frac{\sqrt{Y_0 + Y/k}}{Y_0 - Y} \tag{6.5}$$

where μ is the net signal calculated by subtracting the background from the initial signal; Y_0 the initial signal measured in the first n channels and Y the background measured in m channels; k is defined as m/n. It can be seen from this formula that the RSE is inversely proportional to the brightness of a grain (i.e. number of counts). We study the influence of the RSE threshold used for selecting grains on the estimated D_e, which means investigating whether equivalent doses determined from bright grains are more reliable than those calculated from dim grains. The RSE check was performed on the OSL responses of all five test doses within the SAR procedure.

It is worth noting that the more stringent the rejection criteria, the smaller the percentage of grains that will successfully pass all the tests. Thus, it should be ensured that a statistically significant number of grains are left for a meaningful D_e estimation. However, with too permissive criteria, grains that do not fulfill the basic requirements of the SAR protocol may be accepted and given the same weight as the others. In this case unreliable equivalent doses will be obtained.

6.3.3 Equivalent dose determination

Equivalent doses were calculated by projecting the OSL response of the natural onto the straight line connecting the origin and the OSL response of the first regenerative dose. Roberts *et al.* (1999) have pointed out that this approach should be used with care, since equivalent dose underestimation may occur if this method is applied to single grains that have much larger burial doses than the given regenerative dose. We investigated the systematic error induced in the D_e by using this approach rather than the dose response curve for each grain. Dose-response curves were calculated for one early- and one late-saturating grain as well as for a synthetic aliquot (see next section). In Fig. 6.4 (inset) we show the percentage error introduced by estimating equivalent doses up to 5 Gy when a line between the origin and a 5 Gy regenerative point is used. It can be seen that, for grains that saturate at doses below 50 Gy, the equivalent dose determined using the one data point is overestimated by up to 20% in the range of the expected natural dose. For grains that saturate at doses above 100 Gy, this overestimation is negligible ($< 0.1\%$). For the late-saturating grain presented in Fig. 6.4, the results for the growth curve and single data point approach coincide. Since only few grains saturate at very low doses and the majority show almost-linear growth responses up to 5 Gy, the use of a line drawn between the single regenerative dose point and the origin is feasible.

An alternative approach for calculating equivalent doses using a single regenerative point is by interpolation of the natural OSL signal between the recuperation point ($R_2 = L_2/T_2; D_2 = 0$ Gy) and the first regenerative point (R_1). Although in principle more correct, this approach is impractical for the fact that the recuperated OSL signals from a zero dose are highly scattered from grain to grain, as explained in Section 6.2.3.

The discrepancy between the D_e values for the synthetic aliquot calculated by these two approaches is 5%. This systematic error does not seriously affect the final D_e, since the random errors are three times larger ($\sim 15\%$). However, the systematic error caused by using a single data point can be reduced by using lower regenerative doses, although in this case random errors will increase due to counting statistics.

After application of rejection criteria the best estimate of the burial doses for the two samples were calculated using different methods, such as simple mean, weighted mean and median.

An alternative method for estimating equivalent doses to the ones mentioned above, is to look at the collective light output of the single grains, rather than investigating D_e values from individual grains separately (Henshilwood *et al.*, 2002; Jacobs *et al.*, 2003b). If the OSL responses from the natural dose of those grains that met the rejection criteria requirements are summed together, and with similar summing for the OSL signals from the regenerative and test doses, the equivalent dose for a single synthetic aliquot can be calculated. This technique effectively reduces to a standard SAR protocol used on a single aliquot. However, in such a synthetic aliquot, grains with little sensitivity are not taken into account.

Table 6.4: Results from SG analysis for sample TX02-29. The acceptance criteria used are $RSE < 30\%$ and (post-IR) OSL to OSL ratio $> 30\%$. The early background (EBG) and the late background (LBG) subtraction methods are compared

Sample TX02-29 Expected dose: (0.236 ± 0.010) Gy ($n = 2000$)			
	OSL signal 10 ch	OSL signal 2 ch	
	LBG (5 ch)	LBG (5 ch)	EBG (2ch)
Accepted grains	194 (9.7%)	209 (10.5%)	90 (4.5%)
Rejected as feldspar grains	6 (0.3%)	7 (0.35%)	8 (0.4%)
Single grain	D_e (Gy)	D_e (Gy)	D_e (Gy)
Average	1.166 ± 1.21 (104%)	-0.102 ± 2.56 (2521%)	0.457 ± 0.281 (62%)
Weighted mean	0.284 ± 0.014 (5%)	0.151 ± 0.011 (7%)	0.136 ± 0.032 (16%)
Median	0.817	0.851	0.289
Min	-214	-519	-16
Max	67	101	12
Synthetic Aliquot	0.626 ± 0.027 (4%)	0.526 ± 0.020 (4%)	0.245 ± 0.031 (13%)

6.3.4 Results and discussion

We can now compare the equivalent doses for samples TX02-09 and TX02-31 calculated using different integration time intervals and RSE with those values obtained using single aliquots. The $D_e$values for TX02-09 are given in Tab. 7.2. The single aliquot results have been demonstrated to give D_e values in agreement within one standard deviation with independent age controls (Ballarini *et al.*, 2003). Our aim was to establish what parameters are most appropriate for single-grain dating of young quartz samples.

Single grain

D_e values for TX02-09 calculated using the simple mean are inadequate whichever rejection criterion or background subtraction is used (Tab. 7.2). The median gives estimations for the D_e reasonably close to the expected dose given from single aliquot measurements (0.236 ± 0.010 Gy) only when EBG subtraction is applied. No clear trend for the weighted mean with respect to different background subtraction methods can be inferred.

The effect on equivalent dose distributions by using EBG and LBG subtraction can be seen in Fig. 6.7. A clearly skewed D_e distribution is observed when the initial signal is integrated over the first ten channels and the LBG is used (Fig. 6.7a). The equivalent dose calculated as the mean from the Gaussian fit is overestimated by a factor of two. However, distributions become less skewed when the signal integration interval is shortened (Fig. 6.7b) and in addition the EBG is used (Fig. 6.7c). In this last case, data can be very well fitted by a normal distribution, although the mean equivalent dose of 0.298 ± 0.020 Gy is not consistent with the expected D_e of 0.236 ± 0.010 Gy at two sigma. Results similar to those shown in Fig. 6.7 were obtained for sample TX02-31. It is interesting to note that although the slower OSL components were not completely reset (Fig. 6.7a), standard single aliquot

D_e estimates (blue LED stimulation for 40 s; signal and background integrated over the first 0.8 and over the last 4 s, respectively) were in good agreement with the independent age control. We conclude that the degree of bleaching of the grains was sufficient but not complete and could only be resolved by means of SG analysis.

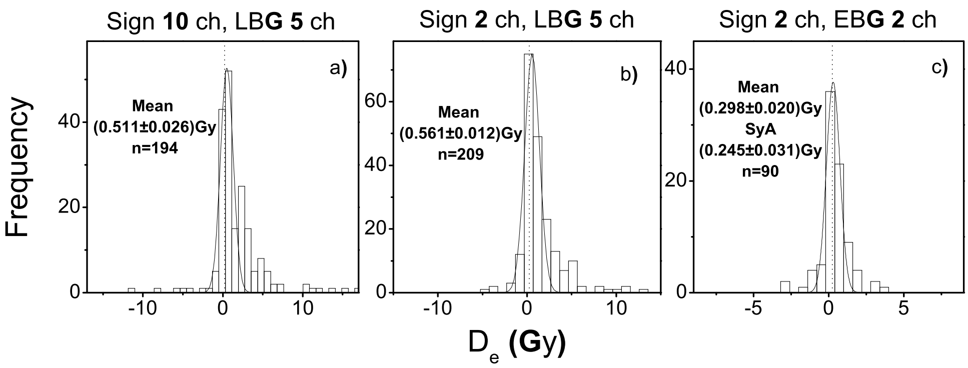

Figure 6.7: Frequency dose distributions for sample TX02-29 (expected D_e 0.236 ± 0.010 Gy) using different signal and background integration intervals after the application of the criterion $RSE < 30\%$. A Gaussian fit for the data and the expected D_e (dotted line) are also shown. The mean values refer to those estimated after Gaussian fitting.

Comparing D_e distributions obtained with different integration intervals for the OSL signal can be used for establishing the degree of bleaching of a sample. Our method is similar to that reported in Bailey (2003), where the estimated equivalent dose as a function of the integration interval ($D_e(t)$) is investigated.

Synthetic Aliquots

In Figs. 8 and 9, D_e values obtained for synthetic aliquots for samples TX02-29 and TX02-31, respectively, are plotted as a function of the RSE threshold; each data set was obtained using the OSL signals for the number of grains that passed the acceptance criteria from an initial number of 200 grains. It can be seen that equivalent doses are accurately recovered by subtracting the EBG, resulting in agreement with the expected value within errors (data shown as circles). When the LBG subtraction is used, the equivalent doses overestimate the expected D_e and increase as a function of the RSE (data shown as squares). This suggests that the higher apparent equivalent doses are associated with dim grains and that these are responsible for the overestimation. Such an effect becomes more evident for the longer integration interval of the OSL signal (data shown as open squares). We suggest that, for the samples under investigation, the medium and/or the slow components were not completely bleached before deposition. In such a scenario, these components contribute to the natural OSL signal if long integration intervals are used. This effect does not occur in the measurement of the regenerated signals, since all the components are bleached to zero by high-temperature optical stimulation at the end of each cycle. We conclude that no reliable equivalent doses can be estimated for these two samples if the LBG subtraction is applied, no matter how short the integration interval for the initial signal.

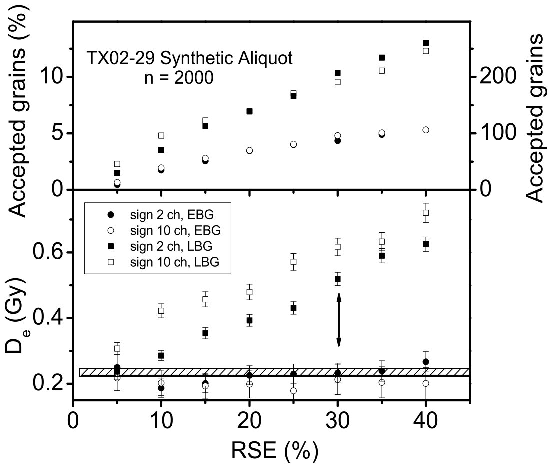

Figure 6.8: Sample TX02-29 (expected D_e 0.236 ± 0.010 Gy), equivalent dose and percentage of accepted grains as a function of the RSE criterion used. The initial signal and the background were calculated in four different ways; 2 ch, 2 ch EBG (filled circles); 10 ch, 2 ch EBG (open circles); 2 ch, 5 ch LBG (filled squares) and 10 ch, 5 ch LBG (open squares). Applied rejection criteria are discussed in the text. The shadowed region represents the expected D_e interval. The data set indicated by the double arrow ($RSE <$ 30%) is the one shown in Tab. 7.2.

If the EBG is used for calculating the net OSL signal, D_e values appear to be in good agreement with the expected D_e within errors for the whole range of RSE values (5-40%). It can be seen from Figs. 6.8 and 6.9 that this is true even when long integration intervals for the OSL signal and the background are used. However, better agreement between estimated and expected D_e is reached when intervals as short as 0.034 s are used for both the signal and the early background. The use of the EBG method also results in a reduction of accepted grains by up to 50% (Figs. 6.8 and 6.9).

In Tab. 7.2 some results from the single-grains and the synthetic-aliquot approach for sample TX02-29 are presented. A 30% threshold was used for the RSE. The choice of this particular value can be justified with two reasons. Firstly, it is not advisable to use a lower RSE threshold as it would reduce too severely the number of grains that can be used for D_e analysis after this check is applied (unless the number of measured grains is far higher than the 2000 grains used here); secondly, with higher RSE thresholds grains with low luminescence sensitivity are included into D_e calculations, which should be avoided.

Results for the synthetic aliquots show that D_e values calculated using standard integration intervals for the OSL signal (0.085 s) and using LBG subtraction (0.17 s) are a factor of two greater than single aliquot results. The overestimation is reduced if the number of channels used for luminescence signal integration is decreased and is fully suppressed when in addition the EBG (0.034 s) subtraction method is applied. In this last case, D_e values

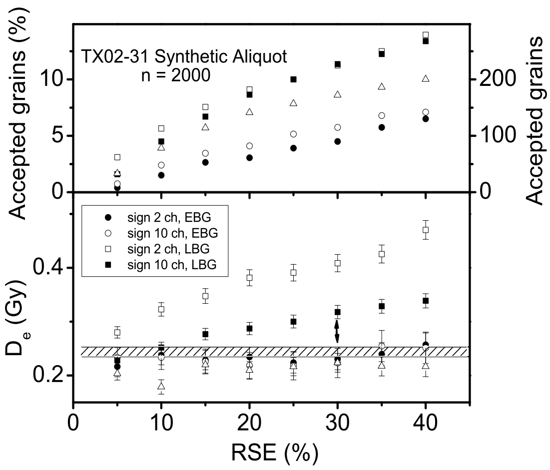

Figure 6.9: 9 Sample TX02-31 (expected D_e 0.244 ± 0.009 Gy), equivalent dose and percentage of accepted grains as a function of the RSE. Notations are the same as those used for Fig. 6.8.

are in agreement with the expected dose within one sigma. Results similar to those shown for sample TX02-29 were obtained for sample TX02-31 (data not shown). The mismatch between synthetic aliquot and SA results for this sample can be explained by means of the different types of OSL stimulations used in these two studies. In the first case, green-laser optical stimulation was employed. Due to the high power of this light source, the fast component is rapidly bleached within the first 0.017 s and the contribution of the medium component becomes substantial within the first 0.034 s (Table 6.3 and Fig. 6.6). In order for the net OSL signal to be made primarily of the fast component, the EBG subtraction was needed. In the case of single-aliquot work, blue diodes were used for optical stimulation. For this light source, the power per square centimeter is three orders of magnitude lower than that of the green laser. As a consequence, the fast and the medium components are bleached much slower. Thus, the optical stimulation time employed in SA works (40 s; first 0.8 and last 4 s for the signal and background subtraction, respectively) had the effect of depleting mainly the fast component traps, and no EBG subtraction was needed.

6.4 Conclusions

By investigating laboratory irradiated quartz grains, we have demonstrated the feasibility of a modified SAR protocol that makes use of an additional bleaching step for reducing recuperation effects, relatively large test doses and a single regenerative dose. These modifications resulted in a protocol suitable for dating young deposits. We have shown that by applying large test doses, more grains can be accepted for equivalent dose analysis.

Expected D_es from young natural sand-dune samples could be successfully retrieved by using short integration intervals for estimating the initial OSL signal and by subtracting the background calculated over the few channels immediately following the initial signal (early background - EBG). D_e values determined by using standard integration intervals were grossly overestimated for these samples, particularly when using late background subtraction (LBG). The equivalent doses obtained using the EBG subtraction appeared to conform to Gaussian distributions. The means gave values of D_e close to the expected equivalent doses for the two samples. Normally-distributed equivalent doses, estimated through the EBG method, are obtained for samples for which at least the fast component was sufficiently bleached. Thus, this method may be used for assessing whether bleaching in nature was sufficient. From our SG analysis we infer that for the samples under investigation only the fast OSL component was reset.

Although we have demonstrated the feasibility of a modified SAR protocol such as explained above, this sould be validated on a larger number of samples, preferably from different depositional environments.

Bibliography

Adamiec, G (2000). Variations in luminescence properties of single quartz grains and their consequences for equivalent dose estimation. *Radiation Measurements*, 32, 427–432.

Bailey, RM (2003). The use of measurement-time dependent single-aliquot equivalent-dose estimates from quartz in the identification of incomplete signal resetting. *Radiation Measurements*, 37, 673–683.

Ballarini, M, Wallinga, J, Duller, GAT, Brouwer, JC, Bos, AJJ and Van Eijk, CWE (2005). Optimizing detection filters for single-grain optical dating of quartz. *Radiation Measurements*, 40, 5–12.

Ballarini, M, Wallinga, J, Murray, AS, Van Heteren, S, Oost, AP, Bos, AJJ and Van Eijk, CWE (2003). Optical dating of young coastal dunes on a decadal time scale. *Quaternary Science Reviews*, 22, 1011–1017.

Banerjee, D, Bøtter-Jensen, L and Murray, AS (2000). Retrospective dosimetry: estimation of the dose to quartz using the single-aliquot regenerative-dose protocol. *Applied Radiation and Isotopes*, 52, 831–844.

Bøtter-Jensen, L, Bulur, E, Duller, GAT and Murray, AS (2000). Advances in luminescence instrument systems. *Radiation Measurements*, 32, 523–528.

Bulur, E, Duller, GAT, Solongo, S, Bøtter-Jensen, L and Murray, AS (2002). LM-OSL from single grains of quartz: a preliminary study. *Radiation Measurements*, 35, 79–85.

Bush, DA and Feathers, JK (2003). Application of OSL single-aliquot and single-grain dating to quartz from anthropogenic soil profiles in the SE United States. *Quaternary Science Reviews*, 22, 1153–1159.

Duller, GAT (1991). Equivalent dose determination using single aliquots. *Nuclear Tracks and Radiation Measurements*, 18, 371–378.

Duller, GAT (2003). Distinguishing quartz and feldspar in single grain luminescence measurements. *Radiation Measurements*, 37, 161–165.

Duller, GAT, Bøtter-Jensen, L and Murray, AS (2000). Optical dating of single sand-sized grains of quartz: sources of variability. *Radiation Measurements*, 32, 453–457.

Duller, GAT, Wintle, AG and Hall, AM (1995). Luminescence dating and its application to key pre-late Devensian sites in Scotland. *Quaternary Science Reviews*, 14, 495–519.

Feathers, JK (2003). Single-grain OSL dating of sediments from the Southern High Plains, USA. *Quaternary Science Reviews*, 22, 1035–1042.

Galbraith, RF (2002). A note on the variance of a background-corrected OSL count. *Ancient TL*, 20, 49–51.

Galbraith, RF, Roberts, RG and Yoshida, H (2005). Error variation in OSL palaeodose estimates from single aliquots of quartz: a factorial experiment. *Radiation Measurements*, 39, 289–307.

Henshilwood, CS, d'Errico, F, Yates, R, Jacobs, Z, Tribolo, C, Duller, GAT, Mercier, N, Sealy, JC, Valladas, H, Watts, I and Wintle, AG (2002). Emergence of modern human behavior: Middle Stone Age engravings from South Africa. *Science*, 295, 1278–1280.

Jacobs, Z, Wintle, AG and Duller, GAT (2003b). Optical dating of dune sand from Blombos cave, South Africa: II – single grain data. *Journal of Human Evolution*, 44, 613–625.

Jain, M, Thomsen, KJ, Bøtter-Jensen, L and Murray, AS (2004). Thermal transfer and apparent-dose distributions in poorly bleached mortar samples: results from single grains and small aliquots of quartz. *Radiation Measurements*, 38, 101–109.

Murray, AS, Olley, JM and Caitcheon, GG (1995). Measurement of equivalent doses in quartz from contemporary water-lain sediments using optically stimulated luminescence. *Quaternary Geochronology (QSR)*, 14, 365–371.

Murray, AS and Roberts, RG (1997). Determining the burial time of single grains of quartz using optically stimulated luminescence. *Earth and Planetary Science Letters*, 152, 163–180.

Murray, AS, Roberts, RG and Wintle, AG (1997). Equivalent dose measurement using a single aliquot of quartz. *Radiation Measurements*, 27, 171–184.

Murray, AS and Wintle, AG (1998). Factors controlling the shape of the OSL decay curve in quartz. *Radiation Measurements*, 29, 65–79.

Murray, AS and Wintle, AG (2000). Luminescence dating of quartz using an improved single-aliquot regenerative-dose protocol. *Radiation Measurements*, 32, 57–73.

Murray, AS and Wintle, AG (2003). The single aliquot regenerative dose protocol: potential for improvements in reliability. *Radiation Measurements*, 37, 377–381.

Olley, JM, Caitcheon, GG and Murray, AS (1998). The distribution of apparent dose as determined by optically stimulated luminescence in small aliquots of fluvial quartz: Implications for dating young sediments. *Quaternary Geochronology (QSR)*, 17, 1033–1040.

Olley, JM, Caitcheon, GG and Roberts, RG (1999). The origin of dose distributions in fluvial sediments, and the prospect of dating single grains from fluvial deposits using optically stimulated luminescence. *Radiation Measurements*, 30, 207–217.

Olley, JM, Pietsch, T and Roberts, RG (2004). Optical dating of Holocene sediments from a variety of geomorphic settings using single grains of quartz. *Geomorphology*, 60, 337–358.

Roberts, RG, Galbraith, RF, Olley, JM, Yoshida, H and Laslett, GM (1999). Optical dating of single and multiple grains of quartz from Jinmium rock shelter, northern Australia: Part II, Results and implications. *Archaeometry*, 41, 365–395.

Roberts, RG, Galbraith, RF, Yoshida, H, Laslett, GM and Olley, JM (2000). Distinguishing dose populations in sediment mixtures: a test of single-grain optical dating procedures using mixtures of laboratory-dosed quartz. *Radiation Measurements*, 32, 459–465.

Singarayer, JS and Bailey, RM (2004). Component-resolved bleaching spectra of quartz optically stimulated luminescence: preliminary results and implications for dating. *Radiation Measurements*, 38, 111–118.

Stokes, S (1994). The timing of OSL sensitivity changes in a natural quartz. *Radiation Measurements*, 23, 601–605.

Thomsen, KJ, Bøtter-Jensen, L, Murray, AS and Solongo, S (2002). Retrospective dosimetry using unheated quartz: a feasibility study. *Radiation Protection Dosimetry*, 101, 345–348.

Thomsen, KJ, Jain, M, Bøtter-Jensen, L, Murray, AS and Jungner, H (2003). Variation with depth of dose distributions in single grains of quartz extracted from an irradiated concrete block. *Radiation Measurements*, 37, 315–321.

Truscott, AJ, Duller, GAT, Bøtter-Jensen, L, Murray, AS and Wintle, AG (2000). Reproducibility of optically stimulated luminescence measurements from single grains of Al_2O_3:C and annealed quartz. *Radiation Measurements*, 32, 447–451.

Wallinga, J (2002a). Optically stimulated luminescence dating of fluvial deposits: a review. *Boreas*, 31, 303–322.

Wintle, AG and Murray, AS (in press). A review of quartz optically stimulated luminescence characteristics and their relevance in single-aliquot regeneration dating protocols. *Radiation Measurements*.

Yoshida, H, Roberts, RG, Olley, JM, Laslett, GM and Galbraith, RF (2000). Extending the age range of optical dating using single 'supergrains' of quartz. *Radiation Measurements*, 32, 439–446.

Chapter 7

Analysis of equivalent dose distributions for single grains of quartz from modern deposits

Quaternary Geochronology, submitted

M. Ballarini[a,b], J. Wallinga[b], Wintle, A.G.[c], A.J.J. Bos[a]

[a] *Delft University of Technology, Faculty of Applied Sciences, Mekelweg 15, NL-2629 JB Delft, The Netherlands*

[b] *Netherlands Centre for Luminescence Dating, Delft University of Technology, Faculty of Applied Sciences, Mekelweg 15, NL-2629 JB Delft, The Netherlands*

[c] *Institute of Geography and Earth Sciences, University of Wales, Aberystwyth, Ceredigion SY23 3DB, UK.*

Abstract

Two modern coastal sands are studied through single-grain optical dating techniques. The first sample is estimated to be less than ten years old by means of independent age control and is known to be well-bleached on the basis of preliminary single-aliquot studies. The second sample is less than a year old, but an age of 73 ± 24 years had been determined through single-aliquot analysis. For both samples we compare equivalent doses obtained from single-grain analysis to those obtained by means of similar single-aliquot methods. We found that results are comparable although equivalent doses determined through single-aliquot methods are more precise. The reason for this may be ascribed to the limited number of grains on which single-grain measurements were carried out. The presence of poorly-bleached grains within a sample could be identified by dose distribution analysis of individual grains.

7.1 Introduction

Optically stimulated luminescence (OSL) is a powerful tool to determine the burial age of mineral grains. In the field of Quaternary geology the age of a deposit can be determined as the time elapsed since the last reworking of the sediment grains. For accurate age estimates it is required that the grains are exposed to sunlight for a sufficient period of time before burial in order to remove the effect of previously absorbed dose. If this zeroing process is incomplete (i.e. grains were poorly bleached) ages obtained by means of optical dating may be overestimated (Murray *et al.*, 1995; Olley *et al.*, 1998). The overestimation due to insufficient bleaching is critical for young deposits, for which the dose retained by the grains may be considerable if compared to the burial dose. Thus, identification of poorly-bleached grains within a sample is of great importance for dating modern deposits.

The major advantage of using single grains for OSL dating is that heterogeneous bleaching within a sample may be recognized through dose-distribution analysis (Feathers, 2003; Jacobs *et al.*, 2003b; Olley *et al.*, 2004; Roberts *et al.*, 1999). However, for a number of reasons optical dating of single grains is not as straightforward as for multiple-grain single-aliquot dating. Firstly, a large number of grains needs to be measured because of the low OSL sensitivity of the majority of the grains (Duller *et al.*, 2000); secondly, for very young samples, natural OSL responses are extremely low and noisy.

In this paper we present single-grain results for a) a well-bleached sample of < 10 years age and b) a poorly-bleached sample known to be < 1 year old. Previous single-aliquot (SA) OSL studies had provided ages of 7.4 ± 1.3 and 73 ± 23 years for the two samples, respectively (Ballarini *et al.*, 2003). The age overestimation for the last sample and the associated large uncertainty suggest that this was not sufficiently bleached before deposition. The aim of our current investigation is to assess whether ages as low as 10 years can be determined for well- and poorly-bleached quartz samples by means of single grain (SG) techniques. The ability to date modern deposits is relevant to environmental dynamics and coastal management applications.

7.2 Samples and instrumentation

Two samples from the island of Texel (The Netherlands) are investigated in this study. Sample TX02-8 is from a coastal embryo dune for which a maximum age of 10 years was established by means of detailed maps for the area. Sample TX02-23 was taken from a small dune formed on a path that is regularly frequented in summertime. Part of the sand from this location is nourishment sand, dumped on the beach to counteract coastal erosion. Its bleaching history is unusual, in that it did not go through numerous bleaching cycles while washed on the beach. Very likely this sample was deposited less than twelve months before collection. Extensive information on these samples, including dose rate and water content, can be found in Ballarini *et al.* (2003).

The instrumentation consisted of a Risø TL/OSL reader equipped with a single-grain attachment (Bøtter-Jensen *et al.*, 2000) in combination with Hoya U-340 optical detection filters of 2.5 mm thickness (Ballarini *et al.*, 2005). The green laser used for optical illumination is capable of delivering 50 W/cm^2 to a grain held in an indentation drilled into a special disc (Bøtter-Jensen *et al.*, 2003). In our experiments, OSL measurements were carried out at 90% of this power. For each sample two thousand grains, each with a diameter in the range of 180-212 mm, were selected for the OSL investigations.

7.3 Experimental details

We used a single-aliquot regenerative-dose (SAR) procedure (Murray and Wintle, 2000) for single-grain analysis of young samples, the exact protocol being that proposed by Ballarini *et al.* (submitted), which is summarized in Tab. 7.1. The modified SAR protocol makes use of an additional bleaching step (step 7 in Table 7.1) at the end of each SAR cycle (Murray and Wintle, 2003), 10 s optical stimulation (0.017 s per data point) at 125°C and a single regenerative point of 5 Gy which is repeated twice and a large test dose of 50 Gy. The luminescence response to a zero dose was also recorded but not taken into account for dose estimations. The equivalent dose (D_e) is calculated from the sensitivity-corrected natural OSL signal (L_n/T_n) using linear interpolation between the origin of the axis and the sensitivity-corrected OSL response to the first regenerative dose (L_1/T_1) as discussed by Ballarini *et al.* (submitted). The luminescence signal is integrated over the first two channels of the OSL decay curve (0.034 s) and the background over the subsequent two channels. We refer to this technique as early background (EBG) subtraction Ballarini *et al.* (submitted). D_e values were also calculated using the more standard late-background (LBG) subtraction method (background integrated over the last 5 channels, 0.085 s). Our assumption is that by using the EBG, only the OSL contribution from the fast component is included in the integrated signal Ballarini *et al.* (submitted). Thus, histograms for D_e values from grains for which the fast component was well bleached are expected to show Gaussian-like trends, as the skewness due to the contribution from slower components should be suppressed.

The validity of the modified SAR protocol was assessed on both laboratory-irradiated and untreated quartz. Details can be found in Ballarini *et al.* (submitted).

Table 7.1: Modified SAR protocol used for D_e estimation of natural quartz from very young samples

Step	treatment	Observed
1	Dose, D_i[1] ($i = 1, \ldots, 4$)	–
2	10 s preheat at 180°C	–
3	10 s OSL at 125°C[2]	L_i
4	Test dose, $D_t = 50$ Gy	–
5	Cut Heat 160°C	–
6	10 s OSL at 125°C[2]	T_i
7	10 s OSL at 210°C	–
8	Return to 1	–
9	Test dose, $D_t = 50$ Gy	–
10	Cut Heat 160°C	–
11	40 s IRSL at room temperature[3]	–
12	10 s OSL at 125°C[2]	T_{IR}

[1] In the first cycle ($i = 1$) no dose was given and the natural OSL signal recorded. The administered regenerative doses were 5, 0 and 5 Gy.

[2] Decay curves were collected in 600 data points (10 s). For the first and the last 5 channels the laser was switched off. OSL data points were collected each 0.017 s.

[3] Feldspar contaminants within grains are checked by comparing the OSL test-dose response prior and subsequent to IR stimulation. This can be achieved by administering a test dose and measuring the OSL response following IR stimulation at the end of the SAR protocol (Duller, 2003). IR stimulation from LEDs at 90% of the maximum power.

7.4 Rejection criteria

For each grain, feldspar contamination was checked by comparing the OSL test-dose response prior to (step 6 for D_4) and subsequent to (step 12) IR stimulation at the end of the SAR dating run (Duller, 2003). We rejected grains that showed an OSL response reduced by 70% or more after 40 s of IR exposure at room temperature. This arbitrary value was purposely chosen to be not too strict, as OSL responses of individual grains to the same given dose are highly scattered.

Many authors have stressed the importance of including for D_e analysis only grains that are able to produce an OSL signal detectable above background. Such a test for sensitivity is usually performed on the OSL response from the first test dose in the SAR protocol. The requirement is a relative standard error (RSE) on the signal that falls below a certain threshold (Thomsen et al., 2002; Bush and Feathers, 2003; Thomsen et al., 2003; Jain et al., 2004). In this paper we present results obtained by using RSE (calculated after Galbraith, 2002; equation (3)) thresholds of 10 and 30%. This check was performed on all of the five test-dose responses within the measurement sequence (7.1). In order to ensure that only grains showing meaningful OSL responses are taken into account for D_e estimation, two more tests were applied for checking grain sensitivity. These are a) non-negative luminescence responses to regenerative doses (L_i) and b) corrected natural responses smaller than corrected regenerated signals ($L_n/T_n < L_1/T_1$). The latter criterion restricts measured D_e values to less than 5 Gy (the value of the regenerative dose).

A recycling-ratio test (Murray and Wintle, 2000; 2003) is usually performed to check the reliability of the SAR protocol for recovering a dose that was administered twice. Here the two OSL responses have to be in agreement with each other within one sigma (Ballarini *et al.*, submitted; submitted). This approach is less strict than the one proposed by Murray and Wintle (2000) and appears to be more realistic in a scenario where sensitivity-corrected responses are small and highly scattered due to small luminescence signals, such as in single grain measurements.

7.5 Equivalent dose calculation

For the grains that passed these criteria, the equivalent doses were plotted as histograms and the burial dose estimated by means of fitting with a Gaussian function. For this purpose, the built-in features of the *Origin 7.5* software package were used. We utilize histograms because parameters of a distribution such as centrality, spread and skewness can be easily determined. Equivalent doses were calculated using the mean and median on the data set (Table 7.2) and by means of fitting on D_e dose distributions (Figs. 7.2 and 7.3). Equivalent dose values calculated for very young samples are expected to be both positive and negative. Although negative equivalent doses have no physical meaning as the true dose is always greater than zero, negative measured D_es can be found. One approach that can be adopted to deal with negative equivalent dose values is to use a truncated D_e distribution in which only positive doses are taken. This method, however, is not investigated in this paper. For D_e calculation from dose distributions, we decided to use the whole set of measured doses (i.e. positive as well as negative) and to use a Gaussian fit on the distribution. In this way, no further data rejection occurs, but largely positive and negative values will be given little weight by the fitting procedure. It must be said that this method does not take into account overdispersion within individual D_e estimates, and equivalent doses obtained through the fitting may be associated with underestimated uncertainties.

As an alternative method for calculating D_es, all the individual signals from the accepted grains were summed together to produce a single natural and a single regenerated response corrected for sensitivity change (Jacobs *et al.*, 2003b) in order to produce a synthetic aliquot. A single value of the D_e is then estimated as for a single aliquot. Grains with equivalent doses smaller or greater than two standard deviations (2 s) from the median were rejected in this approach. In most cases this resulted in excluding few grains only, for which the equivalent dose was in the order of ten times or more the value of the expected D_e (both positive and negative).

It must be noted that radial plot data representation (Galbraith *et al.*, 1999) and age models (Roberts *et al.*, 1999) cannot be used as these methods do not work with negative dose estimates. We do not use the weighted mean approach as dose estimates determined in such a way are biased to low values for distributions made of small doses.

7.6 Results and discussion

7.6.1 Sample TX02-8

In general, D_e values obtained for this sample using the LBG are gross overestimations of the expected dose (Table 7.2). This indicates that the fast and/or the slower components were not entirely bleached before burial. Reduced overestimation can be achieved by using the EBG, which results in less precise but more accurate D_e values. The discrepancy between doses calculated with the EBG and LBG drastically reduces when the RSE threshold is set to 10%. This result suggests that for the LBG method the brightest grains appear to carry doses that relate the most to the last depositional event only (i.e. bright grains are best bleached). Such evidence is corroborated by Fig. 7.1a-b, where individual equivalent doses are plotted against their own RSE values. It can be seen that doses from grains with RSEs up to 10% are relatively accurate and precise, while above this threshold large scatter is observed. Equivalent dose estimates increase as a function of the RSE when the LBG is used (Fig. 7.1b). Synthetic aliquot estimates (using both RSE thresholds of 10 and 30% and EBG) agree with the expected dose and the calculated SA dose within errors (Table 7.2).

Dose distributions (Fig. 7.2) are remarkably broad and skewed when the LBG method is used, but narrower and more symmetric if doses were calculated using EBG subtraction. However, none of the mean doses given in Fig. 7.2 are consistent with either the SA estimate given in Table 7.2 (0.006 ± 0.001 Gy) or the real dose (<0.008 Gy) deduced by means of age control.

Table 7.2: Relevant statistics for samples TX02-8 and TX2-23

Sample (n=2000)	TX02-8				TX02-23			
SA calculated dose	(0.006 ± 0.001) Gy				(0.063 ± 0.020) Gy			
SA calculated age	(7.4 ± 1.3) yr				(73 ± 23) yr			
Independent age	<10 yr				< 1 yr			
Acceptance criteria: $IR > 30\%$ Consistent $R_3 - R_1$ $N < R_1$ D_e within 2σ from the median	$RSE < 30\%$		$RSE < 10\%$		$RSE < 30\%$		$RSE < 10\%$	
Background Accepted grains*	LBG (5 ch) 175 (8.8%)	EBG (2 ch) 87 (4.4%)	LBG (5 ch) 77 (3.9%)	EBG (2 ch) 28 (1.4%)	LBG (5 ch) 169 (8.5%)	EBG (2 ch) 64 (3.2%)	LBG (5 ch) 61 (3.1%)	EBG (2 ch) 21 (1.1%)
	D_e (Gy)		D_e (Gy)		D_e (Gy)		D_e (Gy)	
Average	0.514 ± 0.069	0.036 ± 0.117	0.177 ± 0.032	0.021 ± 0.030	0.536 ± 0.094	0.031 ± 0.157	0.206 ± 0.062	0.150 ± 0.065
Median	0.326	0.057	0.080	0.022	0.362	0.067	0.130	0.063
Min	-2.242	-4.733	-0.531	-0.481	-2.844	-4.851	-1.241	-0.123
Max	2.944	3.717	0.870	0.325	3.844	3.499	1.603	1.236
Synthetic Aliquot	0.121 ± 0.012	0.024 ± 0.021	0.065 ± 0.009	0.016 ± 0.016	0.820 ± 0.020	0.785 ± 0.037	0.091 ± 0.010	0.077 ± 0.016

* Grains for which the individual equivalent dose fell outside two standard deviations from the median were discarded.

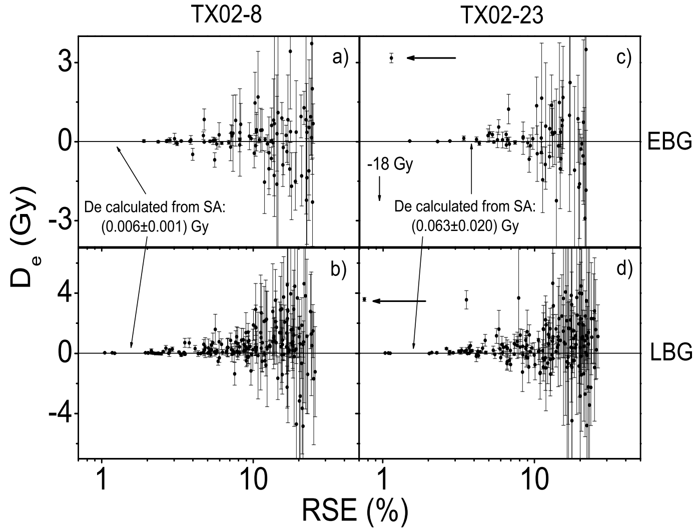

Figure 7.1: Equivalent-dose dependency on the RSE for individual grains from samples TX02-8 (a and b) and TX02-23 (c and d). The EBG (a and c) and LBG (b and d) methods were used for calculating D_e values. Arrows in (c) and (d) show a grain with large D_e value known with high precision.

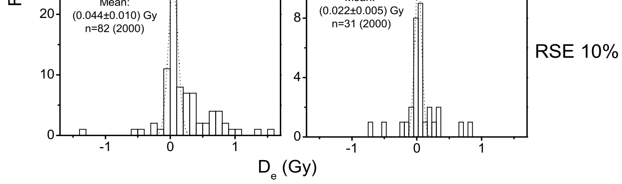

Figure 7.2: Single-grain dose-distribution frequencies from sample TX02-8 obtained by using the EBG and the LBG in combination with RSE thresholds of 10 and 30%. Mean D_e values obtained using the Gaussian fitting software are calculated using all the grains that pass acceptance criteria (n) (see Table 7.2). Graphs are on different scales.

7.6.2 Sample TX02-23

From Table 7.2 it can be seen that the synthetic aliquot D_e value for this sample is consistent with the SA value of 0.063 ± 0.020 Gy when a RSE threshold of 10 and the EBG is used. As in the case of sample TX02-8, we infer that bright grains (low RSEs) are associated with doses that mainly refer to the last depositional event (Figs. 7.1d). However, Figs. 7.1c-d also show the exception of a very bright grain ($RSE{\sim}1\%$) for which an equivalent dose of 3 or 4 Gy was estimated (depending on the signal used for background subtraction, EBG or LBG) with high precision. We suggest that this grain was not sufficiently bleached before deposition and it is excluded from the calculation of the mean in the Gaussian fitting.

Histograms for this sample (Fig. 7.3) show that dose distributions are narrower, and that the mean calculated from Gaussian fitting approaches the real dose, when the EBG and the RSE threshold of 10% are used; in this case, far fewer D_e values are accepted (only 22). However, not even in this last case is the estimated D_e consistent within errors with the 0 Gy dose derived from our geological knowledge of the sample. The mean dose (0.056 ± 0.007 Gy) is consistent with the SA result (0.063 ± 0.020 Gy), although they are both overestimates. It is interesting to note the presence of few outliers in Fig. 7.3, for the case of RSE of 10% and EBG. This may indicate that for some grains even the fast component was not reset, giving rise to the overestimation observed both for the SA analysis and SG analysis.

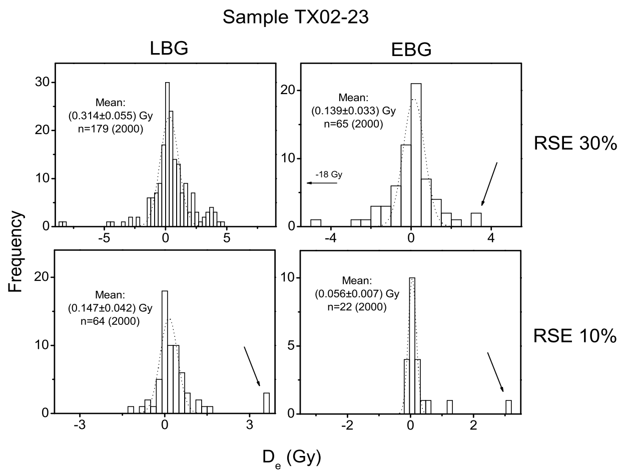

Figure 7.3: Single-grain dose-distribution frequencies from sample TX02-23 obtained by using the EBG and the LBG in combination with RSE thresholds of 10 and 30%. Arrows indicate aberrant grain in Figs. 7.1c and d. Mean D_e values are calculated using all the grains that pass acceptance criteria (see Table 7.2). Graphs are on different scales.

7.7 Conclusions

Based on the results from synthetic aliquots for the cases in which the EBG was used (Table 7.2) and from the shape of the equivalent dose distributions given in Fig. 7.2 (RSE of 10% and EBG), we conclude that sample TX02-8 was sufficiently bleached before deposition and that the previously measured SA dose could be retrieved by means of SG analysis. Both SG and SA equivalent doses are in agreement with the independent age control. SG results were found to be accurate when the EBG method and the RSE threshold of 10% were used, but less precise compared with SA dose estimates.

We found evidence from the results for sample TX02-23 (Figgs.1c-d and 3) that corroborates the hypothesis that for some grains the fast component was insufficiently bleached, as was also determined by the dose estimation from SA analysis. The expected dose of 0 Gy could not be determined by means of our methods. However, we found values for the D_e, by using the average and the synthetic aliquot, similar to that found through SA method when both the EBG and a RSE of 10% (7.2) were employed.

From the above results, we conclude that no precise dose estimates can be determined through SG techniques for quartz samples younger than 10 years using the mean, median, or weighted mean D_e values, or by the construction of a synthetic aliquot using summed light outputs. These estimates may be accurate when the EBG subtraction method and the 10% RSE threshold are used, but large uncertainties are associated. Better statistics on the distributions, and thus more meaningful results, may be achieved by increasing the number of measured grains. Other approaches for D_e determination of young quartz grains not discussed in this paper, such as the use of a truncated dose distribution or the age-model methods, should also be investigated and may represent valid alternatives to the methods presented here.

However, even for the limited data set from this study, useful information that cannot be deduced from the SA results is provided by the SG plots. This provides an insight into the actual dose distribution for the individual grains, which may reveal partial bleaching of the slower components (skewed shape for the distribution, if the LBG is used). Symmetric dose-distributions obtained when using the EBG indicate sufficient bleaching of the fast component, while skewed distributions suggest incomplete resetting. Such information is important when contemplating the dating of modern deposits using single aliquots.

Bibliography

Ballarini, M, Wallinga, J, Bos, AJJ and Wintle, AG (submitted). A modified SAR protocol for optical dating of individual grains from young quartz samples. *Radiation Measurements.*

Ballarini, M, Wallinga, J, Duller, GAT, Brouwer, JC, Bos, AJJ and Van Eijk, CWE (2005). Optimizing detection filters for single-grain optical dating of quartz. *Radiation Measurements*, 40, 5–12.

Ballarini, M, Wallinga, J, Murray, AS, Van Heteren, S, Oost, AP, Bos, AJJ and Van Eijk, CWE (2003). Optical dating of young coastal dunes on a decadal time scale. *Quaternary Science Reviews*, 22, 1011–1017.

Bøtter-Jensen, L, Andersen, C.E., Duller, GAT and Murray, AS (2003). Developments in radiation, stimulation and observation facilities in luminescence measurements. *Radiation Measurements*, 37, 535–541.

Bøtter-Jensen, L, Bulur, E, Duller, GAT and Murray, AS (2000). Advances in luminescence instrument systems. *Radiation Measurements*, 32, 523–528.

Duller, GAT (2003). Distinguishing quartz and feldspar in single grain luminescence measurements. *Radiation Measurements*, 37, 161–165.

Duller, GAT, Bøtter-Jensen, L and Murray, AS (2000). Optical dating of single sand-sized grains of quartz: sources of variability. *Radiation Measurements*, 32, 453–457.

Feathers, JK (2003). Single-grain OSL dating of sediments from the Southern High Plains, USA. *Quaternary Science Reviews*, 22, 1035–1042.

Galbraith, RF (2002). A note on the variance of a background-corrected OSL count. *Ancient TL*, 20, 49–51.

Galbraith, RF, Roberts, RG, Laslett, GM, Yoshida, H and Olley, JM (1999). Optical dating of single and multiple grains of quartz from Jinmium rock shelter, northern Australia: Part I, Experimental design and statistical models. *Archaeometry*, 41, 339–364.

Jacobs, Z, Wintle, AG and Duller, GAT (2003b). Optical dating of dune sand from Blombos cave, South Africa: II – single grain data. *Journal of Human Evolution*, 44, 613–625.

Murray, AS, Olley, JM and Caitcheon, GG (1995). Measurement of equivalent doses in quartz from contemporary water-lain sediments using optically stimulated luminescence. *Quaternary Geochronology (QSR)*, 14, 365–371.

Murray, AS and Wintle, AG (2000). Luminescence dating of quartz using an improved single-aliquot regenerative-dose protocol. *Radiation Measurements*, 32, 57–73.

Murray, AS and Wintle, AG (2003). The single aliquot regenerative dose protocol: potential for improvements in reliability. *Radiation Measurements*, 37, 377–381.

Olley, JM, Caitcheon, GG and Murray, AS (1998). The distribution of apparent dose as determined by optically stimulated luminescence in small aliquots of fluvial quartz: Implications for dating young sediments. *Quaternary Geochronology (QSR)*, 17, 1033–1040.

Olley, JM, Pietsch, T and Roberts, RG (2004). Optical dating of Holocene sediments from a variety of geomorphic settings using single grains of quartz. *Geomorphology*, 60, 337–358.

Roberts, RG, Galbraith, RF, Olley, JM, Yoshida, H and Laslett, GM (1999). Optical dating of single and multiple grains of quartz from Jinmium rock shelter, northern Australia: Part II, Results and implications. *Archaeometry*, 41, 365–395.

Chapter 8

Optical dating of fluvial deposits with excellent age control provided by a wrecked Roman barge (Rhine delta, The Netherlands)

To be submitted

J. Wallinga[a], M. Ballarini[a], P. Vos[b], C. Johns[a]

[a] *Netherlands Centre for Luminescence dating, Delft University of Technology, Faculty of Applied Sciences, Mekelweg 15, NL-2629 JB Delft, The Netherlands*

[b] *Netherlands Institute of Applied Geoscience TNO - National Geological Survey, Geology division, PO Box 80015, NL-3508 TA Utrecht, The Netherlands.*

Abstract

We explore the validity of optically stimulated luminescence (OSL) dating for Holocene fluvial channel deposits by applying the method to deposits with extremely tight independent age control. We date six samples from fluvial channel deposits in and around a beautifully preserved Roman barge which sank between 180 and 200 AD. Single-aliquot equivalent dose distributions are slightly skewed. This indicates that the majority of grains were well bleached but that incomplete resetting of the OSL signal in some grains prior to deposition and burial caused overestimation of the equivalent dose for some aliquots. We investigate methods to identify and remove aliquots which were affected by poor bleaching from the distribution. We find no dependency of equivalent dose on the integral used for the OSL signal (D_e-t methods) for our samples and conclude that identification of poorly bleached aliquots should be based on statistical analysis. After discarding poorly-bleached aliquots we obtain optical ages on the six samples that are in excellent agreement with the independent age control. Further measurements on individual quartz grains from two samples corroborate that the vast majority of grains had their signal completely reset at deposition.

8.1 Introduction

Fluvial systems are one of the most important geomorphic agents shaping the landscape (e.g. Vandenberghe and Maddy, 2000). Both fluvial style and behavior are influenced by external forcing such as climate, sea-level and land use. As a consequence fluvial deposits form an important archive of environmental change. One of the difficulties in interpreting this archive is that chronological information on fluvial deposits is difficult to obtain. Radiocarbon dating, the most used geochronological method for the Holocene, is often not applicable as organic material is sparse. Moreover, if organic material is present, it is likely reworked and therefore not necessarily of the same age as the deposits in which it is incorporated.

Optical dating is an alternative method by which the burial age of sediments can be directly determined. The method uses the optically stimulated luminescence (OSL) signal of quartz or feldspar grains. The method is most suitable for aeolian deposits, where light exposure to grains is sufficient to completely reset the OSL signal prior to deposition. If light exposure is too limited in intensity or duration to completely reset the luminescence signal, the burial age of a sample will be overestimated.

Previous research has shown that optical ages may overestimate the burial ages for fluvial deposits, but that offsets are usually less than a few hundred years for large fluvial systems (see e.g. Wallinga, 2002a). Most previous work uses contemporary fluvial deposits to investigate offsets (e.g. Stokes *et al.*, 2001). Such studies assume that there is no dependency between remnant luminescence signal and preservation potential. Moreover, it is arguable whether the results on modern samples are directly applicable to the dating of palaeosediments as many of the present fluvial systems are no longer in their natural states due to locks and other water works.

To investigate the degree of bleaching in natural state fluvial systems it is essential to study fluvial sediments of known burial age. However, the independent age control on such deposits is often not tight enough to draw firm conclusions on the completeness of resetting at the time of deposition (e.g. Wallinga *et al.*, 2000). In this research we investigate six samples from fluvial channel deposits directly associated with a Roman barge that sank in an old channel of the River Rhine (The Netherlands) between 180 and 200 AD. The aim of our investigation is to determine whether the OSL signal was completely reset at the time of deposition and to validate methods used for the detection of incomplete resetting and for obtaining burial ages on heterogeneously bleached deposits.

8.2 Optical dating

Optically stimulated luminescence dating, or optical dating, makes use of a minute light signal that can be emitted by natural minerals like quartz, feldspar and zircon when stimulated by light (Aitken, 1998). The luminescence signal is set to zero on exposure to sunlight during transport and sedimentation of the sand or silt-sized grains. After burial, the luminescence signal builds up under the influence of natural ionizing radiation from its surrounding (mainly from the Uranium and the Thorium decay chains, and from Potassium) and a small contribution from cosmic rays.

For luminescence dating two quantities are determined. Firstly, the amount of ionizing radiation received by the sample since the last exposure to sunlight. This is called the equivalent dose (D_e), expressed in Gray (Gy). Secondly, the ionizing radiation flux to which the sample is exposed in its natural environment. This is termed the dose rate, expressed in Gy per year. Dividing the equivalent dose by the dose rate gives the burial age of the sample.

Optical dating of quartz has shown to be the most reliable technique with excellent results obtained on samples from a wide range of depositional environments (e.g. Murray and Olley, 2002). The technique can be used for samples of only a few years old (e.g. Ballarini *et al.*, 2003) up to saturation of the quartz OSL signal which occurs after about 150.000 years.

Resetting of the OSL signal

Optical dating methods assume that the OSL signal is completely reset at the time of deposition. Resetting of the quartz OSL signal occurs rapidly in a few seconds of direct sunlight. In a fluvial environment sunlight will be filtered and attenuated by the turbid water column (e.g. Berger and Luternauer, 1987). Whether or not the exposure is sufficient to entirely reset the OSL signal (referred to as bleaching) depends on a great number of parameters including the turbidity of the water, the depth of the system, the transportation length and the previously acquired dose.

A range of methods has been developed to test whether the OSL signal of all grains was completely reset prior to burial (reviewed by Wallinga, 2002a). Most of these methods rely on the assumption that if the signal is not completely reset, the remaining signal and remnant dose will be different from grain to grain. As a result, equivalent dose data obtained on small subsamples (aliquots) consisting of not more than a few hundred grains will show scatter because the signal is dominated by a few bright grains (e.g. Li, 1994). If the scatter in single-aliquot equivalent doses is caused by inhomogeneous resetting, the dose received by the samples after burial (burial dose) will be at the lower end of the distribution obtained. To avoid averaging within aliquots, subsamples should ideally consist of a single grain of quartz (Wallinga, 2002b).

A second group of methods compares the equivalent doses obtained using OSL signals with different optical resetting rates. If the equivalent dose obtained from the different signals is identical it is probable that both signals were reset completely (e.g. Bailey *et al.*, 2003; Larsen *et al.*, 2000). If the equivalent dose obtained using the slow-bleaching OSL signal is greater than the equivalent dose obtained from the fast-bleaching OSL signal, than at least the slow bleaching signal was not completely reset. Complete resetting if the fast-bleaching OSL component is then not guaranteed and the result should be discarded for further analysis.

8.3 The Roman barge

During archaeological investigations preceding construction of a new housing project near the city of Utrecht (Fig. 8.1) remains of a roman barge were encountered (Bazelmans and Jansma, 2005). As the remains were very well preserved, the ship and associated finds were investigated in situ after which the ship was recovered to be preserved. The ship is named 'De Meern 1', and will be exposed in a museum in Utrecht after preservation.

During the first centuries AD the River Rhine formed the northern border (*'Limes'*) of the Roman Empire. The barge was found in channel deposits of the "Heldammer stroom", a former course of the River Rhine (Fig. 8.1). Three activity phases have been identified for the "Heldammer stroom". Starting of activity of the first phase has been dated to 2907 - 2678 BC (4221 ± 37 BP, UtC-11183; Nales and Vis, 2003). In Roman times the "Heldammer stroom" was in its third activity phase. Starting of this phase is not accurately known, but must be later than approximately 550 BC (Berendsen and Stouthamer, 2000; Nales and Vis, 2003). Within overbank deposits of the third phase, wooden remains of a Roman road were found. The remains have been dendrochonologically dated to 123 AD indicating that the channel was active at that time (Berendsen and Stouthamer, 2000). Based on Roman remains preserved within the channel the end of activity is dated to approximately 300 AD (Nales and Vis, 2003).

The ship is a flat bottomed barge made of oak wood, 24.7 m long and 2.7 m wide (Fig. 8.2); it was probably equipped with a mast and a rudder, although neither are preserved. The presence of equipment such as scissors, a mill stone, and arrow heads in the ship indicates that the ship was not sunk on purpose as was the case for other Roman ships found in The Netherlands (Bazelmans and Jansma, 2005).

Dendrochronological investigations show that the ship was built from three oaks that grew in or near The Netherlands and were cut between 142 and 154 AD. It is likely that the ship was built soon after.

Several lines of evidence indicate that the ship sank after 180 AD and before 200 AD. The archaeological context tells that the ship sunk after construction of a road along the River Rhine in 125 AD. In the ship a roof tile with the stamp **'VEX EX GER INF'** was

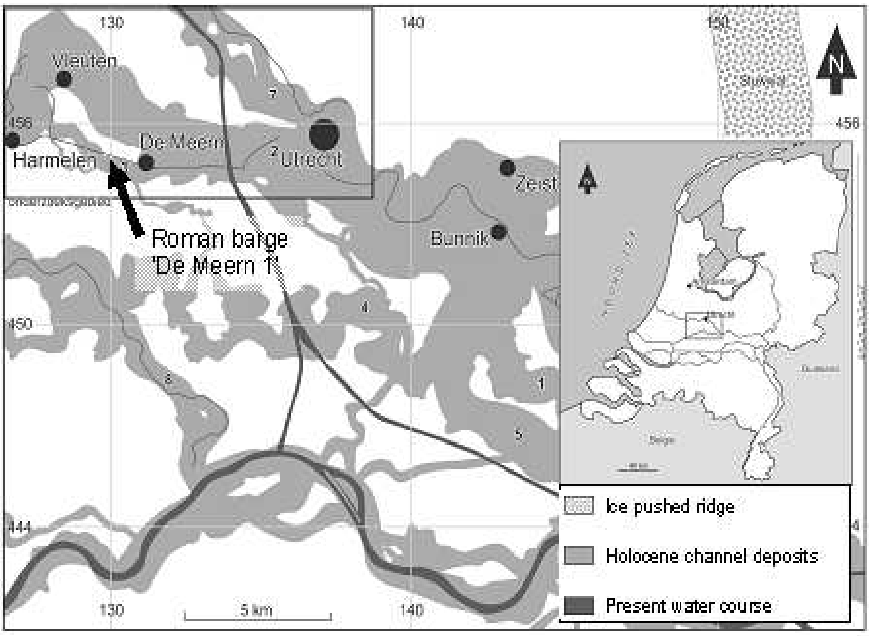

Figure 8.1: Location of the Roman barge and Holocene fluvial deposits (#3 depicts Heldammer stream) in the study area (after Nales and Vis, 2003). Local coordinates of the ship are: (x 129.850, y 454.800, z -2.0).

Figure 8.2: Sampling of fluvial deposits for optical dating.

found. The shape of the stamp was used only between 140 and 180 AD. A drinking cup that was found in the ship has a shape which was developed in 175 AD. Finally, several pairs of shoes were preserved in and around the ship. One of these are made of cork in a style that was manufactured between 180 and 200 AD. This pair however was found outside the ship and may be unrelated. All age evidence is in agreement and suggests sinking of the ship at the end of the second century AD.

The relatively long time between cutting of the trees from which the ship was built and the sinking of the ship suggests that the ship was in use during an extended period. This is corroborated by a large number of repairs that were carried out to plug holes in the body of the vessel. The investigation of the ship has proven two assumptions wrong: 1) the ship was not built in middle or southern Germany, 2) the ship was not built for a single trip downstream and then used as building material. These issues are discussed elsewhere (Bazelmans and Jansma, 2005) and will not be repeated here.

For this study the most important information on the barge is the extremely tight age control. It is also important to note that the wood of the ship is little abraded which indicates that the ship was buried in sediments soon after sinking. This is corroborated by the many finds which are preserved in the ship.

8.4 Samples and experiments

We took six samples from sandy channel deposits in and around the ship. Pairs of samples were taken at either side (samples 1 and 2 on the starboard side (upstream), samples 5 and 6 on the port side (downstream) and samples 3 and 4 from sediments accumulated inside the barge). All samples were taken by driving a light-tight PVC tube into an exposed wall. In the luminescence laboratory the outer parts of the core were used for dose rate analysis whereas the inner part which was not exposed to light was used for equivalent dose determination.

8.4.1 Dose rate determination

The natural dose rate is calculated from the radionuclide concentration of sediments surrounding the sample, in combination with the depth of the sample below the surface and the water content of the sample. About 250 grams of material was dried and ground for assessment of the dose rate. The dry sample was mixed with melted wax and moulded in a puck shape. We determine the radionuclide concentration by high-resolution gamma-ray spectroscopy (Murray *et al.*, 1987); spectral data are converted to activity concentrations and infinite matrix dose rates using the most recent conversion data available (private communication Murray and Nathan, 2004). Several nuclides from the U and Th decay chains were measured to ensure that the samples were in secular equilibrium. The natural dose rate was calculated from the infinite matrix dose rate using attenuation factors given by Mejdahl (1979). A contribution from cosmic rays was included based on the burial depth of the sample following equations presented by Prescott and Hutton (1994). A correction was made for attenuation of the dose rate by water using the attenuation factors given by Zimmerman (1971). The deposits were formed at a few meters water depth and the groundwater table has risen continuously since the early Holocene (Cohen, 2005). We can thus safely assume that the sediments were fully water saturated since deposition; based on the porosity of channel sands ($34 \pm 3\%$; Weerts, 1996) we used a water content of 20% by weight for dose rate calculations.

Uncertainties taken into account for dose rate determination include both systematic and random errors. The systematic errors are calibration of the gamma spectrometer (2%), conversion from activity concentrations into dose rate (3%), uncertainties in water content (3%), a 1% uncertainty in grain-size attenuation, and 10% uncertainty in cosmic dose rate. Random errors arise solely from counting statistics in gamma-spectrometry.

8.4.2 Single aliquot equivalent dose determination

Samples for equivalent dose determination were sieved to obtain the grain size fraction used for analysis (sample 103006: 180-250 μm, all other samples 212-250 μm). This fraction was then treated with HCl and H_2O_2 to remove carbonates and organics, treated with concentrated HF (40%) for 40 minutes to remove feldspars and etch the alpha-exposed outer layer of the quartz grains and washed with HCl to remove fluorides. Finally the sample was sieved again to remove grains that were severely affected by the HF treatment.

Measurements for equivalent dose determination were performed using Risø TL/OSL DA 15 readers (Bøtter-Jensen *et al.*, 2003). The readers use blue LEDs for stimulation (470 ± 30 nm), the OSL signal was detected through a 7.5 mm Hoya U340 filter. The readers are equipped with 1.48 GBq Sr-90 beta sources for irradiation. Stainless-steel discs were mounted with a few hundred grains using silicone spray as an adhesive. Only the center 2 mm of discs was covered with grains to facilitate the detection of scatter in equivalent doses due to inhomogeneous resetting.

The modified SAR procedure (Murray and Wintle, 2003) was used for equivalent dose determination (see Table 8.1 for measurement details). In this protocol the luminescence response to the natural dose and following a range of laboratory doses which encompass the natural dose is measured. Each measurement is followed by measurement of the OSL response to a fixed test dose to monitor and correct for sensitivity changes. The SAR cycles are: 1) measurement of the natural, 2) measurement of OSL response to three regenerative doses, 3) measurement of a zero dose (recuperation), and 4) a repeat measurement of the second regenerative dose (recycling). Finally, the test dose response after a 40 s exposure to infrared stimulation (880 nm) at 50°C was recorded to allow the identification of aliquots which are contaminated with feldspar grains (Duller, 2003).

Stimulation was for 40 s; for routine analysis the signal was integrated over the first 0.32 s, and the background over the last 4 s was subtracted. Equivalent doses were also calculated using integration over four consecutive 0.32 s intervals (i.e. 0.32 - 0.64 s; 0.64 - 0.96 s; 0.96 - 1.28 s; 1.28 - 1.60 s) to investigate the dependency of the equivalent dose on the signal integration interval used. We investigated the dependency of equivalent dose on the preheat temperature used for a selection of samples (Fig. 8.3); a preheat temperature of 225°C was selected for data acquisition. Samples were heated to 200°C before measurement of the test dose response. At the end of each SAR cycle an OSL readout at elevated temperature (245°C) was incorporated to avoid recuperation effects (Murray and Wintle,

Table 8.1: Measurement protocol for single aliquot and single grain analysis

Step	Treatment	Single Aliquot	Single Grain	Record
1	Irradiate[a]	~ 2,4,8,0,4 Gy	~ 5,0,5 Gy	
2	Preheat	10 s at 225°C	10 s at 225°C	
3	OSL[b] measurement	BD 40 s at 125°C	GL 0.90 s at 125°C	L_i
4	Test dose	~ $2-4$ Gy	20 Gy	
5	Cutheat	0 s at 200°C	0 s at 200°C	
6	OSL measurement	BD 40 s at 125°C	GL 0.90 s at 125°C	T_i
7	OSL bleach	BD 40 s at 245°C	GL 0.90 s at 245°C	
8	Repeat 1-7	6 SAR cycles	4 SAR cycles	
9	Test dose	~ $2-4$ Gy	~ 20 Gy	
10	Cutheat	0 s at 200°C	0 s at 200°C	
11	IR bleach	IR 40 s at 50°C	IR 200 s at 75°C	IR
12	OSL measurement	BD 40 s at 125°C	GL 0.90 s at 125°C	${T_{pirb}}^c$

[a] Samples are not irradiated in the first cycle to measure the natural signal.

[b] OSL stimulation provided by blue diodes (BD) for single aliquots and by green laser (GL) for single grain measurements.

[c] Test-dose response after IR stimulation.

2003).

Single-aliquot SAR data were accepted if the recycling ratio was between 0.8 and 1.2 and recuperation was smaller than 10% of the first regenerative dose response. To avoid aliquots with feldspar contamination two criteria were used: 1) a considerable IR response ($>$ 10% of the blue OSL signal) and 2) if the blue stimulated test dose response was reduced by more than 10% following IR exposure. Data were rejected if an aliquot failed either test.

To avoid bias of the results to outliers we iteratively removed single aliquot equivalent doses separated more than 2.5 standard deviations from the sample mean. The mean equivalent dose after iteration is very similar to the median without iteration; advantage of the adopted method is that the uncertainty on the estimate can be given.

Uncertainties taken into account in the equivalent dose include systematic errors in calibration of the beta sources (3%) and random errors due to spread in results obtained on individual aliquots.

8.4.3 Single grain equivalent dose determination

Single-grain measurements on two samples were made using the Risø single grain attachment which allows stimulation of individual grains with green light (532 nm) from a laser (Bøtter-Jensen *et al.*, 2003). A 2.5 mm Hoya U340 filter was used for OSL detection following Ballarini *et al.* (submitted). Based on the single-aliquot investigations, a 225°C preheat and 200°C cutheat were used. Stimulation was for 0.90 s at 125°C; the OSL signal was obtained by integrating over the first 0.02 s of stimulation. For background subtraction we used the late background (signal integrated over the last 0.10 s of stimulation) and early background

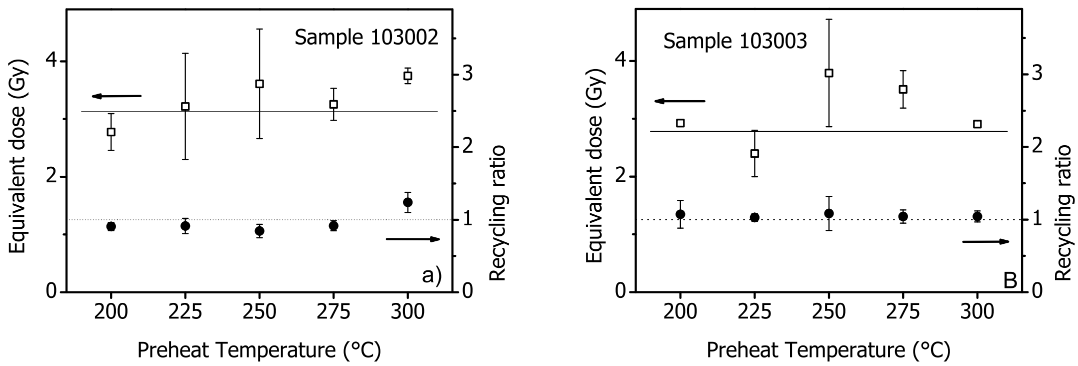

Figure 8.3: Equivalent doses and recycling ratios as a function of preheat temperature for sample 103002 (A) and 103003 (B). The solid line indicates the mean equivalent dose obtained on the sample (Table 8.3), the dotted line indicates a recycling ratio of unity. A preheat temperature of 225°C was used for all subsequent measurements. Each data point represents three replicate measurements.

(signal integrated over 0.02 -0.04 s).

A limited SAR procedure was used with one regenerative dose at 5 Gy. A relatively large test dose of 20 Gy was used to induce a large response and thereby reduce uncertainties (Ballarini *et al.*, submitted). The SAR cycles are: 1) measurement of the natural, 2) measurement of the regenerative dose, 3) measurement of a zero dose (recuperation), and 4) a repeat measurement of the regenerative dose (recycling). Finally, the test dose response after a 200 s exposure to infrared stimulation (880 nm) at 75°C was recorded to allow the identification of contaminating feldspar grains (following Duller, 2003).

We measured 2900 and 2400 grains for sample 103003 and 103005, respectively. We used a combination of rejection criteria to select grains used for analysis: 1) The relative standard error (RSE) on all test dose responses must be less than 30%; 2) the ratio of the test-dose responses with and without prior IR stimulation must be consistent with unity within 2.5 standard deviations; 3) the recycling ratio must be consistent with unity within 2.5 standard deviations; 4) recuperation on the first regenerative dose must be less than 30% and 5) the responses to the regenerative dose must be positive.

We used the same iterative method employed for single aliquots to remove grains for which the measured equivalent dose was more than 2.5 standard deviations removed from the average equivalent dose value.

8.5 Results

8.5.1 Dose rate

Radionuclide activities, cosmic dose rate and total dose rate after attenuation are presented in Table 8.2. There are no indications of secular disequilibrium in the Uranium and Thorium decay chains. Dose rates on the paired samples are very similar.

Table 8.2: Dose rate determination

Sample	Depth	Water Content		Radionuclide concentration (Bq/Kg)						Total dose rate			
	(m)	(%)	s.e.	U-238	s.e.	Th-232	s.e.	K-40	s.e.	(Gy/ka)	s.e.	syst	rand
103001	3.7	20	3	12.1	0.2	11.8	0.3	521	6	1.81	0.07	0.06	0.02
103002	3.7	20	3	13.1	0.2	13.7	0.3	501	4	1.77	0.06	0.06	0.01
103003	3.35	20	3	15.3	0.2	20.2	0.3	380	5	1.61	0.06	0.06	0.01
103004	3.35	20	3	13.1	0.2	16.6	0.4	413	5	1.62	0.06	0.06	0.02
103005	3.75	20	3	18.8	0.3	19.4	0.5	424	4	1.74	0.06	0.06	0.01
103006	3.35	20	3	18.3	0.2	17.8	0.3	477	6	1.84	0.07	0.07	0.02

8.5.2 Single aliquot

Investigation of the dependency of the equivalent dose on preheat temperature used revealed no trends for the whole temperature range from 200 to 300°C (Fig. 8.3). This indicates that there is negligible thermal transfer from less light sensitive traps. We chose a preheat temperature of 225°C for data acquisition.

In Fig. 8.4 we show equivalent doses obtained using the 0.96 - 1.28 s integration interval as a function of the equivalent dose obtained using the standard 0 to 0.32 s integration interval. The rejection criteria with regard to recycling, recuperation and feldspar contamination were used for both integration intervals. Due to lower signals for the later interval, fewer aliquots were accepted for analysis. For most aliquots the equivalent dose estimates are similar with most points falling close to the 1:1 line. In Fig. 8.5 we show equivalent doses for different integration intervals for the five aliquots that gave the highest equivalent dose using the standard 0.32 s integration interval. Results show no clear dependency of the equivalent dose on the integration interval used.

For each sample the equivalent dose was determined for approximately 40 aliquots. All samples showed relatively wide spread in values of equivalent dose. The procedure to remove outliers from the equivalent dose distribution ($>$ 2.5 standard deviation from sample mean) was iterated until no more aliquots had to be discarded. This iteration procedure resulted in the rejection of one to four aliquots per sample. Equivalent doses obtained on individual aliquots and the resulting histograms of the dose distributions are shown in Fig. 8.6.

8.5.3 Single grain

We found no dependency of equivalent dose on the relative standard error for individual grains for both early background subtraction and late background subtraction (data not shown). Since dim grains would be more affected by inappropriate background subtraction, the absence of a trend indicates that the both background estimations are valid. The late background subtraction method was adopted as more grains can be accepted for analysis (Ballarini *et al.*, submitted).

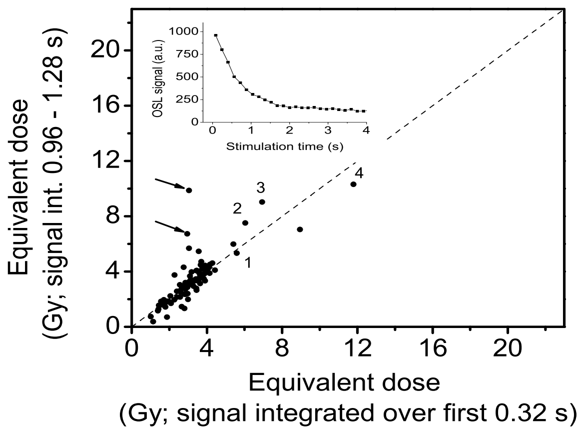

Figure 8.4: Comparison of single-aliquot equivalent doses obtained using the 0 - 0.32 s interval for signal integration and those obtained on the same aliquots using the 0.96 - 1.28 s interval for signal integration. The plot shows all aliquots of the six samples investigated for which both measurements passed the acceptation criteria detailed in the text. Note that both equivalent dose estimates are similar irrespective of the value obtained. The inset shows a typical OSL decay curve.

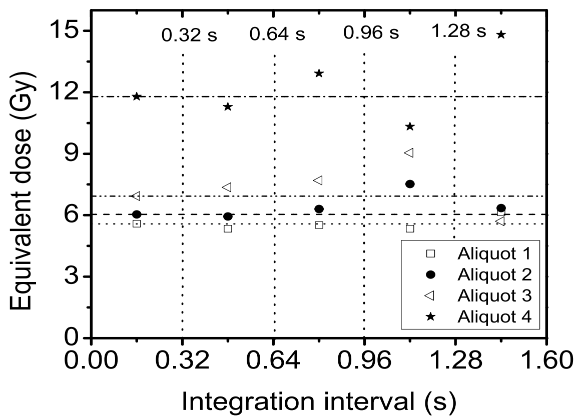

Figure 8.5: Dependency of the equivalent dose on the signal integration interval. Shown are the four aliquots for which all estimates passed the acceptation criteria and which gave the highest equivalent dose values using the standard (0 - 0.32 s) integration interval. Note that there is no dependency of the equivalent dose on integration interval used.

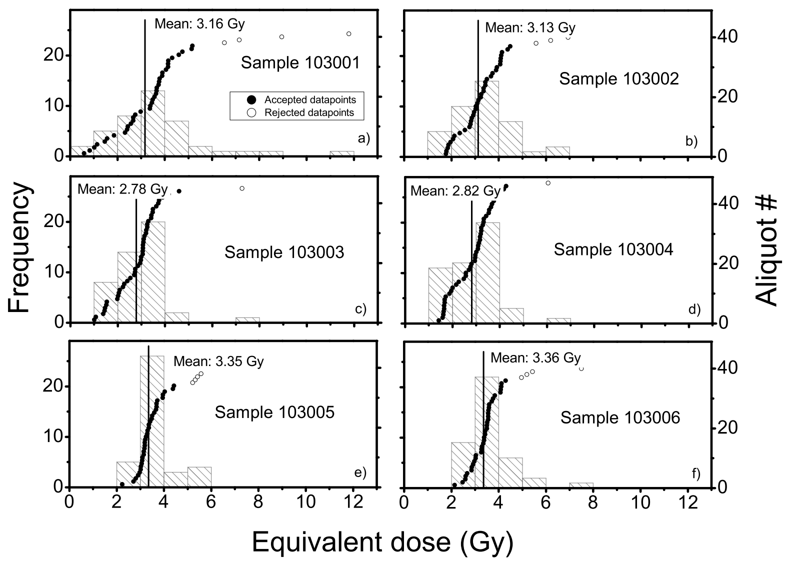

Figure 8.6: Single aliquot dose distributions for the six samples studied. Histograms show all points that past the acceptation criteria (see main text). The bin size is chosen identical (1 Gy) for all samples to allow visual comparison of the distributions. Single-aliquot equivalent doses separated more than 2.5 sigma from the sample mean (indicated in open points) were iteratively discarded for calculation of the mean equivalent dose. The resulting dose distributions are normal, apart from the distribution obtained on sample 103004 which shows some evidence of bimodality.

We investigated the dependency of the equivalent dose on the stringency of the RSE rejection threshold and found no clear dependencies up to a RSE threshold of 50% (Fig. 8.7). Data are displayed with and without the use of the iterative method for discarding grains whose equivalent doses were outside 2.5 standard deviations from the average.

After the rejection criteria were applied (using a RSE threshold of 30%) the accepted grains returned average equivalent doses of 2.64 ± 0.21 Gy (103003; 56 grains) and 2.82 ± 0.31 Gy (103005; 43 grains). Iterative removal of outliers resulted in exclusion of only two and one grain for sample 103003 and 103005, respectively. After iteration, we obtained equivalent dose values of 2.46 ± 0.18 Gy (103003, 54 grains) and 2.68 ± 0.28 Gy (103005; 42 grains). Equivalent dose distributions are presented in Fig. 8.8 for both samples.

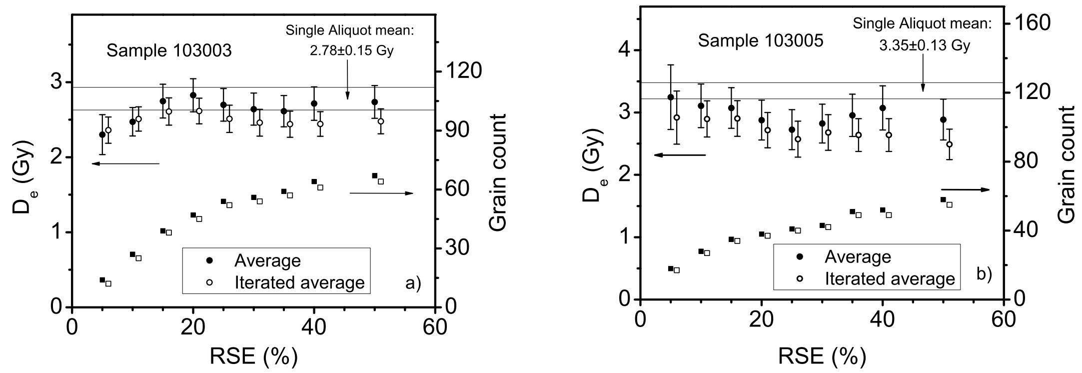

Figure 8.7: Single grain equivalent doses obtained on sample 103005 plotted as a function of the relative standard error (RSE) on the first test dose. Data for early background subtraction and late background subtraction are shown. Neither of the data set shows any dependency of the equivalent dose on the RSE. Late background subtraction was used for further analysis as it allows more grains to be accepted.

8.6 Discussion

8.6.1 Single-aliquot

The observed spread in single-aliquot equivalent doses is likely caused by a combination of: 1) measurement uncertainties; 2) grain-to-grain differences in dose rate in the natural environment; 3) incomplete resetting of the OSL signal prior to burial for some grains. The average equivalent dose obtained is little affected by the first two sources of scatter, but may be overestimated due to the incorporation of poorly bleached grains.

The challenge in analysing data for heterogeneously bleached samples is to identify those aliquots which contain poorly-bleached grains that contribute to the signal, and to ignore results on these aliquots in further analysis. One approach to identify such aliquots is to

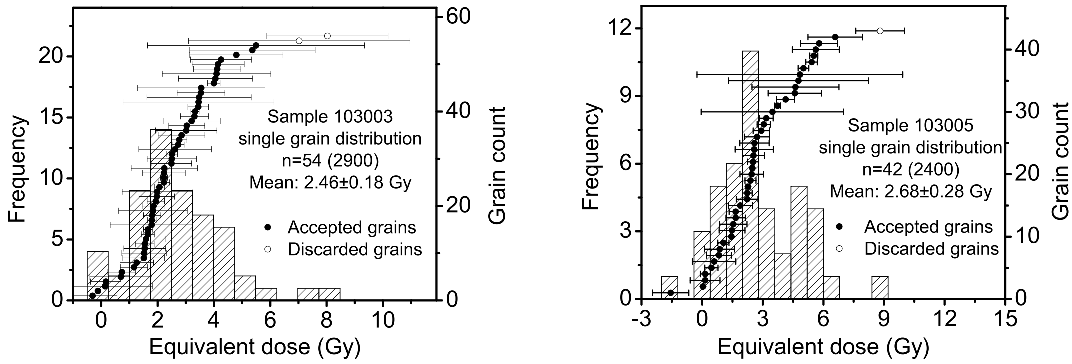

Figure 8.8: Single-grain equivalent dose distributions for sample 103003 (A) and 103005 (B). Method of plotting and rejection of outliers is identical to the single-aliquot results shown in Fig. 8.6.

compare equivalent doses using OSL components with different bleachability. However, we found no dependency of the equivalent dose on the interval used for integration (Fig. 8.4 and 8.5). We therefore conclude that such dependency cannot be used to identify poorly-bleached aliquots in our study. This is contrary to the findings by Bailey *et al.* (2003). Possible reasons why this method does not work are that either our signal arises entirely from the fast component, or the fast and medium components are equally well bleached in the original depositional environment.

As the dependency of equivalent dose on integration interval cannot be used to identify poorly bleached aliquots, rejection has to be based on the properties of the dose distribution itself. We found that through iteratively removing single-aliquot equivalent doses removed by more than 2.5 standard deviations from the sample mean we rejected a limited number of aliquots at the high end of the equivalent dose distribution (Fig.8.6). This corroborates our assumption that these outliers are caused by incomplete resetting of the OSL signal of one or more bright grains in these aliquots.

After discarding outliers, the equivalent doses are normally distributed (according to a Shapiro Wilk normality test) for all samples but 103004. For this sample there is evidence of a bimodal distribution. We hypothesize that the bimodal distribution for this sample arises from sampling a heterogeneous unit with a non-uniform dose rate. Since our dose rate sample was homogenized and given a mean dose rate, we also used the mean equivalent dose (after rejecting a single outlier) for age determination. The average equivalent dose after removal of outliers is presented in Tab. 8.3 and used for calculation of the optical age.

According to the independent age control the barge sank between 180 and 200 AD. Ages obtained by single-aliquot dating of the samples from fluvial deposits surrounding the ship are shown in Tab. 8.3 and Fig. 8.9. The ages are internally consistent and in excellent agreement with the independent age information. It should be noted that even without rejecting poorly bleached aliquots the age obtained (84 ± 102 AD) would have been in agreement with the archaeological age.

Table 8.3: Single-aliquot equivalent doses and ages

Sample	Equivalent dose				Age				Age	
	(Gy)	s.e.	syst	rand	(ka)	s.e.	syst	rand	AD	s.e.
103001	3.16	0.22	0.09	0.20	1.75	0.14	0.08	0.11	252	140
103002	3.13	0.16	0.09	0.13	1.77	0.11	0.08	0.07	237	111
103003	2.78	0.15	0.08	0.13	1.72	0.11	0.08	0.08	279	115
103004	2.82	0.15	0.08	0.12	1.74	0.11	0.08	0.08	264	113
103005	3.35	0.13	0.10	0.08	1.93	0.10	0.09	0.05	75	102
103006	3.36	0.13	0.10	0.08	1.82	0.10	0.09	0.05	181	99
Average					**1.79**	**0.09**	**0.08**	**0.03**	**215**	**89**

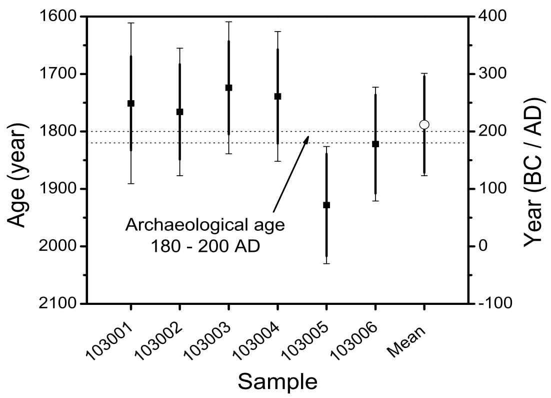

Figure 8.9: Optical ages on the six samples (closed dots) and the overall mean (open circle) as derived from the single-aliquot equivalent dose determinations. Error bars indicate the random error (thick line) and total uncertainty (thin line).

8.6.2 Single-grain

The single-grain dose distributions obtained on samples 103003 and 103005 (Fig. 8.8) corroborate our conclusion from single-aliquot work that the OSL signal of the vast majority of grains was completely reset at deposition.

Burial ages obtained from the single-grain work (459 ± 202 AD and 469 ± 297 AD for sample 103003 and 103005, respectively) are somewhat younger than the independent age control suggests and also younger than results from the single aliquot work. The poor precision on the single-grain equivalent dose estimates however precludes us from drawing firm conclusions regarding the validity of the single-grain ages. Large uncertainties on single grain dose estimates are partially due to the limited number of grains left available after the rejection criteria were applied. In order to obtain a more significant D_e estimate from a distribution, a larger number of grains should be employed.

8.7 Summary and conclusions

We applied single-aliquot optical dating to quartz extracts from six samples taken from fluvial channel deposits in and around the Roman barge with excellent independent age control. For two samples we additionally measured equivalent doses of individual grains of quartz. From our investigation we conclude that:

- there is no dependency of equivalent dose on the OSL integration interval for aliquots giving high equivalent doses. Hence, we cannot use D_e-t dependencies to identify aliquots which contain poorly-bleached grains;
- by using an iterative procedure based on the 2.5 standard deviation threshold around the mean we are able to remove points that are not part of the expected single-aliquot equivalent-dose distribution. The resulting dose distributions are normally distributed;
- the mean equivalent doses from these dose distributions provide burial ages that are internally consistent and in excellent agreement with the expected age of the deposits;
- single-grain equivalent dose distributions corroborate that the vast majority of grains had their OSL signals completely reset prior to deposition. Outliers can be removed by using an iterative procedure identical to that used for single aliquots;
- average single grain equivalent doses are smaller than those obtained for single aliquots and lead to ages that are slightly too young compared to the independent age information.

Bibliography

Aitken, MJ (1998). *An introduction to optical dating.* Oxford University Press.

Bailey, RM, Singarayer, JS, Ward, S and Stokes, S (2003). Identification of partial resetting using d-e as a function of illumination time. *Radiation Measurements*, 37, 511–518.

Ballarini, M, Wallinga, J, Bos, AJJ and Wintle, AG (submitted). A modified SAR protocol for optical dating of individual grains from young quartz samples. *Radiation Measurements.*

Ballarini, M, Wallinga, J, Murray, AS, Van Heteren, S, Oost, AP, Bos, AJJ and Van Eijk, CWE (2003). Optical dating of young coastal dunes on a decadal time scale. *Quaternary Science Reviews*, 22, 1011–1017.

Bazelmans, J and Jansma, E (2005). Das Leben an Bord - Im Schiffsfund von De Meern (Niederlande) ist der Alltag auf einem Römischen Frachter konserviert. *Antike Welt*, 36, 23–29.

Berendsen, HJA and Stouthamer, E (2000). *Palaeogeographic development of the Rhine-Meuse delta, The Netherlands.* Koninklijke van Gorcum.

Berger, GW and Luternauer, JJ (1987). Preliminary fieldwork for thermoluminescence dating studies at the Fraser River delta, British Columbia. *Geological Survey of Canada Paper*, 87, 901–904.

Bøtter-Jensen, L, Andersen, C.E., Duller, GAT and Murray, AS (2003). Developments in radiation, stimulation and observation facilities in luminescence measurements. *Radiation Measurements*, 37, 535–541.

Cohen, KM (2005). 3D Geostatistical interpolation and geological interpretation of paleo-groundwater rise in the holocene coastal prism in the Netherlands. In *River Deltas - Concepts, models, and examples.*, pages 341–364. Giosan, L. & J.P. Bhattacharya (Eds.), SEPM Special Publication edition.

Duller, GAT (2003). Distinguishing quartz and feldspar in single grain luminescence measurements. *Radiation Measurements*, 37, 161–165.

Larsen, NA, Bulur, E, Bøtter-Jensen, L and McKeever, SWS (2000). Use of the lm-osl technique for the detection of partial bleaching in quartz. *Radiation Measurements*, 32, 419–425.

Li, SH (1994). Optical dating: insufficiently bleached sediments. *Radiation Measurements*, 23, 563–567.

Mejdahl, V (1979). Thermoluminescence dating: beta dose attenuation in quartz grains. *Archaeometry*, 21, 61–72.

Murray, AS, Marten, R, Johnston, A and Marten, P (1987). Analysis for naturally occurring radionuclides at environmental concentrations by gamma spectrometry. *Journal of Radioanalytical Nuclear Chemistry*, 115, 263–288.

Murray, AS and Olley, JM (2002). Precision and accuracy in the optically stimulated luminescence dating of sedimentary quartz: a status review. *Geochronometria*, 21, 1–16.

Murray, AS and Wintle, AG (2003). The single aliquot regenerative dose protocol: potential for improvements in reliability. *Radiation Measurements*, 37, 377–381.

Nales, T and Vis, GJ (2003). *De paleogeografie van de Oude Rijn.* Master's thesis, Utrecht University.

Prescott, JR and Hutton, JT (1994). Cosmic ray contributions to dose rates for luminescence and ESR dating: large depths and long-term time variations. *Radiation Measurements*, 23, 497–500.

Stokes, S, Bray, HE and Blum, MD (2001). Optical resetting in large drainage basins: tests of zeroing assumptions using single-aliquot procedures. *Quaternary Science Reviews*, 20, 879–885.

Vandenberghe, J and Maddy, D (2000). The significance of fluvial archives in geomorphology. *Geomorphology*, 33, 127–130.

Wallinga, J (2002a). Optically stimulated luminescence dating of fluvial deposits: a review. *Boreas*, 31, 303–322.

Wallinga, J (2002b). On the detection of OSL age overestimation using single-aliquot techniques. *Geochronometria*, 21, 17–26.

Wallinga, J, Duller, GAT, Murray, AS and Törnqvist, TE (2000). Testing optically stimulated luminescence dating of sand-sized quartz and feldspar from fluvial deposits. *Radiation Measurements*, 32, 691–695.

Weerts, HJT (1996). *On the detection of OSL age overestimation using single-aliquot techniques.* Nederland Geographical Studies.

Zimmerman, DW (1971). Thermoluminescent dating using fine grains from pottery. *Archaeometry*, 13, 29–52.

Summary and Conclusions

Optically Stimulated Luminescence (OSL) dating is a tool used in Quaternary Geology for assessing ages of depositional mineral grains such as quartz, feldspars and zircons. In particular, OSL showed to be exceptionally robust and reliable for dating quartz samples. Such a technique has been successfully applied in the age range of 1.000 up to 150.000 years, but optical dating below and beyond these limits remains a challenge. OSL dating relies on the assumption that the luminescence signal of grains is fully reset to zero by sunlight exposure before deposition. If this requirement is not fulfilled (i.e. grains were "poorly-bleached"), ages may be grossly overestimated. In particular, poor-bleaching can significantly affect age estimations of young sediments, for which the remnant signal may be large relative to the signal built up during burial.

Standard procedures for estimating the burial dose of a sediment make use of a large number of grains (*aliquot*) that is measured simultaneously. This approach has been shown to work well on homogeneously bleached sediments, but to fail if heterogeneous bleaching occurred. An alternative way to investigate poor-bleaching within a sample is to measure the OSL signal from individual grains rather than from aliquots made up of several thousands of grains. The advantage is that individual grains with large doses (possibly due to poor-bleaching) can be identified and dealt with. However, the single grain approach is not without problems. Drawbacks are that only a small percentage of the measured grains produce detectable signals and luminescence responses are weak.

The aim of this thesis it to determine the feasibility of applying dating techniques to individual grains of quartz from deposits formed within the last 300 years.

The problem was tackled step by step.

From single-aliquot to single-grain OSL dating

First we validated multigrain OSL dating using samples for which heterogeneous bleaching was not a significant issue (**Chapter 2**). This gave us the knowledge of the limits of standard luminescence techniques. The south-west of the island of Texel (The Netherlands), which mainly consists of sand-dune deposits formed over the past 300 years, was chosen as a study site. The timing of formation of the sequence of dunes at the study location is accurately known from historical maps and documents. The sand grains in these dunes are likely to have experienced several bleaching cycles during marine and aeolian transport, before being trapped and buried in a coastal dune. We therefore expect these grains to be well bleached (i.e. there should be negligible charge remaining in the easy-to-bleach OSL traps at the time of burial). These unusual conditions, combined with independent age control information, make the site an ideal sampling area for validating OSL dating techniques. It was found that OSL ages from large aliquots were reproducible and in excellent agreement with the expected ages. We showed that aeolian samples as young as ~ 10 years could be successfully dated by quartz single-aliquot dating.

Chapter 3 is a review of the methods reported in literature coping with insufficient bleaching of quartz. Although several authors have developed methods that deal with poor bleaching based on the multi-grain approach, a general opinion is that in order to solve the issue, investigations on a single-grain base are needed.

Optimization of instrumentation and protocol for single grain dating

As a second step before attempting SG age determinations, we tried to optimize existing instruments and measurement procedures for dating individual grains of quartz from young deposits. The need arose from the fact that luminescence signals from extremely young samples are weak and noisy.

The first check on instrumentation we made was to assess whether β-sources used for irradiating samples gave rise to uniform irradiation of sample disks (**Chapter 4**). Since 100 grains are mounted on a single grain disk and these are irradiated simultaneously, it is important that each of them receives the same dose. If not, OSL responses from grains after laboratory irradiation are not comparable. We found that only two β-sources out of four available at the NCL are sufficiently uniform. This could be seen from 3D graphs in which the dose rate from each individual grain was plotted as a function of its position on the disk. We conclude that sources should be checked for uniformity before they are used for single grain measurements.

Another important issue concerning instrument optimization, is to maximize the light detection efficiency. In this regard, both the PM tube and the detection filters play an important role. We investigated a number of alternative filters to be used for single grain measurements and showed that the light efficiency can be increased by mounting filter combinations other then the one which is commonly used (**Chapter 5**). Using the newly selected filter, the luminescence light collection was improved and more grains could be used for analysis.

Although the above changes in the standard instrumentation were significant steps towards optimized single grain measurements of young samples, the major challenge we had to face regarded the protocol used for determining burial doses. Existing protocols were designed and have been shown to work well on relatively old materials (> 1000 years). However, the use of such protocols is impractical for dating young samples. In the case of extremely young samples, such as the ones used in this study, pre-existing protocols needed significant changes. The most important changes were focused on two issues: (a) further increase of the percentage of grains that could be accepted for dose analysis and (b) selection of the OSL component that is more representative of the last depositional event that is to be dated.

The protocol we developed for dating individual young grains was tested on two samples that were previously dated by means of large aliquots (**Chapter 6**). The purpose of this study was to assess whether single grain results were consistent with single aliquot (SA) results and independent age information. For the purpose, two well-bleached samples of 300 years were measured by means of single grain methods. This kind of comparison was of great importance, in that if single grain dating could not provide reliable ages for samples taken from a “perfect" environment, where no bleaching problems are involved, it would have been of little use for single grains from poorly-bleached materials. We showed that single grain dose estimates for the above two samples could be compared to those from SA work if the background for the OSL signal is integrated in the early part of the decay curve (EBG). However, single grain estimates are systematically less precise than the corresponding single aliquot ones. This fact has most likely to be ascribed to the limited number of individual grains on which the final dose was estimated. In general, only 3-5% of the total number of measured grains can be used for equivalent dose analysis. Thus, a way of improving single grain estimates accuracy might be to measure a lot more grains. Although useful for understanding distributions from individual grains, this approach is not convenient for routine dating measurements.

Applications of the modified single grain protocol

The modified protocol was also applied to two more samples from Texel (**Chapter 7**). The first was a well-bleached dune-sand sample estimated to be less than 10 years from single aliquot results and independent age control. The second one is known to be less than one year old but single aliquot work returned an age of 73 ± 24 years. With the first sample the ability of SG techniques to date extremely young sediments was tested; with the second we wanted to determine whether the single grain approach could be used for dating poorly-bleached samples otherwise overestimated by single aliquot results. Our results on these two samples are somewhat disappointing and encouraging at the same time. The well-bleached sample could be correctly dated (within errors) but very large uncertainties are associated with the final dose. For the poorly-bleached sample, no satisfactory dose estimate could be provided. However, in this last case, poorly-bleached grains responsible for the gross overestimation obtained with SA work could be clearly identified.

Another application of the newly developed protocol was attempted on an archaeological site (**Chapter 8**). A very well preserved Roman barge was recently found in The Netherlands in the vicinity of Utrecht (De Meern 1), which has been dated from 180-200 AD by means of archaeological findings. Multi- and singe-grain OSL measurements were performed on samples from fluvial deposits taken in the surroundings of the barge, with the aim of investigating partial bleaching on fluvial deposits. Although in a fluvial environment insufficient bleaching is to be expected, we found that ages determined through the multi-grain method are in good agreement with the expected age. On the other hand, results from SG measurements clearly show that heterogeneous resetting occurred for these samples. However, for reasons that are not yet known, SG ages underestimate the age of the barge determined by archaeological means.

The future of SG dating

We conclude that although the SG approach is still under development, it shows to be the most promising means for analyzing and dating poorly-bleached samples. This optimism is justified by the fact that insufficiently bleached grains can be easily recognized through SG distributions and handled accordingly. Although we found that single-grain estimates are not as precise as multigrain OSL, uncertainties may be decreased by measuring a larger number of grains and by improving our analysis techniques and developing more suitable ones.

For what concerns dating of individual young quartz grains, the future is less easy but more challenging than optical dating of older individual grains. When dealing with extremely young grains, uncertainties become significantly larger due to poor counting statistics. In this case, large errors do not necessarily mean poor reproducibility. The nature of such uncertainties is intrinsic to the fact that doses to be measured are close to zero. Thus, conventional methods based on individual uncertainties (for example the weighted mean) may not represent the most correct approach for this particular case. Also, representing dose estimates obtained from young grains means dealing with distributions centered very close to zero. Several methods for analyzing dose distributions that have been developed for older samples (for example the age models and the leading edge) are not applicable with such distributions and new approaches are required.

The work presented in this thesis clearly shows the feasibility and great potentials of SG dating of young quartz samples - and a suitable protocol for the purpose is proposed. To make optical single-grain dating a robust and reliable tool for dating sediments of less than 300 years old, further investigations and additional innovative approaches are needed.

Samenvatting en conclusies

Optisch geStimuleerde Luminescentie- (OSL) datering is een instrument om de afzettingsouderdom van sediment mineraal korrels zoals kwarts, veldspaat en zirkoon te bepalen. De techniek is succesvol toegepast voor het ouderdomsbereik van 1.000 tot 150.000 jaar; optische datering van afzettingen buiten dit bereik is een uitdaging. Optische datering bouwt op de aanname dat het luminescentiesignaal van de korrels volledig op nul is gesteld door blootstelling aan zonlicht voor afzetting en begraving. Als aan deze voorwaarde niet wordt voldaan (onvolledige 'bleking' van de korrels) dan kan de afzettingsouderdom sterk overschat worden. Onvolledige (ofwel inhomogene) bleking heeft vooral consequenties voor datering van jonge sedimenten; hier kan het restsignaal groot zijn vergeleken met het signaal dat na afzetting is opgebouwd.

Standaardprocedures om de dosis te bepalen die het sediment ontvangen heeft na begraving maken gebruik van submonsters (aliquots) die bestaan uit een groot aantal korrels; deze korrels worden tegelijkertijd gemeten. Deze aanpak werkt goed als het OSL signaal in alle korrels volledig op nul gesteld is voor afzetting en begraving, maar niet als sommige korrels slecht gebleekt waren. Een manier om onvolledige bleking in een monster te onderzoeken is om het OSL signaal van individuele korrels te meten, in plaats van op submonsters die enkele duizenden korrels bevatten. Het voordeel is dat individuele korrels met grote doses (mogelijk door onvolledige bleking) geïdentificeerd kunnen worden en uitgesloten voor verdere analyse. Toch is de individuele korrel aanpak niet zonder problemen. Nadeel is dat slechts een klein percentage van de gemeten korrels een meetbaar OSL signaal geeft, en dat de OSL signalen zwak zijn.

Het doel van dit proefschrift is om te bepalen of het mogelijk is om optische dateringsmethoden toe te passen voor individuele kwartskorrels van afzettingen die tijdens de laatste driehonderd jaar gevormd zijn.

Het probleem wordt stap voor stap aangepakt.

Van meerkorrel naar individuele korrel OSL datering

Om te beginnen hebben we 'meerkorrel' OSL datering gevalideerd voor monsters waarbij heterogene bleking geen rol speelt (**Chapter 2**). Dit gaf ons inzicht in de beperkingen van standaard luminescentietechnieken. Het zuidwesten van het Waddeneiland Texel, dat voornamelijk bestaat uit kustduin afzettingen gevormd tijdens de laatste driehonderd jaar, werd gekozen als onderzoeksgebied. De tijd van vorming van deze duinsequentie is nauwkeurig bekend uit historische kaarten en geschriften. De zandkorrels in de duinen zijn voordat ze begraven raakten blootgesteld aan zonlicht tijdens een aantal cycli van marien en eolisch transport. We verwachtten daarom dat deze korrels volledig zijn gebleekt (dat wil zeggen dat er geen lading meer aanwezig is in de makkelijk-te-bleken OSL-vallen in het kristalrooster ten tijde van begraving). Deze ongebruikelijke condities, gecombineerd met de onafhankelijke ouderdomsinformatie, maken dit gebied ideaal voor het valideren van OSL dateringsmethoden. We vonden dat optische ouderdom van deze monsters (bepaald met OSL meting op submonsters van duizenden kwartskorrels; single-aliquot, SA methoden) reproduceerbaar waren en uitstekend overeen kwamen met de verwachte ouderdom. We toonden dat eolische afzettingen van ongeveer 10 jaar oud met succes gedateerd konden worden met deze methode.

Chapter 3 geeft een overzicht van gesuggereerde methoden voor het omgaan met onvolledige bleking van kwartskorrels uit sedimenten. Hoewel verschillende auteurs meerkorrel methoden hebben ontwikkeld om met onvolledige bleking om te gaan, wordt algemeen verondersteld dat onderzoek aan individuele kwartskorrels noodzakelijk is om het probleem op te lossen.

Optimalisatie van instrumenten en protocol voor individuele korrel datering

Vervolgens hebben we geprobeerd om de bestaande instrumentatie en meetprocedures te optimaliseren voor het dateren van individuele kwartskorrels van jonge afzettingen. Deze optimalisatie was noodzakelijk omdat de OSL signalen van de zeer jonge monsters zwak zijn en veel ruis bevatten.

De eerste controle op de apparatuur was of de beta-bronnen die voor bestraling van de monsters gebruikt worden een uniforme bestraling van het hele monster (een disk met een diameter van 1 cm) gaf (**Chapter 4**). Het is belangrijk dat alle 100 korrels die gelijktijdig worden bestraald op een 'individuele korrel disk' dezelfde dosis ontvangen. Als dit niet het geval is zijn de OSL responsies van de korrels na bestraling in het lab niet vergelijkbaar. We vonden dat slechts twee van de vier beta-bronnen die bij het Nederlands Centrum voor Luminescentiedatering (NCL) aanwezig zijn voldoende uniform zijn voor gebruik voor individuele korrels. Dit bleek uit 3D plots waar het dosistempo voor elke positie op de 'individuele korrel disk' werd geplot als functie van de positie op de disk. We concluderen dat de homogeniteit van bronnen gecontroleerd moet worden voordat ze gebruikt worden voor OSL metingen op individuele korrels.

Een ander belangrijk punt met betrekking tot optimalisatie van de instrumentatie is het maximaliseren van de OSL signaal detectiegevoeligheid. Hier spelen de PM-buis en de detectiefilters een belangrijke rol. We hebben een aantal alternatieve detectiefilters onderzocht die gebruikt kunnen worden voor individuele korrel metingen. We toonden aan dat de detectie gevoeligheid kon worden verbeterd door een andere filtercombinatie te gebruiken dan die standaard gebruikt worden (**Chapter 5**). Met de geselecteerde filter werd de gevoeligheid van de OSL-signaaldetectie verbeterd en konden meer korrels gebruikt worden voor analyse.

Hoewel de bovenstaande veranderingen aan instrumentatie belangrijke stappen waren voor geoptimaliseerde individuele korrelmetingen op jonge monsters, was de voornaamste uitdaging de ontwikkeling van een protocol voor de bepaling van de begravingsdosis. Bestaande protocollen zijn ontworpen en werken goed voor relatief oude materialen ($>$ 1000 jaar). Deze protocollen zijn echter niet bruikbaar voor datering van jonge monsters. Voor datering van zeer jonge monsters, zoals gebruikt in deze studie, moesten bestaande procedures ingrijpend gewijzigd worden. De belangrijkste aanpassingen hebben betrekking op twee onderdelen: a) verdere vergroting van het percentage korrels dat geruikt kan worden voor analyse en b) selectie van de OSL component die het meest representatief is voor het moment van afzetting dat bepaald moet worden.

Het protocol dat we hebben ontwikkeld voor de datering van individuele jonge korrels is getest op twee monsters die eerder met conventionele SA methoden waren gedateerd (**Chapter 6**). Het doel van dit onderzoek was om te bepalen of uitkomsten op individuele korrels overeenkwamen met die van de meerkorrel methode en met onafhankelijke ouderdomsinformatie. Voor dit doel werden twee goed gebleekte monsters van 300 jaar oud gemeten met individuele korrel (SG) methoden. Deze vergelijking was van groot belang, omdat toepassing van SG methoden op onvolledig gebleekte afzettingen geen zin had als op deze monsters met volledige bleking geen goede resultaten werden verkregen. We toonden dat SG dosis bepaling op de twee monsters overeenkwamen met die van eerdere meerkorrel metingen als het achtergrondsignaal voor de OSL meting werd bepaald op het eerdere deel van de 'decay curve' (early background - EBG methode). SG bepalingen zijn echter systematisch minder nauwkeurig dan de corresponderende SA bepalingen. Dit houdt waarschijnlijk verband met het beperkte aantal korrels dat voor de equivalente dosis bepaling kon worden gebruikt. De nauwkeurigheid van de SG methode zou kunnen worden vergroot door veel meer korrels te meten. Hoewel dit zeker nuttig is om SG dosis verdelingen beter te leren begrijpen, is dit niet practish voor routinematige metingen voor datering.

Toepassing van het aangepaste individuele korrel protocol

Het aangepaste protocol werd ook toegepast op twee additionele monsters van Texel (**Chapter 7**). Het eerste was een goed gebleekt duinzand monster dat volgens SA resultaten en volgens onafhankelijke ouderdomscontrole minder dan 10 jaar geleden afgezet werd. Voor het tweede monster gaven SA resultaten een ouderdom van 73 ± 24 jaar, terwijl het zand minder dan een jaar voor bemonstering werd afgezet. Met het eerste monster werd de mogelijkheid van SG methoden om extreem jonge sedimenten te dateren onderzocht; met het tweede monster wilden we bepalen of de SG aanpak gebruikt kon worden voor zeer jonge afzettingen die onvolledig gebleekt waren en waarvoor SA methoden een overschatting gaven. Onze resultaten op de twee monsters zijn tegelijkertijd teleurstellend en hoopgevend. Het goed gebleekte monster kon correct gedateerd worden (binnen de fout) maar gaf een ruime onzekerheidsmarge. Voor het tweede monster kon geen bevredigende dosis bepaald worden, maar konden wel de ongebleekte korrels, die verantwoordelijk waren voor de overschatting bij het gebruik van SA methoden, geïdentificeerd worden.

Vervolgens hebben we het nieuw ontwikkelde protocol toegepast voor een archeologische vondstplaats (**Chapter 8**). Een zeer goed bewaarde Romeinse platbodem (De Meern 1) werd recent gevonden in Leidscherijn, een VINEX locatie dicht bij de stad Utrecht. Het schip is volgens archeologische aanwijzingen gezonken tussen 180 en 200 AD. Zowel SA als SG OSL metingen werden uitgevoerd op monsters van rivierafzettingen uit de directe omgeving van het schip, met als doel de inhomogene bleking van deze afzettingen te onderzoeken. Hoewel in rivierafzettingen onvolledige bleking waarschijnlijk is, vonden we dat de ouderdom bepaald met meerkorrel methoden goed overeenkwamen met de verwachte ouderdom. Ondanks dat toonden SG methoden dat de korrels niet homogeen gebleekt waren. Om onbekende redenen zijn de SG dateringsuitkomsten te jong vergeleken met de onafhankelijk bekende ouderdom van het schip.

De toekomst voor datering van individuele korrels

We concluderen dat de SG methode, hoewel nog in ontwikkeling, de meest veelbelovende aanpak is voor analyseren en dateren van slecht gebleekte monsters. Dit optimisme wordt gerechtvaardigd door het feit dat slecht gebleekte korrels in principe kunnen worden herkend in SG dosis verdelingen en kunnen worden uitgesloten voor verdere analyse. We vonden dat SG dateringen niet zo nauwkeurig zijn als SA OSL dateringen, maar de onzekerheden kunnen verkleind worden door een groter aantal korrels te meten.

Datering van jonge kwarts korrels is minder makkelijk en een grotere uitdaging dan OSL datering van oudere individuele korrels. Voor jonge korrels worden onzekerheden duidelijk groter doordat signalen klein zijn en meetonzekerheden daardoor groter. In dit geval betekenen grote onzekerheidsmarges niet noodzakelijkerwijs slechte reproduceerbaarheid; de onzekerheden zijn onlosmakelijk verbonden met het feit dat de doses dicht bij nul zitten. Daarom zijn conventionele methoden die gebaseerd zijn op individuele onzekerheden (bijvoorbeeld gewogen gemiddelde) mogelijk niet de beste aanpak voor deze monsters. Daarnaast zijn dosisverdelingen op zeer jonge monsters zeer dicht bij het nulpunt gecentreerd. Meerdere methoden voor het analyseren voor dosis verdelingen voor oudere monsters (de ouderdomsmodellen en 'leading edge' methode) zijn niet toepasbaar voor zulke verdelingen en een nieuwe aanpak is nodig.

Het werk dat in dit proefschrift gepresenteerd wordt toont duidelijk de haalbaarheid en het grote potentieel voor datering van individuele kwartskorrels van jonge afzettingen, en een bruikbaar protocol voor deze toepassing wordt voorgesteld. Verder onderzoek en nieuwe innovatieve methoden zijn nodig om betrouwbare optische datering van individuele korrels van monsters jonger dan 300 jaar mogelijk te maken.

Acknowledgements

Ovvero ringraziamenti e pensieri sparsi

Non ci si innamora dell'Olanda a prima vista. Specialmente se piove per due mesi consecutivi dopo che sei appena arrivato. Forse non ci si innamora neanche dopo quattro anni di permanenza, ma almeno si apprezzano quelle cose che il grigio del cielo nasconde. Ecco, se non sono fuggito per tornare al sole caldo lo devo a SuperA. Con lei ho scoperto l'inebraiante esperienza di un salto nel vuoto, lasciare il noto per l'incerto quasi per gioco. Mettersi in discussione e ricominciare. Tutto, daccapo. Spero di ricominciare molte volte con te, SuperA, oppure mai piu', e rimanere per sempre nello stesso posto, coltivando il sogno di andare ad abitare prima o poi in un poggio piu' giu'. Spero che qualsiasi cosa mi capiti, sia con te.

Insomma, l'Olanda...

Adrie J.J. Bos e' la prima persona che ho incontrato in Olanda, per il mio colloquio. Quando e' venuto a prendermi in macchina alla stazione per portarmi all'Universita', ha subito sbagliato strada, facendomi pensare che non buttava per niente bene. Invece e' un bravo ricercatore e lo considero un po' come il mio padre adottivo olandese. Adesso sa anche che ero io a nascondergli la valigetta alla sera, prima che andasse a casa.

Carel e' il secondo olandese che ho incontrato in ordine di tempo. Uomo di raro acume e senso dell'umorismo, un leader nato. A lui devo moltissimo, compreso un grosso aiuto per quell'altro mio progetto, quello dei Selvaggi. Mi ha guidato come Virgilio con Dante, per chi capisce cosa intendo.

Il mio piu' sentito ringraziamento e' per JW, che ha saputo guidarmi con competenza e polso fermo attraverso il mondo della luminescenza. Da lui ho imparato molte cose che mi han fatto crescere sia come persona che come ricercatore. Se adesso so riconoscere meglio i miei limiti lo devo a lui; se riesco a scrivere un articolo decente per conto mio e' piu' per merito suo che per il corso Scientific Writing in English che ho seguito. Critico, ma sempre costruttivo e leale; abbiamo avuto delle divergenze ad un certo punto, ma ci sono servite per crescere insieme.

Ricord con affetto un sacco di altre persone che mi hanno accompagnato durante i miei quattro anni di PhD. Alcuni sono partiti, altri sono rimasti. Ivan e Andrei, storici PhD dei primi anni, e poi Majid, Thea e Jeffrey. Enrichetta Blondel ha portato una ventata

---

di freschezza con la sua risata cristallina e il suo buonumore. Con Andreuz si discute di LaTeX, Linux, calcio e condividiamo il piacere di imparare e migliorare quotidianamente. Abbiamo persino deciso di fare una statua a Greg (non a grandezza naturale, leggermente piu' alta...) da mettere nella coffee room. Greg e' un eclettico, mente analitica e cervello fino. Con lui puoi parlare di tutto e non dice mai cazzate, se non di proposito... Insieme a Gael siamo andati a tutte le partite dell'Ajax in Champions League allo stadio e stiamo ancora aspettando di vedere una partita decente. Gael e' uno che gioca bene a pallone e con lui ci siamo fatti un mucchio di risate. Peccato sia partito.

Un ringraziamento poi a tutti quelli a cui ho rotto le palle durante le ore di lavoro per le mie cose personali. Innanzi tutto Jan Huizenga, che mi riparato un Commodore Kim-1, insegnato a saldare e dato un mucchio di consigli per i miei circuitini. Cosi' come Johan, che piu' che un tecnico e' un guru e ci aiuta a trovare i biglietti per l'Ajax. Sopratutto un ringraziamento a Rob Hollander, per aver tentato l'impresa di riparare un vecchio televisore a valvole senza speranza.

Un pensiero affettuoso va alle "donne" con cui ho diviso l'ufficio per un sacco di tempo: CJ, Femke e Hans. Hans non e' una ragazza ma e' nel nostro stesso ufficio! CJ e' una persona davvero speciale. E' master del *Sudoku* (che lei chiama 'Soduko') e fa del corn bread buonissimo. Regina indiscussa del gossip, e' la vera anima del gruppo. Femke ha un viso d'angelo ma e' terribile! Mi mancheranno gli scherzi e le battute che colorivano le nostre giornate. E come non ricordare con affetto i Pet Shop Boys? Uno di loro, Jan, e' un legionario dell'antica Roma.

Mi mancheranno anche le partite di pallavolo del dopopranzo, con Danang karateka, e Niels che mi insegna a giocare a ping-pong nel seminterrato.

E poi volevo ringraziare il mio amichetto storico Emilio per esserci ancora dopo tanto tempo e nonostante la distanza. Si e' un po' involuto nello snowboard ultimamente, ma e' una delle menti piu' lucide che conosca. Adesso Santa Lidia aspetta un bimbo. Buona fortuna.

E cosi' si arriva alla fine, che e' poi un inizio, a voler ben guardare. L'inizio di una vita, che e' un miracolo, e ogni miracolo e' strabiliante. Un viso che tra milioni di altri possibili si materializza nel mondo. Una manina che stringe un dito, il primo sorriso che non ti aspetti; ecco, se il paradiso esiste deve essere fatto di queste sensazioni. Per spiegarlo, forse, l'unica sarebbe fare un ritratto dell'anima nel momento dell'estasi, se qualcuno ne e' capace. Piccolina, tu sei mia, ma soprattutto sei figlia del mondo. Ti vorrei stringere per sempre e mi prende un groppo alla gola al solo pensiero che invece un giorno partirai. E dovrai farlo, perche' cosi' e' la vita. Ma vicina o lontana, felice o triste, io saro' sempre li' per te, se lo vorrai.

Le ultime righe le voglio dedicare a delle persone speciali. Alla fine, qui, un pensiero pieno di affetto per i miei genitori che hanno sempre creduto in me. E per Culetto a Mandolino, a cui voglio un sacco di bene ma forse non gliel'ho mai detto abbastanza. Vi portero' sempre nel mio cuore.

Curriculum Vitae

Mirko Ballarini was born in Torino, Italy, on April 30, 1974. There he attended the high school and received education in both science and humanities. In 2001 he obtained his master degree in Physics with a thesis on "Analysis of some pigments and bindings commonly used in paintings by means of Photoacoustic techniques". In 2001 he was employed as a PhD by the Technical University of Delft. This thesis is the result of his research.